STATIC CRITICAL PROPERTIES OF THE PURE AND DILUTED HEISENBERG AND ISING MODELS

Mathew Raymond Davies
Magdalen College, Oxford

A thesis submitted for the
degree of Doctor of Philosophy

Trinity Term 1982

ABSTRACT

Real space renormalisation group scaling techniques are used to investigate the static critical behaviour of the pure and dilute, classical, anisotropic Heisenberg model.

Transfer matrix methods are employed to obtain asymptotically exact expressions for the correlation lengths and susceptibilities of the one-dimensional system. The resulting scaling relationships are combined with an approximate bond moving scheme to treat pure and dilute models in higher dimensionalities.

Detailed discussions are given for the dependence of correlation lengths and susceptibilities on temperature, anisotropy and concentration, and for the critical temperature on anisotropy and concentration.

Particular emphasis is given to the weakly anisotropic system near percolation threshold and comparisons are made between the results of the present analysis and those of neutron-scattering experiments on dilute quasi-two- and three-dimensional systems.

STATIC CRITICAL PROPERTIES OF THE PURE AND DILUTED HEISENBERG AND ISING MODELS

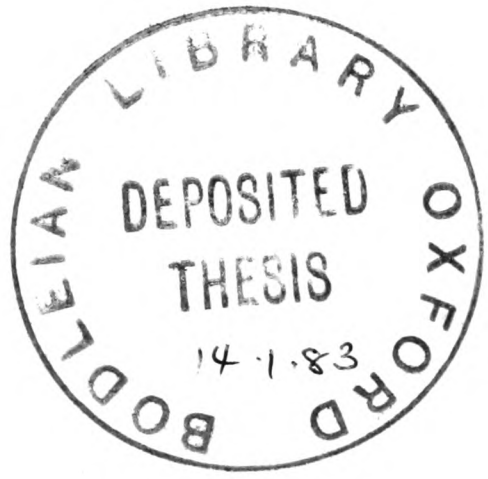
Mathew Raymond Davies

Department of Theoretical Physics
University of Oxford

A Thesis submitted for the degree of

Doctor of Philosophy

at the University of Oxford



Magdalen College

July 1982

This thesis is dedicated
to my daughter Lorna Louise

ACKNOWLEDGEMENTS

I would like to express my gratitude to the following:

Dr. R. B. Stinchcombe, for his constant advice and guidance throughout my time at Oxford.

Prof. R. J. Elliott and all his staff at the Theoretical Physics Department.

My friends and colleagues in the department: especially, Anne Browne, John Chalker, Rashpal Gill, Dick Perkins, Raimundo dos Santos and Andrew Sharland.

The Science Research Council.

The Scott Fund for its generous financial assistance.

Lastly, to my wife for typing this script.

CONTENTS

		Page No.
CHAPTER 1 -	INTRODUCTION	
1 (a)	Background	1-4
1 (b)	$Rb_2Mn_pMg_{1-p}F_4$ As An example Of A Dilute, Quasi-Two-Dimensional System	4-7
1 (c)	Model Systems	7-10
1 (d)	An Intrcduction to Scaling	10-12
1 (e)	Modus Operandi	12-13
CHAPTER 2 -	THE ONE - DIMENSIONAL SYSTEM	
2 (a)	Introduction	14-15
2 (b)	Transfer Matrix Techniques	15-19
2 (c)	An Iteration Scheme	19-24
2 (d)	The Classical Ising Chain	24-25
2 (e)	The Classical Heisenberg Chain	25
2 (f)	The Weakly Anisotropic Heisenberg Chain	25-32
2 (g)	The Dilute, Weakly Anisotropic Heisenberg Chain	32-34
2 (h)	Summary	34-35
CHAPTER 3 -	THE PURE, TWO - DIMENSIONAL SYSTEM	
3 (a)	Introduction	36
3 (b)	The Migdal/Kadanoff Bond Moving Scheme	37-39
3 (c)	Application of the Migdal/Kadanoff Scheme to the Pure, Two-Dimensional System.	39-57
3 (d)	Summary	57-60
CHAPTER 4 -	THE DILUTE, TWO - DIMENSIONAL SYSTEM	
4 (a)	Introduction	61-62
4 (b)	Interaction Probability Distribution Scaling	62-72

CHAPTER 4 (Continued) Page No.

4 (c) Scaling At The Percolation Threshold 72-81

4 (d) Scaling Near The Percolation Threshold 81-93

4 (e) Behaviour Of The Dilute Anisotropic Heisenberg Model Near The Pure Limit 93-96

CHAPTER 5 - THE THREE - DIMENSIONAL SYSTEM

5 (a) Introduction 97

5 (b) The Pure, Three-Dimensional System 97-106

5 (c) The Dilute, Three-Dimensional Model Near Percolation Threshold 106-127

5 (d) The Dilute, Three-Dimensional Model Near The Pure Limit 127-131

CHAPTER 6 - CONCLUSIONS

6 (a) Overview of Results 132-139

6 (b) Qualifications 139-143

6 (c) Comparison With Experiments 143-151

6 (d) Comparison With Existing Theoretical Work 151-157

APPENDIX 1 158-164

APPENDIX 2 165-171

REFERENCES

CHAPTER 1

INTRODUCTION

a) Background

During the last decade, a large number of experiments have been carried out on quasi-low-dimensional magnetic systems. These systems have structures such that over a certain temperature range they may be considered a good approximation to a magnetic system with dimensionality, d^*, lower than the dimensionality, d, of the crystal. For example, a crystalline specimen of the chain-like compound TMMC[tetramethyl ammonium manganese chloride: $(CH_3)_4 NMnCl_3$] exhibits characteristically one-dimensional magnetic behaviour down to less than 2K despite the manifestly three-dimensional nature of the bulk sample. (This being an example of $d^* = 1 < d = 3$) (Birgeneau et al., 1971). Further examples of quasi-low-dimensional magnetic systems are $CsNiF_4$ and Rb_2MnF_4 with $d^* = 1, 2$ respectively. [The reader is referred to the book by de Jongh & Miedema (1974) for a comprehensive review of known examples of systems displaying such behaviour.] The discovery and detailed investigation of these compounds has been part of an enormous upsurge in interest in the statistical mechanics of low-dimensional systems.

At temperatures sufficiently close to a second order phase transition, a system becomes extremely sensitive to certain external perturbations (as shown, for example, by the behaviour of the magnetic susceptibility). Thus, within such a regime, a quasi-low-dimensional system becomes increasingly 'conscious' of its true dimensionality. This, in turn, leads to a change or crossover of behaviour from that characteristic of a d^* - dimensional system to that of a d - dimensional system. Moreover, in any real systems,

especially those with an almost isotropic Hamiltonian, there is the additional crossover behaviour generated by the slight anisotropy in the Hamiltonian to be considered. Far from criticality, such systems would be expected to behave as if their Hamiltonian were totally isotropic whereas on approaching criticality their behaviour would be expected to change to that consistent with a lower symmetry Hamiltonian. These features can be emphasised in some low-dimensional systems where criticality occurs at low temperatures. The anisotropy crossover is particularly striking in systems with an easy spin axis since it induces a change from power law to exponential dependence on temperature in certain thermodynamic functions.

A third type of crossover, which we consider in this thesis, is driven by dilution. If we consider randomly removing a fraction (1-p) of the spins in a magnetic system, the remaining spins start to form isolated groups or 'clusters'. Above some critical value, p_c, of the magnetic ion concentration, a cluster of infinite size exists. Below p_c all spins belong to clusters of finite size. Hence, for values of p less than the critical value, the system will certainly not exhibit long range order (Elliott, Heap, Morgan, Rushbrooke (1960)).

The first investigations of the regime $p \gtrsim p_c$ (Harris(1974)) showed that provided the specific heat exponent was negative, it was plausible that the dilute magnetic system would undergo a second order phase transition at some well defined temperature, $T_c(p)$. Later scaling (Stauffer (1975)) and field theoretic renormalisation group (Lubensky (1975, 1977), Grinstein & Luther (1976)) studies suggested that the only important constraint on the

system for it to undergo such a transition was for the dilution to be uncorrelated.

For a magnetic system with transition temperature $T_c(1) > 0$, random dilution lowers T_c until the critical concentration, p_c, of the magnetic sites is reached whereupon:

$$T_c(p_c) = 0$$

The point in the phase diagram of the dilute magnetic system defined by the equation above is of particular interest. By varying the concentration, p, at $T = 0$ one sees purely geometrical critical behaviour associated with the corresponding percolation problem (Essam (1972)). Varying the temperature exactly at p_c one sees purely thermal critical behaviour. Such a point is termed a multicritical point (Stauffer (1975)).

As a result of introducing dilution into a uniaxially anisotropic magnetic system, we are able to depress the critical temperature arbitrarily close to zero. Thus, the sort of striking effects resulting from the anisotropy crossover in lower dimensional systems may also be observed in the three-dimensional system near the percolation threshold (p_c). Furthermore, it becomes possible to observe a crossover from thermal to percolative behaviour in the vicinity of the multicritical point.

The renormalisation group treatment of dilute magnetic systems may be carried out either by the previously mentioned field theoretic methods or within a real space framework (Young and Stinchcombe (1976)). In this thesis we employ the latter method to investigate the static critical properties of the pure and dilute Heisenberg model with uniaxial exchange anisotropy.

To a large extent, this work was stimulated by the experiments

of Birgeneau et al. (1980) and others on dilute low-dimensional systems such as $Rb_2Mn_pMg_{1-p}F_4$. In the next section we briefly review the salient experimental results on this dilute, quasi-two-dimensional system.

b) $Rb_2Mn_pMg_{1-p}F_4$ As An Example Of A Dilute Quasi-Two-Dimensional System .

The pure system, Rb_2MnF_4, is known to have the K_2NiF_4 crystal structure illustrated in Figure 1. (Balz & Plieth (1955)). Manganese ions within a large crystalline sample can be regarded as forming a series of square nets or layers perpendicular to the c-axis. The superexchange interaction between Mn^{2+} ions is almost isotropic (i.e. Heisenberg-like) but dipolar interactions between the ions result in a small axial anisotropy along the c-axis. The antiferromagnetic superexchange interaction is mediated by F^- ions so that the magnitude of the interaction is expected to decrease rapidly with the number of intermediate F^- ions. As a result, nearest neighbour (n.n.) Mn^{2+} ions within a layer experience a far stronger interaction than n.n. Mn^{2+} ions in different layers. Moreover, due to the symmetry of the crystal structure there would appear to be a great deal of cancellation of n.n. layer interaction. Indeed, within a crystal field type treatment or in the classical Néel state such a cancellation would be complete due to the exchange anisotropy. That such an effect would persist in the presence of quantum or thermal fluctuations is not so obvious although experimental data suggests that it does, even at comparatively high temperatures. Such cancellation implies that any ordering of the system has to be mediated by the extremely weak next nearest

neighbour (n.n.n.) layer interaction or by exchange anisotropy.

Neutron scattering (Birgeneau et al., (1970)) and susceptibility (Breed, 1967) experiments have shown that crystals of Rb_2MnF_4 undergo a phase transition to a state of three-dimensional order at $T_n = 38.5K$ accompanied by critical scattering which is two-dimensional in nature. Within the ordered state two distinct magnetic phases are found. These are illustrated in Figure 2. These observations strongly suggest that there is a delicate balance between dipolar (favouring ferromagnetic alignment) and superexchange (favouring antiferromagnetic alignment) interactions between next nearest neighbour layers: the particular phase occuring in a given region of the crystal being determined by local defects.

The picture which emerges from these experimental observations is that of a layered system with strong intralayer couplings but very weak interlayer interactions. Thus, at temperatures well above T_N all but the intralayer interactions are negligable. As the temperature is reduced towards T_N, the seperate layers begin to order, due to the exchange anisotropy, and the large scale cancellation of n.n. layer interactions sets in. The onset of order within the layers amplifies the n.n.n. layer interaction to such an extent that the system crosses over to three-dimensional long range order. Below T_N, three-dimensional L.R.O. is established but correlations within the layers remain two-dimensional in nature. Within this picture the transition is driven by the intralayer exchange anisotropy. It is of interest to note that using the exchange values given by fitting the inelastic scattering data to spin wave theory and estimating the next nearest layer coupling,

an R.P.A. treatment of the system suggests that in the absence of any exchange anisotropy, the crossover to three-dimensional ordering would not take place until the temperature was of order a few degrees Kelvin. (Tahir-Kheli and Ter Haar (1962))

With the random replacement of a fraction (1-p) of the magnetic Mn^{2+} ions by the non-magnetic Mg^{2+} ions the situation is a little more complicated. The chemical similarity of Mn^{2+} and Mg^{2+} ions suggests that there will be little, if any, clustering effect in the dilute system. However, we might expect some degree of lattice distortion since the lattice constants differ in pure Rb_2MnF_4 and Rb_2MgF_4. The effect of this distortion on the exchange interaction was further investigated by Breed et al. (1973) who showed that it led to a small adjustment in the value of the average exchange interaction parameters from those of the pure system. There is also some question as to whether the previously described nearest neighbour layer interaction cancellation persists in the dilute system. Within a virtual crystal view of the problem, the cancellation is still complete but it is certainly not clear, a priori, that the cancellation persists in the presence of configurational fluctuations. We defer further discussion of this point until we have discussed some experimental data.

Since 1976, a set of neutron scattering experiments has been carried out on $Rb_2Mn_pMg_{1-p}F_4$ for various values of the magnetic ion concentration, p, by Birgeneau et al. (1976, 1980) and Cowley et al. (1977). We have summarised some of their results below.

For magnetic ion concentrations, p, less than p_c (the critical concentration for the square lattice with nearest neighbour bonds

only) no transition to L.R.O. was observed at any temperature. The corresponding diffuse scattering was two-dimensional in nature.

For a magnetic ion concentration , p, greater than p_c, a 'smeared' transition to two-dimensional L.R.O. but with S.R.O. in the third direction was observed. The 'smearing' was thought to be due to chemical inhomogeneities over a length scale of order the size of the specimen although it is possible that this may be a random dipolar field effect due to local concentration fluctuations.

Subsequent neutron scans showed no evidence for two-dimensional or three-dimensional S.R.O. effects indicating that the distribution of Mg^{2+} ions throughout the sample was, on a macroscopic scale, indeed random.

These results suggest that even in the presence of random substitutional disorder there is a large scale cancellation of nearest-neighbour layer coupling. Were this not the case, a transition to three-dimensional L.R.O. would seem inevitable.

We conclude, therefore, that $Rb_2Mn_pMg_{1-p}F_4$ appears to be a 'bona fide' example of a randomly dilute quasi-two-dimensional antiferromagnet within the temperature range investigated.

Having outlined some of our reasons for studying low-dimensional systems, the next section presents and discusses the models we have used in our investigation.

c) Model Systems.

Real systems are notoriously complex. Remarkably, however, much of the behaviour of real systems seems to be reproduced by

models with only very few details of the real system. We now believe that many properties of a system near a second order phase transition are determined by only a small number of relevant factors such as (in the magnetic case) the number of spin components appearing in the order parameter and the dimensionality of the system. For a review of these ideas and the methods by which they were originally obtained, the reader is referred to the book by Ma (1976) . Such universal behaviour of systems depending only on certain relevant parameters allows us to model real systems by very simple Hamiltonians. Of course, not all properties of the system are determined by just these few parameters. For instance, the critical temperature of a system is extremely sensitive to the size of the exchange interactions. Nevertheless, in the following we shall have cause to invoke the ideas of universality in justifying our choice of model.

For the remainder of this thesis, unless stated to the contrary, we will restrict our attention to d-dimensional ($d = 1,2,3$) magnetic model systems on hypercubic lattices and described by the Hamiltonian:

$$\mathcal{H} = -J \sum_{\langle ij \rangle} \left[(1-\delta)\, \underline{\sigma}_i \underline{\sigma}_j + \delta \sigma_i^z \sigma_j^z \right] \qquad 0 \leqslant \delta \leqslant 1 \qquad (1.C.1)$$

where the summation is over nearest neighbour sites on the lattice. Before proceeding any further, we take time to remark on some of the differences between this model Hamiltonian and real systems: in particular Rb_2MnF_4.

Firstly, in order to avoid quantum mechanical commutation problems later on, we follow Fisher (1964) by taking the magnitude of the spin vectors ($\{\underline{S}_i\}$) to infinity after first defining normalised spin vectors through the relationship:

$$\underline{\sigma}_i = \underline{S}_i / S$$

In this limit the spins $\{\underline{\sigma}_i\}$ become classical in that:

$$\lim_{S\to\infty} [\sigma_i^\alpha, \sigma_j^\beta] = \lim_{S\to\infty} (1/S^2)[S_i^\alpha, S_j^\beta] = \lim_{S\to\infty} (i/S)\,\delta_{ij}\,\epsilon_{\alpha\beta\delta}\,\sigma_i^\delta = 0 \qquad (1.C.2)$$

That is, commutators can be neglected.

For the particular case of Mn^{2+} ions with spin-5/2 we expect this approximation to give the correct qualitative behaviour of the real system except, possibly, as the transition temperature tends to zero (e.g. because of dilution or reduced dimensionality) where crossover to essentially quantum behaviour may occur. Of course, by the very nature of this approximation, any such crossover will be entirely neglected within this scheme.

Secondly, we have chosen the interaction between spins to be ferromagnetic whereas Rb_2MnF_4 is an antiferromagnet. For the nearest neighbour Ising model on a hypercubic lattice in the absence of an external field, the static behaviour of the ferromagnet is the same as that for the antiferromagnet since each can be mapped onto the other by relabelling spins on a sublattice. Since we are already dealing with a classical model, universality arguements are anyway sufficient to imply that antiferro- and ferro- magnetic versions of our Hamiltonian have the same static critical properties. One should note, however, that these sorts of statements may not hold for quantum critical behaviour in the Heisenberg limit, and they certainly do not apply to behaviour in a field, nor to dynamic critical behaviour.

Thirdly, we have ignored next nearest neighbour and weaker interactions which are present in the real system. Universality

arguments again lead us to believe that next nearest neighbour interactions will be irrelevant to the static critical behaviour. Note, however, that the omission of some interaction terms precludes the possibility of dimensional crossover. Since, at least in Rb_2MnF_4, no measurable dimensional crossover temperature regime was observed, this last point should not be important here.

Lastly, we have chosen the anisotropy term in our Hamiltonian to be of the exchange type whereas in Rb_2MnF_4 it is probably a single ion term. However, near criticality, we expect the exact nature of the anisotropy to be irrelevant to static critical phenomena: only its effect upon the symmetry of the Hamiltonian being important for long wavelength properties.

The next two sections give a brief outline of the methods we have used to obtain various statistical mechanical properties from these model systems for comparison with experimental data.

d) An Introduction To Scaling (Widom (1965), Griffiths (1965), Kadanoff (1966))

Neutron scattering experiments on magnets with localised spins have shown that large 'patches' or clusters of spins become strongly correlated near a second order phase transition. The resultant behaviour of such systems is, to a large extent, governed by the behaviour of these clusters of correlated spins. It therefore seems reasonable to expect that many details of the system, particularly those on a length scale much smaller than the average cluster size, will not be important or relevant to the critical behaviour of the system. As an example, the underlying lattice (e.g. B.C.C. or S.C.) is irrelevant to such

properties as the system's response to an external magnetic field near criticality. Heuristic arguements of this type lend physical insight into how phenomena such as universality arise. They are also the inspiration behind such theoretical methods as scaling and the renormalisation group (Ma (1976), Pfeuty & Toulouse (1977)) for if we can find a way to dilate the length scale of the system by a factor, b, making sure that we have, in some sense, the same sort of system after the dilation (but not worrying too much about what happens on a length scale much less than the average cluster size) then we can interpret this new system as being the old system at a slightly different temperature (or, equivalently, with different coupling constants in the Hamiltonian). Alternatively, we can turn the procedure on its head by starting off with the average cluster size expressed as a function of the various coupling constants, divide it by a factor b and ask what values of the coupling constants in the original system would have resulted in the same average cluster size. Either way, the nett result is a transformation of the various parameters in the problem which we are free to interpret as having been brought about by a length dilation factor, b. A detailed knowledge of these transformations enables us to deduce a great deal about the functional forms of statistical mechanical quantities such as the specific heat, susceptibility etc. as we show later.

Of course, the discussion above assumes that there is a unique, large, characteristic length scale in the system near criticality: the average cluster size. In the isotropic Heisenberg or Ising model this is conveniently calculated as the correlation length: the length scale over which spin-spin correlations decay. However, in the uniaxially anisotropic Heisenberg model, as we shall show in

Chapter 2, there are two independent spin-spin correlation functions. One is concerned with spin components along the easy axis: the other with components perpendicular to it. In this case, we can define two dominant length scales near criticality. It turns out that it is the competition between these two length scales which gives rise to anisotropy crossover effects in the critical region. Similarly, the thermal/geometric crossover occurring in diluted systems near the percolation threshold can also be interpreted in terms of the competition between the large correlation lengths of the pure thermal and the percolation problem near p_c.

The ideas outlined in this section will be refined and used in later chapters to treat the pure and dilute two- and three-dimensional anisotropic Heisenberg models near criticality.

e) Modus Operandi.

Two- and three-dimensional model systems displaying critical phenomena are notoriously difficult to treat analytically, though, of course, a few exact solutions exist(e.g. that for the two-dimensional Ising model (Onsager, 1944)). As a consequence, we have had to employ an approximation scheme to obtain the qualitative behaviour of our model systems in two and three dimensions. The particular scheme we have chosen to use is due to Migdal (1976). This scheme is also convenient for the treatment of the effects of dilution. However, in order to be able to use this scheme, it is a necessary prerequisite that we solve the corresponding one-dimensional pure problem. This being the case, the rest of this thesis is laid out as follows:

In Chapter 2 we obtain an approximate solution of the corresponding one-dimensional pure problem, including the effects of anisotropy; then generalisation, in a straightforward way, to the dilute one-dimensional case.

In Chapter 3 we incorporate the results of chapter two into the Migdal/Kadanoff (1976) bond moving scheme to obtain results for the pure two-dimensional systems.

In Chapter 4 we extend the work of the previous two chapters to include the effects of dilution into the two-dimensional system.

In Chapter 5 ,again using the results of chapter two, we obtain results for the pure and dilute three-dimensional model systems.

Chapter 6 summarises our results and conclusions.

As pointed out above, before we can progress to the experimentally interesting two- and three-dimensional systems it is necessary to solve the corresponding one-dimensional problem. This is the main purpose of chapter two.

CHAPTER 2

THE ONE-DIMENSIONAL SYSTEM

a) Introduction

As we briefly stated at the end of the last chapter, our reasons for studying the one-dimensional system are not entirely for its interest per se. Some of the results which we obtain in this chapter are essential for the application of the Migdal/ Kadanoff approximation to model systems in higher dimensions. In particular, we need to know how the various parameters in the one-dimensional problem transform when the length scale of the system is dilated by a factor b. [Ma (1976), Pfeuty & Toulouse (1977), Riedel & Wegner (1969)]. One method of obtaining these transformations, and the method which we have employed, is to calculate the long wavelength limit of the two spin-spin correlation lengths which act as the underlying, natural length scales for the system near criticality. Knowing how these two functions of the parameters appearing in the Hamiltonian scale when the length scale of the system is dilated by a factor, b, we obtain two implicit equations for the scaling of the parameters. As a result, the rest of this chapter is concerned with obtaining these correlation lengths although we do make some comparison of our results on this model with those of other authors and in the later sections we show how such results are affected by the presence of dilution.

The method used is a transfer matrix technique, introduced and developed in the following subsections (b), (c) and applied to specific cases in the remainder of the chapter.

As a preliminary we rewrite the Hamiltonian for the system

using a parameterisation originally introduced by Joyce (1967) viz:

$$H = -J \sum_{\langle ij \rangle} [\tanh \mu (\sigma_i^x \sigma_j^x + \sigma_i^y \sigma_j^y) + \sigma_i^z \sigma_j^z] \qquad (2.a.1)$$

In the limits of $\mu \to 0, \infty$ we obtain the classical Ising and Heisenberg models respectively.

b) Transfer Matrix Techniques.

In this section we show how the spin-spin correlation functions and correlation lengths of the classical anisotropic Heisenberg chain may be expressed in terms of the eigenvalues and eigenvectors of an integral operator. In the classical Ising limit ($\mu = 0$) the integral operator becomes the infinite spin analogue of the $(2S+1)$-dimensional transfer matrix which is used in the analysis of spin-S Ising systems [Stanley (1971), Domb (1960)]. In the following section we discuss how successive approximations to these expressions may be obtained by exploiting the form of the operator and its expected eigenvalue spectrum behaviour. The spin-spin correlation functions for a ring of N spins with periodic boundary conditions and a Hamiltonian, H, given by (2.a.1) can be expressed as:

$$\langle \sigma_i^z \sigma_j^z \rangle \equiv \frac{1}{Z} \prod_{r=1}^{N} \left(\int_{\Omega_r} \frac{d^2\underline{\sigma}_r}{4\pi} \right) \cdot e^{-\beta H} \sigma_i^z \sigma_j^z \qquad (2.b.1)$$

$$\langle \sigma_i^x \sigma_j^x \rangle \equiv \langle \sigma_i^y \sigma_j^y \rangle \equiv \frac{1}{Z} \prod_{r=1}^{N} \left(\int_{\Omega_r} \frac{d^2\underline{\sigma}_r}{4\pi} \right) e^{-\beta H} \sigma_i^x \sigma_j^x \qquad (2.b.2)$$

where:

$$Z \equiv \prod_{r=1}^{N} \left(\int_{\Omega_r} \frac{d^2\underline{\sigma}_r}{4\pi} \right) e^{-\beta H} \qquad (2.b.3)$$

$$\beta = 1 / k_B T$$

k_B is Boltzmann's constant, T is the absolute temperature and the integrals in (2.b. 1-3) are over the solid angles for the unit spins at each site. If we now introduce the complete orthonormal set of eigenvectors $\{\mathcal{S}_{r,m}\}$ and corresponding eigenvalues $\{\lambda_{r,m}\}$ of the integral equation:

$$\int_{\Omega_i} \frac{d^2\underline{\sigma}_i}{4\pi} e^{\beta J[\tanh\mu(\sigma_i^x\sigma_j^x + \sigma_i^y\sigma_j^y) + \sigma_i^z\sigma_j^z]} \mathcal{S}_{r,m}(\hat{\underline{\sigma}}_i|\beta J,\mu)$$

$$= \lambda_{r,m}(\beta J,\mu)\,\mathcal{S}_{r,m}(\hat{\underline{\sigma}}_j|\beta J,\mu) \qquad (2.b.4)$$

and use the fact, as pointed out by Rae (1974), that there is a single positive maximum eigenvalue, $\lambda_{0,0}$ of this equation, in the thermodynamic limit ($N \to \infty$), equations (2.b. 1-3) reduce to:

$$\langle\sigma_i^z\sigma_j^z\rangle \equiv \sum_{r,m}\left(\frac{\lambda_{r,m}(\beta J,\mu)}{\lambda_{0,0}(\beta J,\mu)}\right)^{|i-j|}|C_{r,m}|^2 \qquad (2.b.5)$$

$$\langle\sigma_i^x\sigma_j^x\rangle \equiv \langle\sigma_i^y\sigma_j^y\rangle \equiv \sum_{r,m}\left(\frac{\lambda_{r,m}(\beta J,\mu)}{\lambda_{0,0}(\beta J,\mu)}\right)^{|i-j|}|\epsilon_{r,m}|^2 \qquad (2.b.6)$$

$$Z \equiv \sum_{r,m}\lambda_{r,m}^N(\beta J,\mu) \qquad (2.b.7)$$

where:

$$C_{r,m} \equiv \int_\Omega \frac{d^2\underline{\sigma}}{4\pi}\,\mathcal{S}^*_{r,m}(\hat{\underline{\sigma}}|\beta J,\mu)\,\sigma^z\,\mathcal{S}_{0,0}(\hat{\underline{\sigma}}|\beta J,\mu) \qquad (2.b.8)$$

$$\epsilon_{r,m} \equiv \int_\Omega \frac{d^2\underline{\sigma}}{4\pi}\,\mathcal{S}^*_{r,m}(\hat{\underline{\sigma}}|\beta J,\mu)\,\sigma^x\,\mathcal{S}_{0,0}(\hat{\underline{\sigma}}|\beta J,\mu) \qquad (2.b.9)$$

The eigenvectors are the angle spheroidal wave functions [Joyce (1967), Morse & Feshbach (1953)] viz:

$$\varphi_{\rho,m}(\hat{\underline{\sigma}}|\beta J,\mu) \equiv \left\{\frac{2}{\Lambda_{\rho,|m|}(-ih)}\right\}^{1/2} S_{\rho,|m|}(-ih,\cos\theta)\, e^{im\varphi} \qquad (2.b.10)$$

where we have parameterised the spin direction, $\hat{\underline{\sigma}}$, in terms of the polar angles (Θ, φ), and:

$$h \equiv \frac{\beta J}{\cosh \mu} \qquad (2.b.11)$$

Equations (2.b. 10-11) express the important result that the eigenvectors do not depend on the two parameters βJ and μ seperately, but only through the quantity h. In this and the following sections we will frequently use and refer back to this point.

The corresponding eigenvalues are the radial functions [Joyce (1967), Morse & Feshbach (1953)] viz:

$$\lambda_{\rho,m}(\beta J,\mu) \equiv i^{\rho} e_{\rho,|m|}(-ih,\cosh\mu) \qquad (2.b.12)$$

In terms of these functions, our final results for the spin-spin correlation functions (2.b. 5-9) become:

$$\langle \sigma_i^z \sigma_j^z \rangle \equiv \sum_{\rho \text{ odd}} \left(\frac{\lambda_{\rho,0}(\beta J,\mu)}{\lambda_{0,0}(\beta J,\mu)}\right)^{|i-j|} D_\rho(h) \qquad (2.b.13)$$

$$\langle \sigma_i^x \sigma_j^x \rangle \equiv \langle \sigma_i^y \sigma_j^y \rangle \equiv \frac{1}{2} \sum_{\rho \text{ odd}} \left(\frac{\lambda_{\rho,1}(\beta J,\mu)}{\lambda_{0,0}(\beta J,\mu)}\right)^{|i-j|} E_\rho(h) \qquad (2.b.14)$$

where:

$$D_\rho(h) \equiv \Lambda_{00}^{-1}(-ih)\, \Lambda_{\rho 0}^{-1}(-ih) \left\{ \int_{-1}^{1} dx\, x\, S_{00}(-ih,x)\, S_{\rho,0}(-ih,x) \right\}^2 \qquad (2.b.15)$$

$$E_\rho(h) \equiv \Lambda_{00}^{-1}(-ih)\, \Lambda_{\rho,1}^{-1}(-ih) \left\{ \int_{-1}^{1} dx\, (1-x^2)^{1/2} S_{00}(-ih,x)\, S_{\rho,1}(-ih,x) \right\}^2 \qquad (2.b.16)$$

In the limit of large spin seperation we may define two inverse correlation lengths (in units of the lattice spacing) for the system, corresponding to the two dominant length scales in the system near criticality (Riedel (1971), Riedel & Wegner (1969)) i.e.

$$K_{\parallel}(h,\cosh\mu) = \lim_{|i-j|\gg 1}\left(\frac{-\ln\langle\sigma_i^z\sigma_j^z\rangle}{|i-j|}\right)$$

$$= \ln\left\{\frac{\lambda_{0,0}(h,\cosh\mu)}{\lambda_{0,1}(h,\cosh\mu)}\right\} \qquad (2.b.17)$$

$$K_{\perp}(h,\cosh\mu) = \lim_{|i-j|\gg 1}\left(\frac{-\ln\langle\sigma_i^x\sigma_j^x\rangle}{|i-j|}\right)$$

$$= \ln\left\{\frac{\lambda_{0,0}(h,\cosh\mu)}{\lambda_{1,1}(h,\cosh\mu)}\right\} \qquad (2.b.18)$$

Thus, we have obtained closed expressions for the two spin-spin correlations lengths which were mentioned in the introductory part of this chapter. Of course, such expressions are only useful if one can evaluate the eigenvalue ratios involved somehow: even if only approximately. The methods by which we have obtained such information are given in the following sections. Before we consider these, however, we pause to discuss the behaviour of the eigenvalues $\{\lambda_{p,m}\}$ of (2.b.4).

Firstly, we consider the limit of $\mu \to 0^{+}$ (the classical Ising model). Sneddon and Stinchcombe (1978) have shown that the eigenvalue spectrum for the finite spin-s Ising model transfer matrix is dominated by just two eigenvalues as the temperature of the system is reduced to absolute zero. The ratio of this pair tends to unity in the same limit

(Figure 3). This behaviour is compatible with our previous discussion of systems near criticality in that the dominant pair of eigenvalues defines a single, remaining length scale for the system, given by the inverse of equation (2.b. 17) as the temperature is reduced to zero. We have assumed that the eigenvalue spectrum of the infinite spin (classical) Ising model will behave in an analogous manner: a view supported by the work of Thompson (1968).

In the limit of $\mu \to \infty$ (the classical Heisenberg model) we know from Fisher's exact solution (Fisher (1964)) and the subsequent work of Joyce (1967(a)) that the eigenvalue spectrum converges as the temperature is reduced to zero. (Figure 4.) This indicates the presence of as many length scales in the problem as there are degrees of freedom. However, asymptotically close to absolute zero, these length scales all become the same so that we are left with a single length scale in the system given by the inverse of (2.b. 17) and/or (2.b. 18).

In the following sections we shall elaborate on these ideas and utilise the behaviour of the eigenvalue spectrum to obtain approximate forms for the inverse correlation lengths defined in (2.b. 17-18).

c) An Iteration Scheme.

Equations (2.b. 17-18) are of little value unless one can evaluate the eigenvalue ratios involved. The present section develops the framework which we have used to obtain successive estimates of the respective eigenvalues.

From the outset we concentrate our attention on the 'low temperature' regime viz.:

$$\frac{J}{k_B T} = K \gg 1 \qquad (2.c.1)$$

Even within this limited temperature range, a system described by the Hamiltonian (2.a. 1) but with only weak anisotropy, would be expected to show three distinct types of behaviour. Well above some crossover temperature, T_x, which will be in the low temperature regime (2.c. 1) for very weak anisotropy, we expect the system to behave like an isotropic Heisenberg model. As the temperature is lowered towards T_x we expect some change in behaviour as certain fluctuations of the system become 'damped' by the attendant anisotropy. Well below T_x we expect the system to have changed its behaviour drastically from that of the first temperature regime ($T > T_x$) having crossed over to characteristically Ising-like behaviour. As a result, it would seem plausible that the eigenvalue spectrum of the system's transfer matrix (2.b. 4) would mirror these changes (Figure 5) by being fairly closely spaced above T_x (cf. Figure 4), being well seperated below T_x (cf. Figure 3) but with one big difference from the Ising case: the emergence of a third dominant eigenvalue in the system (Riedel (1971)). It turns out that these expectations concerning the eigenvalue spectrum behaviour are borne out by our later calculations. We also show that it is the variable h in equation (2.b. 11) which determines whether the system in question is well above ($h \ll 1$) or well below ($h \gg 1$) the crossover temperature, T_x. Note that this provides us with a rough estimate of the crossover temperature viz:

$$T_x \sim \frac{J}{k_B \cosh\mu}$$

The expected eigenvalue spectrums behaviour well below crossover ($h \gg 1$) implies that on inserting an initial or 'seed' function into the left-hand side of equation (2.b. 4) and iterating the equation many times, the eigenvectors $\mathcal{S}_{0,0}$, $\mathcal{S}_{1,0}$ and $\mathcal{S}_{1,1}$ will be projected out. Moreover, if the 'seed' functions are chosen judiciously, each of the eigenvectors can be projected out seperately. These ideas form the basis of our iteration scheme, the successive approximations to the eigenvectors being used to obtain estimates of their corresponding eigenvalues.

Well above crossover ($h \ll 1$) it is not clear, a priori, that the iteration scheme outlined above will be effective. However, the fact that h is small within this regime allows us to solve eqn (2.b. 4) exactly for the eigenvectors as a power series in h.

Below we quote the results of the iteration scheme but the interested reader is referred to Appendix 1 for details of their derivation.

i) Well Below Crossover: $T \ll T_x$

As discussed briefly above, the iteration scheme consists of inserting a seed function, $S^{(0)}_{pm}(h,x)$, into the left-hand side of equation (2.b. 4), iterating many times and allowing the eigenvalue spectrum to project out eigenfunctions $S_{00}(-ih,x)$, $S_{10}(-ih,x)$ and $S_{11}(-ih,x)$. By choosing the symmetry and form of the seed in an appropriate manner, with regard to the kernal of (2.b. 4), the results of the scheme converge rapidly.

Successive un-normalised approximations to the

spheroidal wave functions S_{oo} , S_{1o} , S_{11} are obtained from:

$$S^{(n+1)}_{o,o}(-ih,x) = \int_o^1 dt.\cosh hxt.S^{(n)}_{o,o}(-ih,t) \qquad (2.c.2)$$

$$S^{(n+1)}_{1,o}(-ih,x) = \int_o^1 dt.\sinh hxt.S^{(n)}_{1,o}(-ih,t) \qquad (2.c.3)$$

$$S^{(n+1)}_{1,1}(-ih,x) = (1-x^2)^{1/2} f^{(n+1)}(-ih,x)$$

$$= (1-x^2)^{1/2}\int_o^1 dt.(1-t^2).\cosh hxt.f^{(n)}(-ih,t) \qquad (2.c.4)$$

[compare equations (A.1. 10) and (A.1. 15) of Appendix 1]

and the corresponding approximations for λ_{oo} , λ_{1o} , λ_{11} , from:

$$\lambda^{(n)}_{oo}(h,\cosh\mu) = \frac{1}{S^{(n)}_{oo}(-ih,1)}\int_o^1 dx.\cosh Kx.S^{(n)}_{oo}(-ih,x) \qquad (2.c.5)$$

$$\lambda^{(n)}_{1o}(h,\cosh\mu) = \frac{1}{S^{(n)}_{1o}(-ih,1)}\int_o^1 dx.\sinh Kx.S^{(n)}_{1o}(-ih,x) \qquad (2.c.6)$$

$$\lambda^{(n)}_{11}(h,\cosh\mu) = \frac{K.\tanh\mu}{2.f^{(n)}(-ih,1)}\int_o^1 dx.(1-x^2).\cosh Kx.f^{(n)}(-ih,x) \qquad (2.c.7)$$

[compare equations (A.1. 11) and (A.1. 16) of Appendix 1]

ii) Well Above Crossover: $T \gg T_x$

Well above crossover ($h \ll 1$) the arguments which were used to justify the iteration scheme (particularly the eigenvalue spectrum behaviour) no longer apply.

However, the fact that h is now a small variable allows us to solve for the respective eigenfunctions and eigenvalues as a power series in h. As a direct consequence, our results in this regime are exact.

The eigenfunctions forms are obtained by solving the following equations as a power series in h and x.

$$\lambda_{oo}(h,1).S_{oo}(-ih,x)=\int_o^1 dt.\cosh hxt.\ S_{oo}(-ih,t) \qquad (2.c.8)$$

$$\lambda_{1o}(h,1)\,S_{1o}(-ih,x)=\int_o^1 dt.\sinh hxt.\ S_{1o}(-ih,t) \qquad (2.c.9)$$

$$S_{11}(-ih,x)=(1-x^2)^{1/2}f(-ih,x) \qquad \text{where:}$$

$$\frac{\partial}{\partial\mu}\lambda_{11}(h,\cosh\mu)\Big|_{\cosh\mu=1} f(-ih,x) = \frac{h}{2}\int_o^1 dt.(1-t^2).\cosh hxt.\ f(-ih,t) \qquad (2.c.10)$$

[cf. equations (A.1. 3), (A.1. 4) and (A.1. 13) of Appendix 1]

The forms so obtained can then be used to calculate the corresponding eigenvalues by using the relationships:

$$\lambda_{oo}(h,\cosh\mu) = \frac{1}{S_{oo}(-ih,1)}\int_o^1 dx.\cosh Kx.\ S_{oo}(-ih,x) \qquad (2.c.11)$$

$$\lambda_{1o}(h,\cosh\mu) = \frac{1}{S_{1o}(-ih,1)}\int_o^1 dx.\sinh Kx.\ S_{1o}(-ih,x) \qquad (2.c.12)$$

$$\lambda_{11}(h,\cosh\mu) = \frac{K.\tanh\mu}{2.f(-ih,1)}\int_o^1 dx.(1-x^2)\cosh Kx.\ f(-ih,x) \qquad (2.c.13)$$

[cf. equations (A.1. 6), (A.1. 7) and (A.1. 14) of Appendix 1]

In the next two sections we illustrate the use of this and the iteration scheme applied to the Ising and

isotropic Heisenberg limits of our model respectively.

d) The Classical Ising Chain

The classical Ising model has previously been investigated by Thompson (1968). Comparison with his results allows us to assess the accuracy of our iteration scheme in this limit ($\mu=0$).

The eigenvalue λ_{11} is identically zero for the Ising model. (See Appendix 1). This corresponds to there being only one characteristic length scale in the system. Starting with the 'seed' functions:

$$S_{\infty}^{(0)}(-iK, x) = \delta(x-1) + \delta(x+1)$$

$$S_{10}^{(0)}(-iK, x) = \delta(x-1) - \delta(x+1)$$

the iteration scheme (2.c. 2-3 & 5-6) produces:

$$\left\{ \frac{\lambda_{10}(K)}{\lambda_{\infty}(K)} \right\}^{(1)} = 1 - 8Ke^{-2K} + \ldots$$

$$\left\{ \frac{\lambda_{10}(K)}{\lambda_{\infty}(K)} \right\}^{(2)} = 1 - 8Ke^{-2K}(\ln K + O(1))$$

$$\left\{ \frac{\lambda_{10}(K)}{\lambda_{\infty}(K)} \right\}^{(3)} = 1 - 8Ke^{-2K}[\ln 4K + \gamma + O(\ln K/K)]$$

where $\gamma \doteq 0.578$ is Euler's constant.

We note that this result implies that for the classical Ising chain: (2.b. 17)

$$K_{11}^{\text{ISING}}(K) = 8Ke^{-2K}[\ln 4K + \gamma + O(\ln K/K)] \quad : \quad (K \to \infty) \qquad (2.d.1)$$

This result agrees with that of Thompson (1968) and with other methods of calculation of the same quantity (Davies, Harris & Stinchcombe (1981)).

e) The Classical Heisenberg Chain ($\mu \to \infty$)

It is well known [Joyce(1967(a)), Morse & Feshbach (1953)] that in the limit of $h \to 0^+$ the spheroidal wave functions reduce to Legendre polynomials. The same result is easily obtained by expanding the spheroidal wave functions in a power series in h and x in equations (2.c. 8-10). The resultant eigenvalue ratios are (2.c. 11-13):

$$\frac{\lambda_{10}(K)}{\lambda_{00}(K)} \equiv \frac{\lambda_{11}(K)}{\lambda_{00}(K)} = \coth K - \frac{1}{K}$$

and, hence:

$$K_{/\!/}^{HEIS.}(K) \equiv K_{\perp}^{HEIS}(K) = -\ln\left\{\coth K - \frac{1}{K}\right\} \sim \frac{1}{K} \qquad (K \gg 1) \qquad (2.e.1)$$

in agreement with the exact result of Fisher (1964).

In the next section, armed with the results of applying our scheme to the Ising and Heisenberg chains, we treat the weakly anisotropic Heisenberg model, which includes both types of limiting behaviour.

f) The Weakly Anisotropic Heisenberg Chain. ($\cosh\mu \gg 1$)

When applied to the weakly anisotropic Heisenberg model, the iteration scheme yields:

i) Well Above Crossover ($T \gg T_x$; $h \ll 1$)

As outlined in section (c), within this regime we are able to solve exactly for the eigenfunctions of equation (2.b. 4) as a power series in h and x to obtain:

$$S_{oo}(-ih,x) \sim 1 - \frac{h^2}{3.3!} + \frac{h^2x^2}{3!} + O(h^4) \qquad : h \to 0^+$$

$$S_{10}(-ih,x) \sim 3^{1/2}.x.\left\{1 - \frac{3h^2}{50} + \frac{h^2x^2}{10} + O(h^4)\right\} \qquad : h \to 0^+$$

$$S_{11}(-ih,x) \sim \left\{\frac{3}{2}(1-x^2)\right\}^{1/2}\left\{1 - \frac{h^2}{50} + \frac{h^2x^2}{10} + O(h^4)\right\} \qquad : h \to 0^+$$

By inserting the above forms into equations (2.c. 10-13) we can evaluate the corresponding eigenvalues in this limit as:

$$\lambda_{oo}(h,\cosh\mu) = \frac{\sinh K}{K}\left(1 - \frac{h^2}{3K} + \frac{h^2}{3K^2} + O(h^4)\right) \qquad : h \to 0^+$$

$$\lambda_{10}(h,\cosh\mu) = U(K)\frac{\sinh K}{K}\left(1 - \frac{h^2}{5K} + \frac{2h^2}{5K^2} + O\left(\frac{h^2}{K^3}\right) + O(h^4)\right) \qquad : h \to 0^+$$

$$\lambda_{11}(h,\cosh\mu) = \tanh\mu.U(K).\frac{\sinh K}{K}.\left(1 - \frac{2h^2}{5K} + \frac{4h^2}{5K^2} + O\left(\frac{h^2}{K^3}\right) + O(h^4)\right) \qquad : h \to 0^+$$

$$U(K) \equiv \coth K - 1/K$$

Thus, well above crossover, the inverse correlation lengths are given exactly by:

$$K_{/\!/}(h,\cosh\mu) \sim \frac{1}{K} - \frac{2h^2}{15K} + O(1/K^2) \qquad : h \to 0^+ \qquad (2.f.1)$$

$$K_{\perp}(h,\cosh\mu) \sim \frac{1}{K} + \frac{1}{15}\frac{h^2}{K} + O(1/K^2) \qquad : h \to 0^+ \qquad (2.f.2)$$

ii) Well Below Crossover ($T \ll T_x$; $h \gg 1$)

Well below crossover, successive approximations to the eigenfunctions and eigenvalues of (2.b. 4) may be obtained by iterating equations such as (2.c. 2-4) from the 'seed' functions:

$$S_{oo}^{(o)}(-ih, x) = \delta(x-1) + \delta(x+1)$$

$$S_{1o}^{(o)}(-ih, x) = \delta(x-1) - \delta(x+1)$$

$$S_{11}^{(o)}(-ih, x) = (1-x^2)^{\frac{1}{2}} \cosh hx$$

Hence using equations (2.c. 2-3) and (2.c. 5-6) we have:

$$K_{//}^{(1)}(h, \cosh\mu) = \ln\left\{\frac{\lambda_{oo}(h, \cosh\mu)}{\lambda_{1o}(h, \cosh\mu)}\right\} \simeq \frac{4e^{-2h}}{\cosh\mu} \quad : h \gg 1$$

$$K_{//}^{(2)}(h, \cosh\mu) = \ln\left\{\frac{\lambda_{oo}(h, \cosh\mu)}{\lambda_{1o}(h, \cosh\mu)}\right\} \simeq \frac{8he^{-2h}}{\cosh\mu} \quad : h \gg 1$$

$$K_{//}^{(3)}(h, \cosh\mu) = \ln\left\{\frac{\lambda_{oo}(h, \cosh\mu)}{\lambda_{1o}(h, \cosh\mu)}\right\} \simeq \frac{16he^{-2h}}{\cosh\mu} \quad : h \gg 1 \qquad (2.f.3)$$

Unfortunately, it proved extremely difficult to go beyond one iteration for the third eigenvalue. However, using our optimum expressions for λ_{oo} viz:

$$\lambda_{oo}^{(3)}(h, \cosh\mu) = \frac{e^{K}}{2h(\cosh\mu + 1)}\left\{1 + \frac{1}{2K} + O\left(\frac{1}{K^2}\right)\right\}$$

— INSERT —

To be specific, figure #6 shows a plot of both the longitudinal and transverse inverse correlation lengths obtained from the iteration scheme via:

$$K_{\parallel}(h,\cosh\mu) = \ln\left\{\frac{\lambda_{00}^{(3)}}{\lambda_{10}^{(3)}}\right\} \quad : \quad K_{\perp}(h,\cosh\mu) = \ln\left\{\frac{\lambda_{00}^{(3)}}{\lambda_{\parallel}^{(3)}}\right\}$$

where:

$$\lambda_{00}^{(3)}(h,\cosh\mu) = \frac{1}{S_{00}^{(3)}(-ih,1)} \int_0^1 dx \cosh kx \; S_{00}^{(3)}(-ih,x)$$

$$\lambda_{10}^{(3)}(h,\cosh\mu) = \frac{1}{S_{10}^{(3)}(-ih,1)} \int_0^1 dx \sinh kx \; S_{10}^{(3)}(-ih,x)$$

$$\lambda_{\parallel}^{(1)}(h,\cosh\mu) = \frac{k.\tanh\mu}{2 f_{\parallel}^{(1)}(-ih,1)} \int_0^1 dx \; (1-x^2) \cosh kx \; f_{\parallel}^{(1)}(-ih,x)$$

and;

$$S_{00}^{(3)}(-ih,x) = \frac{1}{h}\int_0^{2h} dz \cosh[x(z-h)] \frac{\sinh z}{z}$$

$$S_{10}^{(3)}(-ih,x) = \frac{1}{h}\int_0^{2h} dz \sinh[x(z-h)] \frac{\sinh z}{z}$$

$$f_{\parallel}^{(1)}(-ih,x) = \frac{\cosh h(1+x)}{h^2(1+x)^2} + \frac{\cosh h(1-x)}{h^2(1-x)^2}$$

$$- \frac{\sinh(h(1+x)}{h^3(1+x)^3} - \frac{\sinh h(1-x)}{h^3(1-x)^3}$$

Well above crossover ($h \to 0^+$) the forms above reduce to the exact results (2.f.1-2) of the text.

we have been able to obtain:

$$K_{\perp}^{(0)}(h,\cosh\mu)=\ln\left\{\frac{\lambda_{00}^{(3)}(h,\cosh\mu)}{\lambda_{11}^{(0)}(h,\cosh\mu)}\right\}\simeq\frac{1}{2}.\ln\left\{\frac{\cosh\mu+1}{\cosh\mu-1}\right\}+\frac{3}{2K}\quad:h\gg1$$

$$K_{\perp}^{(1)}(h,\cosh\mu)=\ln\left\{\frac{\lambda_{(11)00}^{(3)}(h,\cosh\mu)}{\lambda_{11}(h,\cosh\mu)}\right\}\simeq\frac{1}{2}.\ln\left\{\frac{\cosh\mu+1}{\cosh\mu-1}\right\}-\frac{1}{2K}\quad:h\gg1$$

(2.f.4)

Figure 6 shows these results in graphical form.
[Please see insert to left].

Equations (2.f. 3-4) are the main results which we set out to obtain in this chapter. Before we go on to use them to analyse the two- and three-dimensional counterparts of this model, we compare our results with those of other authors. Finally, for completeness, we obtain approximate forms for the susceptibility of the one-dimensional system and show how all these results are modified in the presence of dilution.

The uniaxially anisotropic classical Heisenberg chain has been investigated by many other authors. Satija (1980) mapped the statistical mechanical problem defined by the Hamiltonian (2.a. 1) onto a quantum field theory to obtain:

$$K_{//}\sim\begin{cases}\frac{1}{K}\left(1-\frac{2h^2}{15}\right) & :h\ll1\\ \frac{c_0}{\cosh\mu}he^{-2h} & :h\gg1\end{cases}$$

$$K_{\perp}\sim\begin{cases}\frac{1}{K}\left(1+\frac{1}{15}.h^2\right) & :h\ll1\\ 1/\cosh\mu & :h\gg1\end{cases}$$

These results agree with equations (2.f. 1-4) except in the value of c_0 . Satija estimated this constant to be of order of

7.5 whereas our iteration scheme suggests a value nearer 16.

Nakamura and Sasada (1978) employed a functional approach to obtain the following forms well below crossover ($h \gg 1$):

$$K_{/\!/} \sim \frac{c_o}{\cosh\mu} e^{-2h}$$

$$K_{\perp} \sim \frac{1}{\cosh\mu}\left(1 - \frac{1}{2h}\right)$$

This expression for the transverse inverse correlation length agrees with equation (2.f. 4). Its longitudinal counterpart differs from our result (2.f. 3) in the exponential prefactor, where we obtain a factor of h.

Faria and Pires (1978) used an expansion of the spheroidal wave functions and radial functions in terms of Legendre and Bessel functions respectively to obtain:

$$K_{/\!/} \sim c_o h e^{-2h}$$

well below crossover. Again, our result differs, this time by a factor $1/\cosh\mu$, with the exponential prefactor.

Feigel'man (1976) used a transfer matrix method to obtain·

$$K_{/\!/} \sim \frac{4}{\cosh\mu} . e^{-2h}$$

$$K_{\perp} \sim \frac{1}{\cosh\mu}$$

The same type of result was obtained by Stinchcombe (1980) using an approximate decimation procedure. As with the results of Nakamura and Sasada, we disagree by a factor of h.

Our numerical results compare well with those of Loveluck et al. (1975) and McGurn & Scalapino (1975) in the appropriate limits.

All the authors above agree on the exponential form of the longitudinal correlation length well below crossover, and on the finite but anisotropy dependent form of the transverse correlation length in the same limit. We feel that the exponential prefactor in the longitudinal correlation length is of the form given by Satija and ourselves since the iteration scheme produced the other results as lower approximations. Figure 7 shows the results of our scheme for the case of $\cosh\mu = 8.3$. This is of particular interest as it can be compared with the numerical work of Blume et al. (1975) which was used by Birgeneau et al. (1980) in their interpretation of experimental data from neutron scattering from $Rb_2Mn_pMg_{1-p}F_4$ systems.

Equations (2.f. 3-4) also allow us to obtain an approximate expression for the wave-vector dependent susceptibility of the weakly anisotropic Heisenberg chain, viz:

$$\chi_{/\!/}(q) = \frac{1}{Nk_BT}\sum_{\langle i,j\rangle} e^{iq\cdot(r_i - r_j)} \langle \sigma_i^z \sigma_j^z \rangle \qquad (2.f.5)$$

$$\chi_{\perp}(q) = \frac{1}{Nk_BT}\sum_{\langle i,j\rangle} e^{iq\cdot(r_i - r_j)} \langle \sigma_i^x \sigma_j^x \rangle \qquad (2.f.6)$$

Well below crossover ($h \gg 1$) equations (2.b. 13-14) may be approximated by:

$$\langle \sigma_i^z \sigma_j^z \rangle = \sum_{p\,odd} \left(\frac{\lambda_{p,o}(h,\cosh\mu)}{\lambda_{o,o}(h,\cosh\mu)}\right)^{|i-j|} D_p(h) \sim \left(\frac{\lambda_{1,o}(h,\cosh\mu)}{\lambda_{o,o}(h,\cosh\mu)}\right)^{|i-j|} D_1(h)$$

$$\langle \sigma^x \sigma_j^x \rangle = \sum_{p\,odd} \frac{1}{2}\left(\frac{\lambda_{p,1}(h,\cosh\mu)}{\lambda_{o,o}(h,\cosh\mu)}\right)^{|i-j|} E_p(h) \sim \left(\frac{\lambda_{11}(h,\cosh\mu)}{\lambda_{oo}(h,\cosh\mu)}\right)^{|i-j|} \frac{E_1(h)}{2}$$

since λ_{oo}, λ_{1o} and λ_{11} are so much larger than the rest of the eigenvalue spectrum. The accuracy of this approximation is rapidly enhanced with increasing spin seperation, so that for long wavelength

correlations well below crossover we expect this to be a very good approximation.

The approximation above is exact in the Isotropic Heisenberg limit (h=0). Thus, by substituting the above two forms into our expressions for the two wave-vector dependent susceptibilities (2.f. 5-6) we obtain approximate forms for these which are exact well above crossover, asymptotically exact for small q below crossover and provide a useful interpolation between these two regimes viz:

$$\langle \sigma_i^z \sigma_j^z \rangle \simeq \left(\frac{\lambda_{o1}(h,\cosh\mu)}{\lambda_{oo}(h,\cosh\mu)} \right)^{|i-j|} D_1(h) = e^{-|i-j| K_{/\!/}(h,\cosh\mu)} D_1(h)$$

$$\langle \sigma_i^x \sigma_j^x \rangle \simeq \frac{1}{2} \left(\frac{\lambda_{11}(h,\cosh\mu)}{\lambda_{oo}(h,\cosh\mu)} \right)^{|i-j|} E_1(h) = e^{-|i-j| K_{\perp}(h,\cosh\mu)} E_1(h)$$

so that:

$$\chi_{/\!/}(q) \simeq \frac{D_1(h)}{k_B T} \cdot \left(\frac{1 - e^{-2K_{/\!/}}}{1 + e^{-2K_{/\!/}} - 2e^{-K_{/\!/}} \cos q} \right) \qquad (2.f.7)$$

$$\chi_{\perp}(q) \simeq \frac{E_1(h)}{2k_B T} \cdot \left(\frac{1 - e^{-2K_{\perp}}}{1 + e^{-2K_{\perp}} - 2e^{-K_{\perp}} \cos q} \right) \qquad (2.f.8)$$

The functions $D_1(h)$ and $E_1(h)$ may be estimated by substituting the approximate eigenfunctions obtained from the iteration scheme into equations (2.b. 15) and (2.b. 16). In this manner we obtain:

$$D_1(h) \sim \begin{cases} 1 & ; h \gg 1 \\ 1/3 & ; h \ll 1 \end{cases}$$

$$E_1(h) \sim \begin{cases} 1/h & ; h \gg 1 \\ 2/3 & ; h \ll 1 \end{cases}$$

The small q limit for the wave-vector dependent susceptibility of the weakly anisotropic Heisenberg chain is then given by:

(a) Well Above Crossover

$$\chi_{\parallel}(q) \sim \chi_{\perp}(q) \sim \frac{1}{3}\frac{1}{k_B T}\left(\frac{2K_{\parallel,\perp}}{K_{\parallel,\perp}^2 + q^2}\right) \qquad \left\{\begin{matrix} K_{\parallel}, K_{\perp} \ll 1 \\ q \ll 1 \\ h \to 0^+ \end{matrix}\right\}$$

(b) Well Below Crossover

$$\chi_{\parallel}(q) \sim \frac{1}{k_B T}\left(\frac{2K_{\parallel}}{K_{\parallel}^2 + q^2}\right)$$

$$\chi_{\perp}(q) \sim \frac{\cosh\mu}{2J}\left(\frac{2K_{\perp}}{K_{\perp}^2 + q^2}\right) \qquad \left\{\begin{matrix} K_{\parallel}, K_{\perp} \ll 1 \\ q \ll 1 \\ h \gg 1 \end{matrix}\right\}$$

Equations (2.f. 7-18) agree exactly with the results of Thorpe (1975) in the Isotropic Heisenberg limit, where:

$$D_1(0) = \frac{E_1(0)}{2} = \frac{1}{3}$$

In the next section we show how the effects of dilution may be incorporated into our treatment of the anisotropic chain.

g) The Dilute, Weakly Anisotropic Heisenberg Chain.

If the spins at a fraction (1-p) of the sites in the chain are removed at random, the probability of n consecutive sites being occupied is just p^n. Hence, the spin-spin correlation function in the dilute chain is given by:

$$\langle \sigma_i^{\alpha} \sigma_j^{\alpha} \rangle_{\text{dilute}} = p^{|i-j|+1} \langle \sigma_i^{\alpha} \sigma_j^{\alpha} \rangle_{\text{pure}} \qquad (2.g.1)$$

where $\langle \sigma_i^{\alpha} \sigma_j^{\alpha} \rangle_{pure}$ is given by either (2.b. 13) or (2.b. 14). Using (2.b. 17) and (2.b. 18) to obtain the corresponding expressions for the long wavelength behaviour of the correlation length gives:

$$K_{//,\perp}(h,\cosh\mu,p) = K_{//,\perp}(h,\cosh\mu,p=1) + \ln(1/p) \qquad (2.g.2)$$

This equation is exact. The inverse correlation lengths of the system are simply the sum of the pure thermal and percolative inverse correlation lengths. This sort of result will prove to be important in later Chapters (4,5) when we investigate analagous behaviour in higher dimensional systems. Thus, the fact that dilution prevents the divergence of thermodynamic functions in one-dimension is clearly illustrated by the finite, non-zero value of $K_{//}$ at absolute zero. Equation (2.g.2) also illustrates the idea of crossover from thermal to percolative behaviour which we discussed in the first chapter. If we start at the multicritical point (which in this one-dimensional system lies at T= 0, p= 1) and increase the temperature, the only contribution to the right-hand side of (2.g.2) is thermal since $\ln(1/p) = 0$. Alternatively, staying precisely at T= 0 but reducing p we see only percolative behaviour since the thermal contribution to the R.H.S of (2.g.2) is constant in such a process. At a general temperature and dilution, it is the competition between the two contributions in the R.H.S of(2.g.2) which gives rise to thermal/percolative crossover. Figure 8 shows the effect cf dilution on the inverse correlation lengths.

In a similar manner, the susceptibility of the dilute chain, within the approximation outlined in section f., becomes:

$$\chi_{//}(q,p) = \frac{D_1(h)}{k_B T}\left(\frac{1 - p^2 e^{-2K_{//}}}{1 + p^2 e^{-2K_{//}} - 2pe^{-K_{//}}\cos q}\right) \qquad (2.g.3)$$

$$\chi_{\perp}(q,p) = \frac{E_1(h)}{2k_B T}\left(\frac{1 - p^2 e^{-2K_{\perp}}}{1 + p^2 e^{-2K_{\perp}} - 2pe^{-K_{\perp}}\cos q}\right) \qquad (2.g.4)$$

At the isotropic Heisenberg limit, h= 0, we have:

$$\chi_{//}(q,p) = \chi_{\perp}(q,p) = \frac{1}{3k_B T}\left(\frac{1 - p^2 e^{-2K_{//}}}{1 + p^2 e^{-2K_{//}} - 2pe^{-K_{//}}\cos q}\right)$$

in complete agreement with Thorpe (1975).

Thus, at low temperature and small q:

$$\chi_{//}(q,p) \sim \frac{D_1(h)}{k_B T}\left\{\frac{1 - p^2 + 2p^2 K_{//}}{(1-p)^2 - 2p^2 K_{//} + 2pK_{//} - pq^2}\right\}$$

where, in all the above equations:

$$K_{//,\perp} \equiv K_{//,\perp}(h, \cosh\mu, p=1)$$

h) Summary.

The main aim of this chapter was to obtain approximate, but analytic, forms for the spin-spin correlation lengths in the one-dimensional anisotropic model. This was achieved in equations (2.f. 1-4).

We have also shown how approximate forms for the wave vector dependent susceptibilities of the anisotropic chain may be obtained as in equations (2.f. 7-8).

Lastly, we have shown how diluting the chain affects its correlation functions and susceptibilities.

In the next chapter we use the results obtained here to treat the pure, two-dimensional system.

Chapter 3

The Pure, Two-Dimensional System

a) Introduction

In the previous chapter we obtained approximate analytic expressions for the spin-spin correlation lengths of the Heisenberg chain with weak uniaxial exchange anisotropy. The present chapter uses these results to obtain information about the pure, two-dimensional, anisotropic system.

In Section (b) we introduce and discuss the Migdal/Kadanoff bond moving scheme.

In Section (c) we show how the results of Chapter 2 are combined with the bond moving scheme in order to obtain the transformation of the various parameters in the two-dimensional problem when the underlying length scales of the system are dilated by a factor b. The transformations so obtained are then used to derive limiting functional forms for the inverse correlation lengths and wavevector dependent susceptibilities of the two-dimensional system near criticality. The effect of the anisotropy upon the transition temperature is also investigated.

In Section (d) we compare the results of this chapter with those of previous authors and experiments.

To begin with, however, we introduce the approximation scheme which plays a central role in the in the rest of this and the following two chapters.

b) The Migdal/Kadanoff Bond Moving Scheme

In order to use the scaling ideas outlined in Chapter 1, we have first to be able to dilate the underlying length scales of the two-dimensional system by a factor, b. For the analagous one-dimensional system, this could be carried out in a variety of ways. For instance, a trace could be taken over alternate spins of the chain (Figure 9). This 'decimation' process leaves the partition function for the system unaltered but changes the length scale of the system by a factor b = 2. The accompanying change in the spin-spin couplings gives the transformation for the Hamiltonian parameters under the length scale dilation. Alternatively, the same transformations could be obtained by evaluating the spin-spin correlation lengths (as we did in Chapter 2) and simply dividing by a factor of b = 2. Unfortunately, the situation in two dimensions is more complex. Unlike the one-dimensional case, it is extremely difficult to calculate the spin-spin correlation lengths ab initio. Furthermore, taking the trace over some subset of spins, or decimating, is not directly applicable either, since the increased connectivity of two-dimensional lattices introduces new couplings into the problem. For example, in the square lattice, each spin has four nearest neighbours. If the spins interact with nearest neighbours only, taking the trace over one spin introduces next nearest neighbour interactions. (Figure 10). As a result, the system we obtain after decimation is not of the same type as we started from. In the terminology of the renormalisation group (Ma (1976)) we have had to increase the dimensionality of our parameter space. Each subsequent length dilation brings higher order couplings into existence and so renders this approach extremely difficult.

In order to combat the problems outlined above, Migdal (1976) and Kadanoff (1976) suggested an approximation scheme in which the interactions or 'bonds' between spins were moved so that decimation could be carried out along one of the lattice axes without introducing higher order couplings. The bond movements involved for a length scale dilation by a factor b = 2 on a square lattice are shown in Figures 11 (a-d). For the sake of notation, the x and y axes are taken to coincide with the directions of the primitive vectors for the square lattice (Fig. 11(a)). The first step of the approximation scheme consists of moving alternate bonds lying perpendicular to the y axis as shown in Figure 11(b). This leaves a subset of the spins (those marked with a cross) with only two nearest neighbour interactions. It is then possible to take the trace over these spins without introducing higher order couplings. The parameter transformations brought about by such a decimation are just those we obtained in Chapter 2 since the weak links coupling the double bonds are merely short, one-dimensional chains. (e.g. the link A-B-C in fig. 11(b)). The resultant system (fig. 11 (c)) has the length scales in the y-direction dilated by a factor b = 2. In order to dilate length scales in the x-direction by the same factor we simply rotate the whole system through $\pi/2$ and repeat the process above. The nett result is a dilation of the underlying, characteristic length scales in the two-dimensional system by a factor b = 2. Although only an approximation, Kadanoff (1976) has suggested that the scheme becomes asymptotically exact in the limit of strong coupling near the lower critical dimensionality. However, our strongest justification for applying the scheme to the anisotropic Heisenberg model is that it is known to give the correct leading

order behaviour for the thermal parameters in both the isotropic Heisenberg and Ising limits.

Before moving on to discuss the effect of the bond moving scheme on a single bond, we pause to point out two further problems with this approximation. Firstly, it effectively sets the critical exponent η to zero. This problem is inherent in the decimation part of the scheme (Kadanoff (1976)). Secondly, the bond combination and decimation processes from which the scheme is built up, do not commute. This latter problem is, however, far less serious and as pointed out by Kirkpatrick (1977) may be overcome by taking the infinitesimal limit of the length dilation factor:

$$b = 1 + \epsilon \qquad \epsilon \ll 1 \qquad (3.b.1)$$

in which case the two component operations commute to $O(\epsilon)$.

In the following section we employ the M-K scheme and the one-dimensional results of the previous chapter to investigate the pure, two-dimensional, anisotropic system. Before leaving this discussion of the M-K scheme, however, we should mention that Martinelli and Parisi (1981) have recently taken an entirely different view of the M-K scheme in which it contributes only the zeroth order term to an expansion in the 'small' quantity:

$$\delta \equiv (1 - \text{fraction of bond moved}).$$

c) Application Of The Migdal/Kadanoff Scheme To The Pure, Two-Dimensional System.

As we pointed out at the end of the previous section, the effect of the M-K scheme on a single bond may be viewed as the result of two distinct operations. Under the first of these operations,

(cf. the trace over spin B in fig. 11(b)), the bond parameters transform in the same way as the parameters of the one-dimensional model considered in Chapter 2 under dilation by a factor b. This part of the transformations may be obtained by noting that under such a dilation the inverse correlation lengths (I.C.L.) of the one-dimensional problem scale as:

$$\mathcal{D}_b : K_\perp(h,\Theta) \longrightarrow K'_\perp(h,\Theta) = bK_\perp(h,\Theta)$$

$$\mathcal{D}_b : K_{/\!/}(h,\Theta) \longrightarrow K'_{/\!/}(h,\Theta) = bK_{/\!/}(h,\Theta)$$

where the operator $\mathcal{D}_b$ represents dilation of the chain by a factor b, and we have defined the variable:

$$\Theta \equiv \frac{1}{2} \ln\left(\frac{\cosh\mu + 1}{\cosh\mu - 1}\right) \qquad (3.c.1)$$

Since the system is of the same type before and after the dilation, these equations may be simplified to:

$$K'_\perp(h,\Theta) = K_\perp(h',\Theta') = bK_\perp(h,\Theta) \qquad (3.c.2)$$

$$K'_{/\!/}(h,\Theta) = K_{/\!/}(h',\Theta') = bK_{/\!/}(h,\Theta) \qquad (3.c.3)$$

Here the change in the underlying length scales has been reinterpreted as a set of parameter transformations.

For the Ising model, where both Θ and $K_{/\!/}$ diverge, equation (3.c.3) becomes (cf. eqn. (2.d.1)):

$$K^{ISING}(h',\Theta') \simeq 8h'e^{-2h'} = b.8he^{-2h} = bK^{ISING}_{/\!/}(h,\Theta)$$

whence:

$$h' \simeq h - \frac{1}{2}\ln b \qquad (\Theta \to \infty) \qquad (3.c.4)$$

For the isotropic Heisenberg model (where $K_{\perp}^{HEIS.} \equiv K_{/\!/}^{HEIS} \equiv K^{HEIS}$) equations (3.c. 2-3) become (cf. eqn. (2.e.1)):

$$K^{HEIS.}(h',\Theta') = \frac{\Theta'}{h'} = \frac{b\Theta}{h} = bK^{HEIS}(h,\Theta) \qquad (3.c.5)$$

For the weakly anisotropic Heisenberg chain well below crossover ($h \gg 1 : 0 < \Theta \ll 1$) equations (3.c. 2-3) become (cf. eqns. (2.f. (3-4)):

$$K_{\perp}(h',\Theta') \simeq \Theta'\left(1 - \frac{1}{2h'}\right) = b\Theta\left(1 - \frac{1}{2h}\right) \simeq bK_{\perp}(h,\Theta)$$

$$K_{/\!/}(h',\Theta') \simeq 16.h'.\Theta'.e^{-2h'} = b\,16\,h\Theta e^{-2h} \simeq bK_{/\!/}(h,\Theta)$$

so that

$$\left.\begin{aligned}\Theta' &\simeq b\Theta \\ h' &\simeq h\end{aligned}\right\} \quad (h \gg 1 ; 0 < \Theta \ll 1) \qquad (3.c.6)$$

whereas, for the weakly anisotropic Heisenberg chain well above crossover ($h \ll 1 ; 0 < \Theta \ll 1$) equations (3.c. 2-3) become (cf. eqns. (2.f. 1-2)):

$$K_{\perp}(h',\Theta') \simeq \frac{\Theta'}{h'}\left(1 + \frac{1}{15}.h'^{2}\right) = b.\frac{\Theta}{h}\left(1 + \frac{1}{15}.h^{2}\right) = bK_{\perp}(h,\Theta)$$

$$K_{/\!/}(h',\Theta') \simeq \frac{\Theta'}{h'}\left(1 - \frac{2}{15}h'^{2}\right) = b.\frac{\Theta}{h}.\left(1 - \frac{2}{15}.h^{2}\right) = bK_{/\!/}(h,\Theta)$$

Thus, under a length dilation by a factor b the approximate transformations for the weakly anisotropic system well above crossover are:

$$\left.\begin{aligned}\Theta' &= b\Theta \\ h' &= h\end{aligned}\right\} \quad (h \ll 1 ; 0 < \Theta \ll 1). \qquad (3.c.7)$$

The transformations in equations (3.c. 4-7) may be combined into the

approximate expressions:

$$\left.\begin{aligned} \Theta' &= b\Theta \\ h' &= h - \frac{1}{2}\ln b.\tanh\Theta \end{aligned}\right\} \quad (3.c.8)$$

Of course, in theory we could write the exact transformations down but this would require a complete knowledge of the I.C.L. forms for general anisotropy and temperature. However, our approximate transformations (3.c. 8) certainly contain both the Ising and isotropic Heisenberg limits exactly and are compatible with our expressions for the weakly anisotropic system. Our strongest justification for using these forms (3.c. 8) is provided a posterii by our later results.

Expressions (3.c. 8) are the final transformation equations for the bond parameters h and Θ under the first step of the M-K scheme: the dilation of the corresponding one-dimensional system by a factor of b.

The second, and final, step of the M-K scheme involves the combination of bonds (cf. bonds. A-D and B-E in figs. 11(a) and 11(b)). 'in parallel'. Such an operation leaves the anisotropy parameter unaltered but multiplies the interaction strengths (J) by a factor b. Under this operation, the parameters h and Θ scale as:

$$\left.\begin{aligned} h'' &= bh' \\ \Theta'' &= \Theta \end{aligned}\right\} \quad (3.c.9)$$

Combining equations (3.c. 8-9), we obtain the parameter transformations under dilation of the two-dimensional system by a factor b as:

$$h'' = b.h' = b[h - \tfrac{1}{2}.\ln b.\tanh\Theta]$$

$$\Theta'' = \Theta' = b\Theta$$

Taking the limit of:

$$b = 1 + \epsilon \quad ; \quad \epsilon \ll 1$$

(cf. the discussion leading up to (3.b.1)) and discarding terms of $0(\epsilon^2)$:

$$\left.\begin{aligned} h'' &= (1+\epsilon)h - \frac{\epsilon}{2}\tanh\Theta \\ \Theta'' &= (1+\epsilon)\Theta \end{aligned}\right\} \quad (3.c.10)$$

Thus, by combining the results of Chapter 2 (on the dilation of the one-dimensional system) with the M-K bond moving scheme, we have obtained expressions (3.c. 10) for the transformations of the two parameters in the two-dimensional system under an infinitesimal dilation of the characteristic length scales by a factor $b = 1 + \epsilon$ With the aid of these transformations (3.c. 10) or modified forms of them, we can determine the limiting forms of various statistical mechanical properties such as inverse correlation lengths and wavevector dependent susceptibilities. It is, however, convenient to first find a 'scaling' function:

$$u \equiv u(h,\Theta)$$

such that under the transformations (3.c. 10), u transforms as:

$$\begin{aligned} u''(h,\Theta) \equiv u(h'',\Theta'') &= bu(h,\Theta) \\ &= (1+\epsilon)u(h,\Theta) \end{aligned} \quad (3.c.11)$$

By looking for solutions of (3.c. 11) of the form:

$$u(h,\Theta) \equiv h + f(\Theta)$$

we obtain:

$$f(\Theta) \equiv \frac{\Theta}{2}\left\{\int_1^{\Theta} \frac{\tanh x}{x^2}\, dx + k_o\right\}$$

where k_o is an undetermined constant which can be chosen conveniently . (Since u and Θ are scaling functions, so is any fixed linear combination of them.) Thus, our transformations (or scaling equations) become:

$$\left.\begin{aligned} \Theta'' &= (1+\epsilon)\Theta \\ u'' &= (1+\epsilon)u \end{aligned}\right\} \quad (3.c.12)$$

with:

$$\Theta \equiv \frac{1}{2}\ln\left(\frac{\cosh\mu + 1}{\cosh\mu - 1}\right)$$

$$u \equiv h - \frac{\Theta}{2}\int_{\Theta}^{\infty} \frac{\tanh x}{x^2}\, dx \qquad (3.c13)$$

(employing here and hereafter a particular choice of k_o .)
In the following two subsections we set about the task of determining the forms of the I.C.L's and wavevector dependent susceptibilities of the two-dimensional model using equations (3.c. 12).

.i) Inverse Correlation Length (I.C.L.) Behaviour In The Two-Dimensional Anisotropic System.

Both I.C.L's of the two-dimensional system will be functions of the two parameters (h,Θ) or equivalently, (Θ,u). Using the latter parameterisation:

$$K_{//,\perp} \equiv K_{//,\perp}(\Theta, u) \qquad (3.c.14)$$

where, as in the one-dimensional case, the subscripts $\perp$ and $//$ refer to spin components perpendicular or parallel to the easy axis. Dilating the length scales of the lattice by a factor b results in the following transformations:

$$\Theta \rightarrow \Theta' = b\Theta$$

$$u \rightarrow u' = bu$$

$$K_{\perp,//} \rightarrow K'_{\perp,//} = bK_{\perp,//}$$

The first two equations follow directly from equations (3.c. 12) whereas the third is just a restatement of the fact that spin-spin correlation lengths constitute the characteristic length scales of the system near criticality.

Since the system we are left with after dilation is of the same type as that which we started from, the last equations (3.c. 14) may be rewritten as:

$$K'_{\perp,//}(\Theta, u) = K_{\perp,//}(\Theta', u') = K_{\perp,//}(b\Theta, bu)$$

$$= bK_{\perp,//}(\Theta, u)$$

Thus, $K_\perp$ and $K_{//}$ are both homogeneous functions of degree one in Θ and u. Substituting $b = \Theta^{-1}$ in the last equality we obtain:

$$K_{\perp,//}(\Theta, u) = \Theta\, \Phi_{\perp,//}(u/\Theta) \qquad (3.c.15)$$

where:

$$\Phi_{\perp,//}(x) \equiv K_{\perp,//}(1,x)$$

In order to obtain more information about the functions $\Phi_{\perp,//}(x)$ in equation (3.c. 15) we have to consider various limits of the parameters Θ and u (or h).

α) The Ising Limit.

In this limit we have:

$$h(=K) \gg 1$$
$$\Theta \to \infty$$

so that using (3.c. 13) the variable u becomes:

$$u \sim h - \frac{\Theta}{2}\int_{\Theta}^{\infty} \frac{dx}{x^2}$$

$$\sim h - \frac{1}{2}$$

and

$$K_{//}^{ISING}(\Theta,u) = \Theta\,\Phi_{//}(u/\Theta)$$

If $K_{//}^{ISING}$ is to be finite and non-zero over any temperature range we must have:

$$\lim_{|x|\to 0^+} \Phi_{//}(x) = a_0|x| \qquad (3.c.17)$$

where a_0 is an undetermined constant, so that the prefactor Θ in expression (3.c. 15) for $K_{//}^{ISING}$ cancels to leave a finite result.

Thus, in the Ising Limit, the longitudinal I.C.L. has the form:

$$K_{//}^{ISING}(h, \Theta \to \infty) = a_0 |K - K_c^{ISING}| \qquad (3.c.18)$$

where $K_c^{ISING} = 1/2$

The expression (3.c. 18) has a zero at $K = K_c$ which we interpret as the occurrence of a second order phase transition at temperature:

$$T_c^{ISING} = \frac{2J}{k_B}$$

Although the value of T_c^{ISING} is not reliable, since we previously restricted our analysis to the regime:

$$K \equiv \frac{J}{k_B T} \gg 1 \qquad [\text{cf. eqn. (2.c.1)}]$$

the qualitative behaviour of expression (3.c. 18) is correct (viz. power law decay to a finite temperature transition with exponent equal to unity). [Montrell, Potts and Ward (1963)] .

β) The Isotropic Heisenberg Limit.

In this limit we have:

$$\left.\begin{array}{l} h \to 0^+ \\ \Theta \to 0^+ \end{array}\right\} h/\Theta = K \gg 1$$

$$u = h - \frac{\Theta}{2}\int_{\Theta}^{\infty} dx \, \frac{\tanh x}{x^2} \sim h + \frac{1}{2}\Theta \ln \Theta + O(\Theta)$$

Thus:

$$K_{//}^{HEIS.}(\Theta, u) - K_{\perp}^{HEIS}(\Theta, u) = \Theta \, \Phi_{\perp,//}(u/\Theta)$$

$$= \Theta \, \Phi_{\perp,//}\left(K + \tfrac{1}{2}\ln\Theta + O(1)\right)$$

In order that $K^{HEIS}_{//,\perp}$ be finite but non-zero over any temperature range yet independent of Θ we must have:

$$\lim_{x \to -\infty} \Phi_{//}(x) = \lim_{x \to -\infty} \Phi_{\perp}(x) = C_0 e^{-2x} \qquad (3.c.19)$$

Thus, the I.C.L. of the isotropic Heisenberg model must vary as:

$$K^{HEIS}(\Theta, u) = C_0 e^{-2K} \qquad (3.c.20)$$

The exponential decay of K^{HEIS} to zero at absolute zero temperature is in qualitative agreement with the exact result of Polyakov (1975) although the exponent in (3.c. 20) differs from that of Polyakov by a factor of π .

By considering the isotropic Heisenberg and Ising limits of equation (3.c. 15) we have obtained sufficient information about the functions $\Phi_{//,\perp}(x)$ to be able to treat the weakly anisotropic system.

γ.) The Weakly Anisotropic Heisenberg Model.

In the weakly anisotropic limit of the Heisenberg model we have:

$$0 < \Theta \sim \frac{1}{\cosh \mu} \ll 1$$

but the variable h may vary from small to large values. To treat these two limits we rewrite:

$$u(h,\Theta) \equiv h - \frac{\Theta}{2} \int_{\Theta}^{\infty} dx \, \frac{\tanh x}{x^2} \equiv h - h_c(\Theta) \qquad (3.c.21)$$

where:

$$h_c(\Theta) \equiv \frac{\Theta}{2} \int_{\Theta}^{\infty} dx \, \frac{\tanh x}{x^2} \qquad (3.c.22)$$

The corresponding expressions (3.c. 15) for the I.C.L.'S of the weakly anisotropic model become:

$$K_{//,\perp}(u, 0<\Theta\ll 1) = \Theta \oint_{//,\perp} \left(\frac{h-h_c(\Theta)}{\Theta}\right)$$

Within the regime:

$$x \equiv \left|\frac{h-h_c(\Theta)}{\Theta}\right| \ll 1$$

we may use (3.c. 17) to obtain:

$$K_{//}(u, 0<\Theta\ll 1) \sim |h-h_c(\Theta)| \quad :\{|h-h_c(\Theta)| \ll \Theta\} \qquad (3.c.23)$$

This expression has a zero at $h = h_c(\Theta)$ which we interpret as being a second order phase transition. Thus, for the weakly anisotropic Heisenberg system in two dimensions our transformations predict:

$$\frac{1}{T_c(\Theta)} = \frac{k_B}{J}\cdot\cosh\mu\cdot h_c(\Theta) \sim \frac{k_B}{2J}\cdot\int_{\Theta}^{\infty} dx\cdot\frac{\tanh x}{x^2}$$

$$\sim \frac{k_B}{2J}\{\ln(1/\Theta) + O(1)\}$$

so that;

$$T_c(\Theta) \sim \frac{2J}{k_B \ln(1/\Theta)} \qquad \Theta \ll 1 \qquad (3.c.24)$$

Equation (3.c. 24) is in qualitative agreement with an R.P.A. treatment of the same system.

In fact, the parameterisation (3.c. 21) and the subsequent identification of $h = h_c(\Theta)$ as the value of h at which a second order phase transition takes place is valid for all values of the anisotropy due to the form of $\Phi_{//}(x)$ as $|x|$ tends to zero[cf. eqn. (3.c. 17)] .

Thus, in general we have:

$$\frac{1}{T_c(\Theta)} = \frac{k_B}{2J}.\Theta.\cosh\mu.\int_{\Theta}^{\infty} dx.\frac{\tanh x}{x^2} \quad : \quad (3.c.25)$$

Figure 12 shows a plot of the transition temperature as a function of the parameter δ occuring in equation (1.c.1).

Within the regime

$$\frac{h_c(\Theta) - h}{\Theta} \gg 1$$

we may use the asymptotic form of $\Phi_{//,\perp}(x)$ given in equation (3.c. 19) to obtain the I.C.L. behaviours well above the critical temperature viz:

$$K_{//}(u, 0<\Theta\ll 1) \sim K_{\perp}(u, 0<\Theta\ll 1) \qquad (3.c.25a)$$

$$\sim C_0\Theta e^{-\frac{2}{\Theta}(h-h_c(\Theta))} \quad : \{h_c(\Theta) - h \gg \Theta\}$$

In the case of the weakly anisotropic system this reduces to:

$$K_{//} \sim K_{\perp} \sim C' e^{-2K} : \left\{ \frac{h_c(\Theta) - h}{\Theta} \gg 1 \right\} : (3.c.26)$$

From the aforegoing discussion we conclude that it is the variable:

$$x \equiv \left| \frac{h - h_c(\Theta)}{\Theta} \right| \qquad (3.c.27)$$

which determines whether the two-dimensional system is well above ($x \gg 1$) or well below ($x \ll 1$) crossover.

So far, we have determined the forms of the longitudinal I.C.L. well below crossover (eqn. (3.c. 23)) and well

above crossover for temperatures greater than the critical temperature (3.c. 26). We have also determined the form of the transverse I.C.L. well above crossover for temperatures greater than the critical temperature (3.c. 26). To determine the asymptotic form of the transverse I.C.L. well below crossover, we note that in this limit the variable

$$X \equiv \left| \frac{h - h_c(\Theta)}{\Theta} \right|$$

tends to zero in equation (3.c. 15). In order that $K_\perp$ remain finite but non-zero in this limit we must have:

$$\lim_{|x| \to 0^+} \Phi_\perp(x) = \alpha_0$$

where α_0 is a constant.

Thus:

$$\lim_{|x| \to 0^+} K_\perp = \alpha_0 \Theta \qquad (3.c.28)$$

Unfortunately, the scheme outlined above gives no information about the behaviour of $\Phi_{//,\perp}(x)$ for x large and positive (well above crossover with temperatures much less than the critical temperature). However, if we assume that $\Phi_{//,\perp}(x)$ are functions of the modulus of x in the large x limit (as they are in the limit $|x| \to 0^+$) we obtain the qualitative picture sketched in figure 13. For regions in which the variable x in equation (3.c. 27) is very much greater than unity, the behaviour of the system is typically Heisenberg-like. For regions in which the variable x is much less than unity, the behaviour is typically Ising-like. This information enables us to estimate the two crossover temperatures of the two-

dimensional system through the implicit equation:

$$X_x \equiv \left| \frac{h - h_c(\Theta)}{\Theta} \right|_{T_x} \sim 1 \qquad (3.c.29)$$

Having obtained the limiting forms for the two I.C.L.'s in the two-dimensional anisotropic system well below and well above cross-over, we now apply a similar type of analysis to the wavevector dependent susceptibilities.

ii) Wavevector Dependent Susceptibility (W.D.S.) Behaviour In The Two-Dimensional Anisotropic System.

When the underlying, characteristic length scales of a system are dilated by a factor b near criticality, the W.D.S.'s transform as:

$$D_b : \chi_{//,\perp}(u,\Theta,q) \longrightarrow \chi'_{//,\perp}(u,\Theta,q) = \chi_{//,\perp}(u',\Theta',q') = b^{-\gamma}\chi_{//,\perp}(u,\Theta,q) \qquad (3.c.30)$$

Although we have not detailed its derivation here, the last equality follows from a consideration of the free energy density scaling in the presence of an external magnetic field. Under the same dilation, the other parameters scale as:

$$\Theta \rightarrow \Theta' = b\Theta$$

$$u \rightarrow u' = bu$$

$$q \rightarrow q' = bq$$

The first two transformations were introduced in the previous subsection (3.c. 15) and the last transformation follows from the fact that q is an inverse length. As the system is of the same type after dilation as before, equation (3.c. 30) becomes:

$$\chi_{//,\perp}(u',\Theta',q') = \chi_{//,\perp}(bu, b\Theta, bq) = b^{-\gamma}\chi_{//,\perp}(u,\Theta,q)$$

Substituting:

$$b = \Theta^{-1}$$

we obtain:

$$\chi_{//,\perp}(u,\Theta,q) = \Theta^{-\gamma}\,\Gamma_{//,\perp}\left(\frac{u}{\Theta},\frac{q}{\Theta}\right) \qquad (3.c.31)$$

where:

$$\Gamma_{//,\perp}(a,b) \equiv \chi_{//,\perp}(a,1,b)$$

Equation (3.c. 31) is the W.D.S.'s analogue to equation (3.c. 15) for the I.C.L.'s. Thus, proceeding in a similar manner, we obtain further information about the functions $\Gamma_{//,\perp}(x,y)$ and exponent(s), γ, by examining the Ising and isotropic Heisenberg limits of equation (3.c. 31). To begin with we consider the Ising limit of the longitudinal W.D.S:

$$\chi_{//}(u,\Theta,q) = \Theta^{-\gamma}\,\Gamma_{//}\left(\frac{u}{\Theta},\frac{q}{\Theta}\right) \qquad (3.c.32)$$

where

$$\Theta \to \infty \;;\quad u = K - K_c^{ISING}$$

Imposing the condition that $\chi_{//}^{ISING}$ be finite and non-zero over some temperature range we obtain:

$$\lim_{x,y\to 0} \Gamma_{//}(x,y) = C_0\,|x|^{-\gamma_I}\,\Phi_{//}^{<}(y/x) \quad : \quad (3.c.33)$$

and hence:

$$\chi_{//}^{ISING}(u,\Theta,q) = C_0\,|K-K_c^{ISING}|^{-\gamma_I}\,\Phi_{//}^{<}(q/|K-K_c^{ISING}|)$$

$$\sim |K_{//}^{ISING}|^{-\gamma_I}\,\Phi_{//}^{<}(q/K_{//}^{ISING}) \quad : \quad (3.c.34)$$

where, in the last step, we have used equation (3.c. 18). From our final equation above we deduce that the exponent, γ_I appearing in equations (3.c. 33-34) is the W.D.S. exponent for the two-dimensional Ising model.

We now turn our attention to the isotropic Heisenberg limit of

equation (3.c. 32) where:

$$\Theta \to 0^{+} \; ; \; \frac{u}{\Theta} = K + \tfrac{1}{2}\ln\Theta \to -\infty$$

In order that the W.D.S.'s be finite and non-zero away from the critical temperature we require:

$$\lim_{|x|,|y|\to\infty} \Gamma_{//}(x,y) = d_0 e^{-2\gamma_H |x|} \; \Phi^{>}_{//}(y e^{-2|x|}) \qquad (3.c.35)$$

so that:

$$\chi^{HEIS}_{//}(u,\Theta,q) = \chi^{HEIS}_{\perp}(u,\Theta,q) = d_0 e^{2\gamma_H K} \; \Phi^{>}_{//,\perp}(q e^{2K})$$

$$\sim (K^{HEIS}_{//,\perp})^{-\gamma_H} \; \Phi^{>}_{//,\perp}(q / K^{HEIS}_{//,\perp}) \qquad (3.c.36)$$

From equation (3.c. 36) we conclude that the exponent, γ_H , appearing in equation (3.c. 35) is the two-dimensional Heisenberg W.D.S. exponent.

Using equations (3.c. 33) and (3.c. 35) we can now determine the limiting behaviour of the weakly anisotropic system's longitudinal W.D.S. Well below crossover and with small wavevector we use the former equation to obtain:

$$\chi_{//}(u,\Theta,q) \sim c_0 |u|^{-\gamma_I} \; \Phi^{<}_{//}(q/|u|) \quad \{q, |u| \ll \Theta\}$$

$$\sim (K_{//})^{-\gamma_I} \; \Phi^{<}_{//}(q/K_{//}) \qquad (3.c.37)$$

The last expression follows from equation (3.c. 23)

In the limit:

$$q_{//}/K_{//} \to 0^{+}$$

(wavevector tending to zero at finite $|T - T_c|$) the susceptibility should remain finite and, hence:

$$\chi_{//}(K_{//},\Theta,q) \sim \frac{\lambda_0 (K_{//})^{2-\gamma_I}}{(K_{//})^2 + \beta_0 q^2} \; : \; (q \ll K_{//} \ll \Theta) \qquad (3.c.38)$$

where we have expanded $\Phi^{<}_{//}(x)$ as a power series in x.

By taking the limit:

$$q/K_{//} \rightarrow \infty$$

(approaching T_c at finite wavevector) we obtain similarly:

$$\lim_{|x|\rightarrow\infty} \Phi^{<}_{//}(x) \sim h_0 |x|^{-\gamma_I}$$

Thus:

$$\chi_{//}(K_{//}, \Theta, q) \sim \frac{h_0}{q^{\gamma_I}} \quad : (K_{//} \ll q \ll \Theta) \qquad (3.c.39)$$

Equations (3.c. 38-39) imply that for a two-dimensional, weakly anisotropic system well below crossover ($|u| \ll \Theta$) the longitudinal W.D.S. behaves as:

i) $$\chi_{//} \sim \frac{h_0}{q^{\gamma_I}} \quad : (q \gg K_{//})$$

ii) $$\chi_{//} \sim \frac{\lambda_0 (K_{//})^{2-\gamma_I}}{K_{//}^2 + \beta_0 q^2} \qquad (q \ll K_{//})$$

The difference in the form of the two expressions arises from the fact that in the regime $q \gg K_{//}$, the characteristic length scale over which the system is being viewed (viz. $1/q$) is much smaller than the characteristic length scale over which fluctuations in the system are well correlated (viz. $\xi_{//} = 1/K_{//}$) and the system appears to be at criticality. In the second regime ($q \ll K_{//}$) the converse is true, hence we obtain an Ornstein-Zernicke form. In this and later chapters, the expressions for the W.D.S. always have the critical exponent η equal to zero. This is due to the decimation step in the Migdal-Kadanoff bond moving scheme which, although exact in one dimension, is known to set η to zero in higher dimensions (Niemeijer & van Leeuwen, 1976).

For the two-dimensional, weakly anisotropic system well above crossover we employ equation (3.c. 35) to obtain:

$$\chi_{//}(u,\Theta,q) \sim d_0 [\Theta e^{2\gamma|u/\theta|}]^{-\gamma_H} \Phi^{>}_{//}(q/\Theta e^{2|u/\theta|})$$

and, using equation (3.c. 25a) we have:

$$\chi_{//}(K_{//},q) \sim K_{//}^{-\gamma_H} \Phi(q/K_{//}) \quad : (|u|, q \gg \Theta)$$

(3.c.40)

Hence, in the limit:

$$q/K_{//} \to 0^+$$

the expression for the W.D.S. becomes:

$$\chi_{//}(K_{//},q) \sim f_0 \cdot \frac{(K_{//})^{2-\gamma_H}}{K_{//}^2 + \sigma_0 q^2} \quad ; (|u|, q \gg \Theta \; ; \; q/K_{//} \to 0^+)$$

(3.c.41)

Likewise, in the limit

$$q/K_{//} \gg 1$$

we have:

$$\chi_{//}(K_{//},q) \sim \frac{f_0}{q^{\gamma_H}} \qquad (|u|, q \gg \Theta \; ; \; q/K_{//} \gg 1)$$

(3.c.42)

The determination of the transverse W.D.S. behaviour for the weakly anisotropic Heisenberg model is a little more complex due to the fact that in the Ising limit this W.D.S. is identically zero. However, we know that at $T_c(\Theta)$, the transverse I.C.L. is finite which implies that the transverse W.D.S. will also be finite at $T_c(\Theta)$. Thus for Θ finite but $T = T_c(\Theta)$:

$$\chi_{\perp}(K_{//}=0 \; ; \Theta, q) \sim \Theta^{-\gamma_I} \Psi_{\perp}(q/\Theta)$$

where:

$$\Psi(x) \equiv \Gamma_{\perp}(0,x)$$

Even at $q = 0$ the transverse W.D.S. should remain finite so we may expand the function $\Psi(x)$ about $x = 0$ to obtain:

$$\chi_{\perp} \sim \frac{\alpha_0 \Theta^{2-\gamma_I}}{\Theta^2 + \beta_1 q^2} \qquad (T = T_c, q \ll \Theta)$$

(3.c. 43)

Well above crossover, the transverse W.D.S. becomes the same as the longitudinal W.D.S. so that:

$$\chi_\perp \sim f_0 \cdot \frac{K_\perp^{2-\gamma_H}}{K_\perp^2 + \sigma_0 q_\parallel^2} \quad : \left\{ |\omega|, q_\parallel \gg \Theta \; ; \; \frac{q_\parallel}{K_\perp} \to 0^+ \right\} : (3.c.44)$$

$$\sim \frac{f_0}{q_\parallel^{\gamma_H}} \quad : \left\{ |\omega|, q_\parallel \gg \Theta \; ; \; \frac{q_\parallel}{K_\perp} \gg 1. \right\} : (3.c.45)$$

Similar results can also be obtained in various other limits by means of the arguments and methods introduced in the last two subsections but we have not detailed them here.

In the next section we summarise our results from this chapter and compare them with those of other authors and experiments.

d) Summary.

In the previous section we obtained the limiting forms of the longitudinal and transverse correlation lengths and wavevector dependent susceptibilities in the two-dimensional anisotropic Heisenberg model, well above and below the anisotropy induced crossover. The temperature at which the crossover occurred was determined by the variable:

$$x \equiv \left| \frac{\omega}{\Theta} \right| \equiv \left| \frac{h - h_c(\Theta)}{\Theta} \right|$$

which, in the limit of weak anisotropy becomes:

$$x \sim \frac{J}{k_B T} \left| 1 - \frac{T}{T_c(\Theta)} \right| \qquad (0 < \Theta \ll 1)$$

For values of x much smaller than unity, the weakly anisotropic system displays characteristically Ising-like behaviour. For instance, the longitudinal I.C.L. decays to zero like:

$$K_\parallel \sim \frac{1}{\cosh\mu} \frac{J}{k_B T} \left| 1 - \frac{T}{T_c(\Theta)} \right| \qquad (x \ll 1)$$
$$[\text{cf. eqn. } (3.c.23)]$$

For values of x much greater than unity, the weakly anisotropic system shows characteristically isotropic Heisenberg-like behaviour with the I.C.L.'s

$$K_{\parallel} \sim K_{\perp} \sim e^{-2J/k_B T} \qquad (x \gg 1) \qquad \text{[cf. eqn. (3.c.26)]}$$

At the Ising limit itself, we obtain a power law decay for the longitudinal I.C.L. viz.

$$K_{\parallel}^{ISING} \sim \frac{J}{k_B T} \left| 1 - \frac{T}{T_c^{ISING}} \right| \qquad \text{[cf. eqn. (3.c.18)]}$$

with:

$$T_c^{ISING} = \frac{2J}{k_B}$$

The value of T_c^{ISING} is fortuitously close to the exact result for the spin-$\frac{1}{2}$ model on a square lattice [$T_c = 4J/k_B \cdot \sinh^{-1} 1$]

As pointed out in the text, the form of eqn. (3.c. 18) is in qualitative agreement with the exact solution (Montrell et al (1963)).

At the isotropic Heisenberg limit, we obtain an exponential decay of the I.C.L.'s given by:

$$K_{\parallel}^{HEIS} = K_{\perp}^{HEIS} \sim e^{-2J/k_B T} \qquad \text{[cf. eqn. (3.c.20)]}$$

This result is in qualitative agreement with the earlier work of Polyakov (1975) and Belavin & Polyakov (1975) who obtained the expression:

$$K_{\parallel}^{HEIS} = K_{\perp}^{HEIS} \sim e^{-2\pi J/k_B T} \qquad (T \ll J/k_B)$$

The dependence of the critical temperature on anisotropy was found to be:

$$\frac{1}{T_c(\Theta)} = \left(\frac{k_B}{2J}\right) \cdot \Theta \cdot \cosh\mu \cdot \int_0^{\infty} dx \cdot \frac{\tanh x}{x^2} \qquad \text{[cf. eqn. (3.c.25)]}$$

which in the limit of weak anisotropy ($\Theta \ll 1$, $\cosh\mu \gg 1$) becomes:

$$T_c(\Theta \ll 1) \sim \frac{(2J/k_B)}{\ln(\cosh\mu) + O(1)} \sim \frac{2J}{k_B \cdot \ln(\cosh\mu)} \qquad \text{[cf. eqn. (3.c.24)]}$$

The logarithmic dependence of the transition temperature on the anisotropy in this limit agrees with the results of an R.P.A. treatment of the system. Stinchcombe (1981) has treated the same problem using the Suzuki-Takano (1979) method. Our results for the transition temperature dependence on anisotropy, in the strong and weak limit qualitatively agree with his.

Using the exchange constants quoted by Birgeneau et al. (1970) the present scheme predicts a transition temperature of $\gtrsim 40K$ for Rb_2MnF_4 in the absence of interlayer couplings. This is fairly close to the experimentally observed value of 38.4K.

Below we have displayed the results of our scheme for the inverse correlation lengths and wavevector dependent susceptibilities in various limits in table form.

INVERSE CORRELATION LENGTH BEHAVIOUR

SYSTEM	WELL ABOVE CROSSOVER	WELL BELOW CROSSOVER
ISING SYSTEM	N/A	$K_{\parallel} \sim \frac{a_0}{T}\left\lvert 1 - \frac{T}{T_c^{ISING}}\right\rvert$ $K_{\perp}^{-1} \equiv \xi_{\perp} \equiv 0$
WEAKLY ANISOTROPIC SYSTEM	$K_{\parallel} \sim K_{\perp} \sim e^{-2J/k_BT}$	$K_{\parallel} \sim \frac{a_0}{T}\frac{1}{\cosh\mu}\left\lvert 1 - \frac{T}{T_c(\Theta)}\right\rvert$ $K_{\perp} \sim \xi_0\Theta$
ISOTROPIC HEISENBERG SYSTEM	$K_{\parallel} = K_{\perp} \sim e^{-2J/k_BT}$	N/A

$$T_c(\Theta) \sim \frac{(2J/k_B)}{\ln(1/\Theta) + O(1)} \qquad \Theta \ll 1$$

WAVEVECTOR DEPENDENT SUSCEPTIBILITY BEHAVIOUR

SYSTEM	WELL ABOVE CROSSOVER	WELL BELOW CROSSOVER
ISING SYSTEM	N/A	$\chi_{\parallel} \sim \frac{\lambda_0 \cdot K_{\parallel}^{2-\gamma_I}}{K_{\parallel}^2 + \beta_0 q^2}$ $(q \ll K_{\parallel})$ $\chi_{\parallel} \sim h_0 q^{-\gamma_I}$ $(q \gg K_{\parallel})$
WEAKLY ANISOTROPIC SYSTEM $\chi_{\parallel}$	$\frac{C_0 K_{\parallel}^{2-\gamma_H}}{K_{\parallel}^2 + \beta_1 q^2}$: $(q \gg \Theta, q \ll K_{\parallel})$ $g_0 q^{-\gamma_H}$: $(q \gg \Theta, q \gg K_{\parallel})$	$\frac{\lambda_0 K_{\parallel}^{2-\gamma_I}}{K_{\parallel}^2 + \beta_0 q^2}$: $(q \ll K_{\parallel})$ $h_0 q^{-\gamma_I}$: $(q \gg K_{\parallel})$
$\chi_{\perp}$		$\frac{a_0 K_{\perp}^{2-\gamma_I}}{K_{\perp}^2 + \beta q^2}$: $(T = T_c ; q \ll K_{\perp})$
ISOTROPIC HEISENBERG SYSTEM	$\frac{C_0 K_{\parallel,\perp}^{2-\gamma_H}}{K_{\parallel,\perp}^2 + \beta_1 q^2}$: $(q \ll K_{\perp,\parallel})$ $g_0 q^{-\gamma_H}$: $(q \gg K_{\perp,\parallel})$	N/A

In the next chapter we incorporate the effects of dilution into the Migdal/Kadanoff bond moving scheme in order to treat the dilute, two-dimensional Heisenberg model with exchange anisotropy.

Chapter 4

The Dilute Two-Dimensional System

a) Introduction

In the previous chapter we obtained qualitative information about the behaviour of the pure, two-dimensional anisotropic system. In the present chapter we show how the framework which was set up to treat the pure system may be extended to include the effects of dilution.

In real systems (e.g. $Rb_2Mn_pMg_{1-p}F_4$) dilution may be carried out by randomly removing a fraction (1-p) of the magnetic ions and replacing them with chemically similar non-magnetic ions. As we pointed out in Chapter 1, one of the effects of such 'site' dilution is to depress the critical temperature of a system from its corresponding pure value (assumed finite). When the fraction , p, of magnetic ions in the system is decreased below a critical value, p_c, no transition to long range order occurs. Precisely at p_c (the percolation threshold) the transition temperature is depressed to absolute zero.

In the following sections we show how the concept of dilution may be introduced into the Migdal/Kadanoff bond moving scheme. In contrast to the pure system, where there was a unique, well-defined interaction strength, J, in the dilute system we are led to consider the scaling of a probability distribution for the continuous variable, J. Furthermore, in order to facilitate use of the bond moving scheme, we consider models in which a fraction (1-p) of the interactions (or 'bonds') between spins are randomly removed. That is, we replace

the real site dilution problem by a bond dilution problem. (Essam (1972)). We do not expect this replacement to change the essential aspects of the model's behaviour since universality arguments lead us to believe that quantities such as critical exponents and amplitude ratios will be the same for both types of dilution. We note, however, that the site dilution case has previously been treated for Ising systems by Yeomans and Stinchcombe (1979).

b) Interaction Probability Distribution Scaling.

Before treating the dilute magnetic system itself we introduce some of the basic formalism which will be used in later sections.

In a bond-diluted magnetic model, the interactions (or bonds) between neighbouring ions (or sites) are assumed to be absent with independent probability (1-p). This corresponds to the random removal of a fraction (1-p) of the bonds from a pure model. Hence, in contrast to the pure model, the interactions between spins become random variables, $\{\underline{K}_i\}$, described by the probability distribution

$$P(K_i) = (1-p)\,\delta(\underline{K}_i) + p\,\delta(\underline{K}_i - \underline{K}) \qquad (4.b.1)$$

where the vector $\underline{K}$ represents the strength and anisotropy of interactions which are present.

In the remainder of this section we consider how models described by the probability distribution (4.b.1) may be treated within the framework of the Migdal/Kadanoff (M/K)bond moving scheme. To this end, we consider each of the operations from which the scheme is built up, in turn, and outline their respective effects upon the bond probability distribution (p.d.). In order to simplify the

following discussion we point out that for real systems in which all bonds have the same initial anisotropy, the anisotropy scaling decouples from that of the concentration, p, and thermal parameters. This result is derived in detail in Appendix 2 (eqn. A.2.12). For our immediate purposes however we need only note that the expression for the bond (p.d.) in eqn. (4.b.1) may be simplified in this case to:

$$P(u_i) = (1-p)\,\delta(u_i) + p\,\delta(u_i - u) \qquad (4.b.2)$$

where u is a scalar, thermal parameter, whose value is zero when a bond is absent.

In the first step of the M/K scheme (Figure 11(a)), alternate sets of bonds perpendicular to the y-axis are moved parallel to the y-direction (Figure 11(b)). In this step, there is no resultant effect upon bonds such as A-B-C or D-E-F. A trace is then taken over the subset of spins with only two nearest neighbour bonds (e.g. spins B,E,... in fig. 11(b)). For a triplet of spins such as A-B-C in figure 11(b), the resulting bond between A and C, after taking the trace over spin B, is described by the p.d:

$$P'(u_{AC}) = \int du_{AB} \int du_{BC}\, P(u_{AB})\, P(u_{BC})\, \delta(u_{AC} - D[u_{AB}, u_{BC}]) \qquad (4.b.3)$$

where P(u) is as given in eqn. (4.b.2) and $D[u_{AB}, u_{BC}]$ represents the thermal parameter obtained after taking a trace over spin B if the initial bonds between A-B and B-C had thermal parameters u_{AB} and u_{BC} respectively. Under the same operation, we show in appendix 2 that the accompanying anisotropy scaling is exactly the same as in the pure system viz: (cf. A.2. 8-11).

$$\Theta \rightarrow \Theta' = b\Theta = 2\Theta \qquad (4.b.4)$$

where Θ was previously defined in equation (3.c.1). The subsequent bond combination step gives the resultant interaction p.d. scaling under a length scale dilation by a factor b = 2 as:

$$P''(u_i) = \int du_{AC} \int du_{DF}\, P'(u_{AC})\, P'(u_{DF}).$$

$$\delta\{u_i - L(D[u_{AB}, u_{BC}], D[u_{DE}, u_{EF}])\} \qquad (4.b.5)$$

where $L(D[u_{AB}, u_{BC}], D[u_{DE}, u_{EF}])$ represents the thermal parameter obtained on combining the new bonds A-C and D-F 'in parallel' (cf. bonds A-D and B-E in figs. 11(a,b)).

Unfortunately, the new probability distribution, $P''(u_i)$ is no longer of the binary form we started from (cf. equation 4.b.2) so that it is difficult to see how the initial and final distributions may be usefully compared. Under repeated transformations, the distribution becomes increasingly complex. In general the probability distribution obtained after n length scalings, $P^{(n)}(u_i)$ is of the form:

$$P^{(n)}(u_i) = (1-p^{(n)})\,\delta(u_i) + p^{(n)}\,Q^{(n)}(u_i) \qquad (4.b.2(a))$$

Our initial binary, or physical, form (4.b.2) is a special case of (4.b.2(a)) with:

$$Q^{(0)}(u_i) = \delta(u_i - u)$$

By substituting the more general form for $P^{(n)}(u_i)$ (4.b.2(a)) into (4.b.5) and using the identities:

$$L(x,0) = x \;\; ; \;\; D(x,0) = 0$$

we obtain the combined interaction p.d. scaling under a length scale

dilation by a factor b = 2 as:

$$P^{(n+1)}(u_i) = (1-p^{(n)2})\,\delta(u_i) + 2p^{(n)2}(1-p^{(n)2}) \int du_a \int du_b \, Q^{(n)}(u_a) Q^{(n)}(u_b) \, \delta(u_i - D[u_a, u_b]) + p^{(n)4} \int du_a \int du_b \int du_c \int du_d \, Q^{(n)}(u_a) Q^{(n)}(u_b) Q^{(n)}(u_c) Q^{(n)}(u_d) \, \delta(u_i - L\{D[u_a, u_b]; D[u_c, u_d]\})$$

$$= (1-p^{(n+1)})\,\delta(u_i) + p^{(n+1)} Q^{(n+1)}(u_i) \qquad (4.b.6)$$

By equating coefficients of the term $\delta(u_i)$ we immediately obtain the scaling of the parameter p as:

$$p^{(n+1)} = 1 - (1-p^{(n)2})^2 \qquad (4.b.7)$$

and, hence,

$$p^{(n+1)} Q^{(n+1)}(u_i) = 2p^{(n)2}(1-p^{(n)2}) \int du_a \int du_b \, Q^{(n)}(u_a) Q^{(n)}(u_b) \, \delta(u_i - D[u_a, u_b]) + p^{(n)4} \int du_a \int du_b \int du_c \int du_d \, Q^{(n)}(u_a) Q^{(n)}(u_b) Q^{(n)}(u_c) Q^{(n)}(u_d) \, \delta\{u_i - L[D[u_a, u_b]; D[u_c, u_d])\}. \qquad (4.b.8)$$

The anisotropy scaling is the same as that in the pure system, viz:

$$\Theta'' = 2\Theta \qquad (4.b.9)$$

This result is derived in Appendix 2 (equation (A.2.12)).

Equations (4.b. 7-9) are our basic scaling equations which we will use in subsequent sections to investigate the behaviour of the dilute, anisotropic, two-dimensional model. Before we do so, however, we consider some of the techniques used so far, and

discuss the qualitative forms of our scaling equations.

To begin with, it is clear that we have not used the infinitesimal form of the M/K scheme which we employed in the investigation of the pure system. Hence, within the present scheme, the operations of bond combination and decimation do not commute. Our reason for using the finite b = 2 form of the scheme is the difficulty encountered in extending the ideas of p.d. scaling to non-integer b values. However, previous work on the Ising and isotropic Heisenberg limits of the dilute model have shown the operation order employed by us here to give the correct qualitative behaviour in these two limits.

Secondly, we have yet to give the functional form of the thermal parameter u. In fact, as we show later on, the choice of u can be crucial within certain approximation schemes. We defer a full discussion of this point until we consider the approximation schemes in question.

Lastly, as pointed out in the discussion leading to eqn. (4.b.2 (a)) if we start with a delta function form for $Q(u)$ viz:

$$Q^{(0)}(u) = \delta(u - u^{(0)})$$

corresponding to all bonds present having the same strength, equation (4.b.8) tells us that, in general, after a single length dilation by a factor b = 2, Q becomes the sum of two delta-functions. Thus, our system after dilation is not of the same form as that we started from. This, in turn, implies that we are no longer able to apply the simple scaling argements we used to analyse the pure model to investigate the dilute, two-dimensional model. Instead, we look to the Renormalisation Group (Ma (1976)) to provide us with an interpretation

of these observations.

To begin with we consider an [N + 2] dimensional space in which one of the axis corresponds to the magnetic-ion concentration parameter, p, another to the anisotropy parameter, Θ , and the remaining N(possibly infinite) characterise the probability distribution, $Q(u)$. Thus, for every dilute, two-dimensional, anisotropic Heisenberg model at a given temperature, T, there exists a corresponding point in this multi-dimensional space. Under a dilation of the underlying length scales of any such system, the point representing that system moves, or 'flows', to another point within the space. Certain special points in the space do not move under the effects of length dilation. These are referred to as fixed points. Associated with each partially unstable/ non-trivial fixed point there is a characteristic subspace such that under the transformation corresponding to dilation points within this subspace flow towards, and eventually arrive at, the fixed point. This subspace is referred to as the critical surface of the fixed point. The Renormalisation Group formalism shows how the singular critical behaviour of all dilute magnetic systems can be determined by the behaviour of representative points very close to a critical surface under repeated dilation transformations: in particular, the way in which such points eventually move away from the associated fixed point. Systems at criticality correspond to points on the critical surface itself. As a result, we now set about determining the fixed points in the space corresponding to dilute, anisotropic, two-dimensional magnets using our scaling equations. (4.b. 7-9). The fixed point values for the concentration and anisotropy parameters are obtained from equations (4.b.7) and (4.b.9) respectively. If we denote these values by p^* and Θ^* , we have:

$$p^* = 1 - (1 - p^{*2})^2$$

$$\Theta^* = 2\Theta^*$$

and, hence:

$$p^* = 0, p_c, 1 \quad ; \; p_c = (\sqrt{5} - 1)/2 \qquad (4.b.10)$$

$$\Theta^* = 0, \infty \qquad (4.b.11)$$

We will be particularly interested in the solution, p_c for the concentration parameter. The values 0,1 correspond to no bonds present and pure system respectively. The former case is trival and the latter corresponds to the pure system we investigated in Chapter 3.

The fixed point values for Θ^* in equation (4.b. 11) correspond to the isotropic Heisenberg and Ising limits respectively. We now restrict our attention to the percolation threshold itself (i.e. $p = p_c$) in which case equation (4.b. 8) becomes:

$$Q^{(n+1)}(u) = (1 - p_c^3) \int du_1 \int du_2 \, Q^{(n)}(u_1) Q^{(n)}(u_2) \, \delta[u - D(u_1, u_2)]$$

$$+ p_c^3 \prod_{i=1}^{4} \left\{ \int du_i Q^{(n)}(u_i) \right\} . \delta\{u - L(D[u_1, u_2]; D[u_3, u_4])\}$$

$$\equiv R_b \{ Q^{(n)}(u) \} \qquad (4.b.12)$$

after n + 1 iterations.

In order to discuss the fixed point structure of the function $Q(u)$ we have to decide upon a particular means of parameterisation. For simplicity we choose to parameterise $Q^{(n)}(u)$ through its moments, viz:

$$m_\alpha^{(n)} = \int du\, Q^{(n)}(u).\, u^\alpha \qquad (4.b.13)$$

Thus, if we start from a real system in which all bonds initially have the same strength and anisotropy value (given by either of the solutions (4.b. 11)), viz:

$$Q^{(0)} = \delta(u - u^{(0)}) \qquad (4.b.14)$$

$$\Theta = \Theta^*$$

our initial moments are:

$$m_\alpha^{(0)} = \int du\, Q^{(0)}(u)\, u^\alpha$$

$$= \int du\, \delta(u - u^{(0)})\, u^\alpha$$

$$= [u^{(0)}]^\alpha \qquad (4.b.15)$$

As we pointed out previously, even after one iteration from the seed function (4.b. 14), Q changes its functional form and so, as a result, do all its moments. In order to obtain the fixed point values of the moments, it is necessary to find a function, $Q^*(u)$, such that under a length dilation by a factor b, all moments of Q^* are left invariant. In general, finding such a function explicitly is very difficult. However, it is possible to employ various approximation schemes which can give a great deal of qualitative information about the fixed point values of the moments. We now consider one such approximation scheme known as the binary approximation.

The binary approximation consists of replacing the new function obtained from eqn. (4.b. 14) after a dilatation transformation by a single delta-function whose argument is chosen to 'preserve' the first moment of the distribution $P(u)$ in equation (4.b. 6). In order to implement this scheme, however, one must decide on a choice of thermal parameter, u. Of course, if one was to solve the scaling equation

(4.b. 12) exactly for the function Q^*, any choice of u would give the same final result. However, it is well known that one has to be far more careful when employing a scheme such as the binary approximation. Since we are only interested in the Ising and isotropic Heisenberg limits of equation (4.b. 12) here, we will consider the two cases seperately and introduce the appropriate thermal parameters.

i) The Ising Limit ($\Theta \to \infty$).

In this limit we choose the thermal parameter to have an exponential nature following Young and Stinchcombe (1976) viz:

$$u \equiv e^{-2K}$$

Thus, if we start from a distribution:

$$Q^{(0)}(u) \equiv \delta(u - u^{(0)})$$

and iterate once using equation (4.b. 12) we obtain:

$$Q^{(1)}(u) = (1-p_c^3)\,\delta(u-2u^{(0)}) + p_c^3\,\delta(u-4u^{(0)2})$$

where we have employed results (A.2.10) in Appendix 2. Approximating the new function $Q^{(1)}$ by:

$$Q^{(1)}(u) \sim \delta(u - u^{(1)})$$

we determine $u^{(1)}$ by preserving the first moment viz:

$$\int du.\,\delta(u-u^{(1)})\,u = u^{(1)}$$

$$= (1-p_c^3).2u^{(0)} + 4p_c^3.u^{(0)2}$$

This result is easily generalised to the $n^{\underline{th}}$. iterate as:

$$u^{(n+1)} = (1-p_c^3).2.u^{(n)} + 4p_c^3\,u^{(n)2}$$

The fixed point value of u is thus:

$$u = 0$$

implying

$$m_\alpha^* = 0$$

for the moments of the fixed point distribution and hence that the temperature, is zero.

ii) The Isotropic Heisenberg Limit ($\Theta = 0$)

In this limit we choose the thermal parameter to have the form:

$$u = \frac{1}{K} = \frac{k_B T}{J}$$

If we start from the distribution

$$Q^{(n)}(u) = \delta(u - u^{(n)})$$

and iterate once using equation (4.b. 12) we obtain:

$$Q^{(n+1)}(u) = (1 - p_c^3)\,\delta(u - u^{(n)}/2) + p_c^3\,\delta(u - u^{(n)})$$

where we have used equations (A.2.11) of Appendix 2. Thus, matching the form above to:

$$Q^{(n+1)}(u) \sim \delta(u - u^{(n+1)})$$

we have:

$$u^{(n+1)} = (1 - p_c^3)\,\frac{u^{(n)}}{2} + p_c^3\,u^{(n)}$$

The fixed point value of u is, therefore;

$$u^* = 0$$

implying

$$m_\alpha^* = 0 \quad : \forall \alpha$$

and hence zero temperature:

$$T = 0$$

It is important to note that the binary approximation only ever requires the combination of, or decimation over, bonds with the same strength. In order to improve on this approximation we have to know how to combine or decimate over bonds of different strengths.

In summary, we have shown, using the binary approximation that the two percolation fixed points of the dilute, anisotropic, two-dimensional model occur at:

$$p^* = p_c \,,\ \Theta^* = 0 \,,\ T^* = 0 \qquad \text{[Heis, fixed pt.]}$$

$$p^* = p_c \,,\ \Theta^* = \infty \,,\ T^* = 0 \qquad \text{[Ising fixed pt.]}$$

or in terms of the parameters $\{m_\alpha\}$:

$$p^* = p_c \,,\ \Theta^* = 0 \,,\ m_\alpha^* = 0 : \forall \alpha \qquad \text{[Heis fixed pt. : } u = 1/K \text{]}$$

$$p^* = p_c \,,\ \Theta^* = \infty \,,\ m_\alpha^* = 0 : \forall \alpha \qquad \text{[Ising fixed pt. : } u = e^{-2K} \text{]}$$

In fact, as we will show later on, these results are exact and can be derived directly from (4.b. 12). Having determined the fixed point structure of our multi-dimensional space, in the next section we show how the behaviour of points near the critical surface determines the critical behaviour of the corresponding systems.

c) Scaling At The Percolation Threshold

In this section we show how the scaling of the moments $\{m_\alpha\}$

introduced in section (b), may be obtained from the solution of an integral equation. We then determine the explicit scaling equations for a system at the percolation threshold.

Consider equation (4.b. 12) for the transformation of the probability distribution, $Q^{(n)}(u)$, at p_c viz:

$$Q^{(n+1)}(u) = R_b\{Q^{(n)}(u)\} \qquad (4.c.1)$$

Following Stinchcombe & Watson (1976) we introduce the set of functions $\{f_j(u-u^*)\}$, where u^* is the fixed point value of the thermal parameter, u, such that under the action of the operator R_b in equation (4.c.1) the $\{f_j\}$ retain their 'shape' but change their scale i.e.

$$R_b\{f_j(u-u^*)\} = \frac{1}{\lambda_j} f_j\left(\frac{u-u^*}{\lambda_j}\right) \qquad \forall_j \qquad (4.c.2)$$

Assuming the set $\{f_j\}$ form a complete set we expand our initial probability distribution as:

$$Q^{(0)}(u) = \sum_j c_j f_j(u-u^*) \qquad (4.c.3)$$

We parameterise the functions, $Q^{(n)}(u)$, by their moments about the fixed point value of u viz:

$$m_\alpha^{(n)} = \int du\, Q^{(n)}(u)\,[u-u^*]^\alpha \qquad (4.c.4)$$

After n iterations from the seed function (4.c.3) we have:

$$Q^{(n)}(u) = R_b^n\{Q^{(0)}(u)\} = \sum_j c_j\, R_b^n\{f_j(u-u^*)\}$$

$$= \sum_j c_j\, \frac{1}{\lambda_j^n} f_j\left(\frac{u-u^*}{\lambda_j^n}\right)$$

so, evaluating the moments of this new function about u^* (using equation (4.c.4)) we obtain:

$$m_\alpha^{(n)} = \int du\, Q^{(n)}(u)\,[u-u^*]^\alpha = \sum_j c_j \int \frac{du}{\lambda_j^n} f_j\left(\frac{u-u^*}{\lambda_j^n}\right)[u-u^*]^\alpha$$

$$= \sum_j c_j\, \lambda_j^{n\alpha} \int du\, f_j(u-u^*)\,[u-u^*]^\alpha \qquad (4.c.5)$$

If we assume that only one of the set $\{\lambda_j\}$ is greater than unity, equation (4.c.5) implies that:

$$\lim_{n\to\infty} \frac{m_\alpha^{(n+1)}}{m_\alpha^{(n)}} = \lambda_{max}^\alpha \qquad (4.c.6)$$

where

$$\lambda_{max} = \max\{\lambda_j\} \qquad (4.c.7)$$

That is after iterating a large number of times from any seed function, $Q^{(o)}(u)$, all moments of the resulting distribution about the fixed point value of the thermal parameter, u^*, become dependent. In particular:

$$m_1^{(n+1)} \sim \lambda_{max}\, m_1^{(n)} \quad : n\to\infty \qquad (4.c.8)$$

Thus, wwe can describe the transformation of all thermal parameters in the dilute magnetic system at percolation threshold via the one scaling equation:

$$(u-u^*)' = b^{1/\nu_u}(u-u^*) \qquad (4.c.9)$$

where, in the last equation we have substituted:

$$\nu_u \equiv \frac{\ln b}{\ln \lambda_{max}} \qquad (4.c.10)$$

We are now in a position to discuss the full scaling of a dilute magnetic system at percolation threshold by combining equations (4.b. 10) and (4.c. 9) viz:

$$\left.\begin{aligned} \Theta' &= b\Theta \\ (u-u^*)' &= b^{1/\nu_u}(u-u^*) \end{aligned}\right\} \quad (4.c\ 11)$$

In the remainder of this section we employ the previously introduced binary approximation and a perturbation scheme to explicitly calculate the nature of the thermal parameter, u, and the corresponding exponent, ν_u , for a weakly anisotropic, dilute, two-dimensional magnetic system at p_c.

i) Binary Approximation at Percolation Threshold.

As we discussed in section (b) of the present chapter, the 'correct' type of thermal variable to employ with the binary approximation at the isotropic Heisenberg limit is:

$$u_{HEIS} = 1/K$$

whereas at the Ising limit, one should use an exponential-like variable viz:

$$u_{ISING} = e^{-2K}$$

In the weakly anisotropic system, we expect isotropic Heisenberg-like behaviour well above some crossover temperature, but Ising-like behaviour well below it. Consequently, we require a thermal variable which mimics this behaviour if we are to obtain meaningful results from the binary approximation. One possible candidate for this variable is the inverse, longitudinal correlation length of the corresponding one-dimensional system, $K_{//}^{(d-1)}(h,\Theta)$, where h and

Θ are now taken to refer to a particular bond in the dilute, two-dimensional system. Thus, well above the corresponding one-dimensional crossover temperature (viz: $h \ll 1$ for all bonds) the application of the binary approximation results in:

$$(U-U^*)' = \frac{1}{K'} = (1-p_c^3).\frac{2}{K} + p_c^3.\frac{1}{K} = (2-p_c^3)\frac{1}{K}$$

$$= (2-p_c^3)(U-U^*) \qquad (4.c.12)$$

by comparison with equation (4.c.8) we deduce:

$$\lambda_{max} \sim 2-p_c^3 \qquad (h \ll 1)$$

or, equivalently,

$$\nu_u \sim \frac{\ln 2}{\ln (2-p_c^3)} \qquad (h \ll 1) \qquad (4.c.13)$$

Well below the one-dimensional crossover temperature ($h \gg 1$ $\forall$ bonds) we obtain:

$$(U-U^*)' = K_{//}'$$

$$= (1-p_c^3).2K_{//} + O(K_{//}^2)$$

$$\sim 2(1-p_c^3)(U-U^*)$$

so that in this limit we have:

$$\nu_u \sim \frac{\ln 2}{\ln 2(1-p_c^3)} \quad : (h \gg 1) : \quad (4.c.14)$$

The binary approximation therefore predicts that the thermal and anisotropy scaling variables at the percolation threshold are (Θ, t) where Θ is as defined in (3.c.1) and:

$$t \begin{cases} [K_{//}^{(d=1)}]^{\frac{\ln 2}{\ln 2(1-p_c^3)}} & ; h \gg 1 ; \Theta \ll 1 \\ [K_{//}^{(d=1)}]^{\frac{\ln 2}{\ln (2-p_c^3)}} & ; h \ll 1 ; \Theta \ll 1 \end{cases}$$

Our definition of a 'scaling variable' corresponds to a variable which scales by b under the length dilation. Thus:

$$\Theta' = b\Theta$$
$$t' = bt \qquad (4.c.15)$$

We now consider this problem with the aid of an analytic perturbation scheme and some exact results.

ii) Perturbation Scheme Treatment At Percolation Threshold.

In the following argument it is convenient, but not necessary, to choose the thermal variable for the weakly anisotropic system to be the inverse longitudinal correlation length of the corresponding one-dimensional system i.e.

$$u \equiv K_{//}^{(d=1)}(h,\Theta)$$

In this case, the zero temperature distribution of bonds is given by:

$$Q^*(u) = \delta(u) \qquad (4.c.16)$$

The distribution (4.c. 16) is infinitely sharply peaked around the zero temperature fixed point value ($u^* = 0$) viz:

$$m_\alpha = \int du . Q(u) . u^\alpha = 0 \qquad \forall \alpha$$

If we now consider a real system asymptotically close to zero temperature i.e.

$$Q^{(0)}(u) = \delta(u - \epsilon) \qquad \epsilon \ll 1 \qquad (4.c.17)$$

and iterate (4.b.12) n times, the resultant distribution will approximate more and more closely to the shape-invariant form,

$\int_{max}^{(u)}$, discussed earlier in this chapter. However, by choosing the value of ϵ sufficiently close to zero, we can arrange for the width of the resulting distribution to be arbitrarily small. Thus, if the characteristic width of $Q^{(n)}(u)$ is of order δ i.e.

$$m_\alpha^{(n)} \sim \delta^\alpha$$

and we iterate a further p times, we obtain:

$$m_\alpha^{(n+p)} \sim [\lambda_{max}^\alpha]^p \delta^\alpha \sim [\lambda_{max}^\alpha]^p m_\alpha^{(n)}$$

If we further arrange for δ to be sufficiently small such that:

$$\delta << \frac{1}{\lambda_{max}^p}$$

we need only consider the scaling of m_1 to determine the value of λ_{max} provided the distribution $Q^{(n+p)}(u)$ still has small width viz:

$$m_1^{(n+1)} \simeq \lambda_{max} m_1^{(n)} \qquad (4 \text{ c } 18)$$

We now apply these 'small width' ideas to the scaling of the weakly anisotropic model, at p_c, well below the crossover temperature of the corresponding one-dimensional system (i.e. all bonds which are present have $h \gg 1$).

If we start from a real system asymptotically close to zero temperature, as described by equation (4.c. 17), and scale n times, we can arrange for the resulting distribution to have an arbitrarily small width, δ . Using equation (4.b. 12), we can evaluate the $(n+1)^{th}$ iterate as:

$$Q^{(n+1)}(u) = (1-p_c^3)\int du_1 \int du_2\, Q^{(n)}(u_1) Q^{(n)}(u_2)\, \delta[u - D(u_1,u_2)]$$

$$+ p_c^3 \prod_{i=1}^{4} \left\{ \int du_i Q^{(n)}(u_i) \right\} \delta[u - L\{D(u_1,u_2); D(u_3,u_4)\}]$$

Moreover, we show in Appendix 2 that if u is chosen as the inverse, longitudinal correlation length of the corresponding one-dimensional system, the functional D takes the form:

$$D(u_1,u_2) \sim u_1 + u_2 \quad : \quad (h_1, h_2 \gg 1)$$

(cf. equations A.2. 6-7), whereas L becomes:

$$L\{D(u_1,u_2); D(u_3,u_4)\} \sim O((u_1+u_2)(u_3+u_4))$$

Thus, the scaling of the first moment is given by:

$$m_1^{(n+1)} = \int du\, Q^{(n+1)}(u).u$$

$$= (1-p_c^3) \int du_1 \int du_2 . Q^{(n)}(u_1) Q^{(n)}(u_2) [u_1+u_2] +$$

$$p_c^3 \prod_{i=1}^{4} \left\{ \int du_i Q^{(n)}(u_i) \right\} O((u_1+u_2).(u_3+u_4))$$

$$= 2(1-p_c^3) m_1^{(n)} + O(m_1^{(n)\,2})$$

However, since the width of the distribution is arbitrarily small, we may discard the last term to obtain the asymptotic form of the moment scaling as:

$$m_1^{(n+1)} \simeq 2(1-p_c^3) m_1^{(n)}$$

and, hence, the corresponding results for the value of λ_{max} in equation (4.c.8) and ν_u in equation (4.c. 11) are:

$$\lambda_{max} = 2(1-p_c^3)$$
$$\nu_u = \frac{\ln 2}{\ln 2(1-p_c^3)} \qquad (4.c.19)$$

The exact results (4.c. 19) agree with those obtained by the binary approximation in this regime. (Equation 4.c. 14)

In order to investigate the probability distribution scaling well above the crossover temperature of the associated one-dimensional system (i.e. all bonds present have $h \ll 1$) we note that in this regime, the thermal variable is:

$$u \equiv K_{//}^{(d=1)} \sim \frac{1}{K}$$

so that the scaling equations so obtained are entirely analagous to the dilute Heisenberg model at percolation threshold. As pointed out by Stinchcombe (1979) this latter problem may be mapped exactly onto the dilute resistor network problem which was treated by Stinchcombe and Watson (1976). Their results show that the value of ν_u so obtained in equation (4.c. 11) is:

$$\nu_u \equiv \nu_{HEIS} \simeq 1.23$$

This value differs from that obtained with the binary approximation by ~ 0.01

In summary, we find that the transformation equations for the thermal and anisotropy parameters at percolation threshold under a length dilation of the system by a factor $b = 2$ are:

$$\Theta' = b\Theta$$
$$t' = b\Theta \qquad (4.c.20)$$

where Θ is defined in (3.c.1) and:

$$t \sim \begin{cases} [K_{//}^{(d=1)}]^{\nu_{ISING}} : h \gg 1 \\ [K_{//}^{(d=1)}]^{\nu_{HEIS}} : h \ll 1 \end{cases} \qquad (4.c.21)$$

$$\nu_{ISING} = \ln 2 \,/ \ln 2(1-p_c^3) \simeq 1.64$$

$$\nu_{HEIS} \simeq 1.23$$

This completes our investigation of the system at p_c. In the next section we show how the system near percolation threshold may be approximately treated using the binary approximation.

d) Scaling Near The Percolation Threshold

In the last two section we considered the thermal variable scaling precisely at the percolation threshold ($p = p_c$). In the present section we show how our previous discussion may be extended to include the effects of concentration scaling by working with models whose bond concentrations lie in a small width neighbourhood, δp, of the critical concentration p_c. In order to obtain a simple, yet qualitatively correct, picture of the resultant scaling, we again, employ the binary approximation.

Consider a model in which only a fraction:

$$p = p_c \pm |\delta p| \qquad \delta p \ll 1 \qquad (4.d.1)$$

of the bonds are present. If all bonds have the same anisotropy value, Θ, and strength, J, we may immediately carry across the results of our discussion leading up to equations (4.b. 7-9) to obtain the scaling equations for p, Θ and the thermal variable probability distribution, $Q^{(n)}(u)$ as:

$$\Theta' = 2\Theta \qquad (4.d.2)$$

$$p' = 1 - (1-p^2)^2 \qquad (4.d.3)$$

$$p' Q^{(n+1)}(u) = 2p^2(1-p^2) \int du_1 \int du_2 \, Q^{(n)}(u_1) Q^{(n)}(u_2) \, \delta[u - D(u_1, u_2)]$$
$$+ p^4 \prod_{i=1}^{4} \left\{ \int du_i \, Q^{(n)}(u_i) \right\} \delta\{ u - L[D(u_1,u_2); D(u_3,u_4)] \}$$

(4.d.4)

By substituting the form (4.d.1) into equations (4.d. 3-4) and keeping terms to $O(\delta p)$ only we have:

$$\delta p' = (p' - p_c) = \lambda_p \delta p$$

(4.d. 5)

$$\lambda_p = 4p_c(1-p_c^2)$$

$$(p_c + \delta p') Q^{(n+1)}(u) = (p_c + \lambda_p \delta p) Q^{(n+1)}(u)$$

$$= [p_c(1-p_c^3) + 4p_c(1-2p_c^2)\delta p]$$

(4.d.6)

$$\int du_1 \int du_2 \, Q^{(n)}(u_1) Q^{(n)}(u_2) \, \delta\{u - D(u_1,u_2)\}$$

$$+ [p_c^4 + 4p_c^3 \delta p] \prod_{i=1}^{4} \left\{ \int du_i \, Q^{(n)}(u_i) \right\} \delta\{ u - L[D(u_1,u_2); D(u_3,u_4)] \}$$

Using the binary approximation as outlined in section (c) but discarding terms of second or higher order in the variables δp and $u \equiv K_{//}^{(d=1)}$ (assumed infinitesimal) our final scaling equations for the anisotropy, concentration and thermal parameters under a length dilation transformation by a factor $b = 2$ become:

i) Well Below Crossover $(h \gg 1)$

$$\Theta' = 2\Theta$$
$$\delta p' = \lambda_p \delta p$$
$$(u - u^*) = K_{//}^{(d=1)'} = \lambda_p (u - u^*)$$
$$= \lambda_p K_{//}^{(d=1)}$$

(4.d.7)

where:

$$K_{//}^{(d=1)} \equiv K^{(d=1)}(h,\Theta)$$

$$K_{//}^{(d=1)\prime} \equiv K^{(d=1)}(h',\Theta')$$

and λ_p was previously defined in (4.d.5).

Thus, well below crossover, the thermal and concentration variables scale with the same factor, λ_p, under a length dilation transformation. This result is valid beyond the binary approximation and in arbitrary dimensionality in agreement with the exact result obtained from the field theoretic treatment of the problem given by Wallace and Young (1978).

ii) Well Above Crossover ($h \ll 1$).

$$\Theta' = 2\Theta$$

$$\delta p' = \lambda_p \delta p \qquad (4.d.8)$$

$$(u-u^*)' = K_{//}^{(d=1)\prime} = (\lambda_p + p_c^3)(u-u^*)$$
$$= (\lambda_p + p_c^3) K_{//}^{(d=1)}$$

It is important to note that these results imply that asymptotically close to zero temperature and the critical concentration, p_c, the thermal variable scaling is unaffected, to lowest order, by the accompanying concentration scaling. This may be confirmed by comparing the thermal variable scaling in equations (4.d. 7-8) with those obtained precisely at percolation threshold ($\delta p = 0$) in equations (4.c. 13-14). By assuming that this behaviour is true beyond the binary approximation but asymptotically close to zero temperature and the percolation threshold, we may incorporate the exact results, equations (4.c. 20-21) into this scheme to obtain our final results

for the anisotropy, concentration and thermal variable scalings under a length dilation of our system by a factor $b = 2$ as:

$$\left.\begin{aligned} \Theta' &= b\Theta \\ t' &= bt \\ (\delta p')^{\nu_p} &= b(\delta p)^{\nu_p} \end{aligned}\right\} \qquad (4.d.9)$$

where:

$$t \sim \begin{cases} \left(K_{//}^{(d=1)}\right)^{\nu_{HEIS}} & : h \ll 1 \\ \left(K_{//}^{(d=1)}\right)^{\nu_p} & : h \gg 1 \end{cases} \qquad (4.d.9(a))$$

$$\nu_p = \frac{\ln 2}{\ln 4p_c(1-p_c^2)}$$

$$\nu_{HEIS} \simeq 1.23$$

We now consider the implications of equations (4.d.9) for the behaviour of inverse correlation lengths and wavevector dependent susceptibilities of the dilute, anisotropic two-dimensional magnetic system at low temperatures near percolation threshold.

iii) Inverse Correlation Length Behaviour At Low Temperatures Near p_c

As a matter of notation, and to avoid possible confusion, we will denote the inverse correlation lengths of the two-dimensional model near percolation threshold as:

$$\frac{1}{\xi_{//}} \equiv \frac{1}{\xi_{//}(\delta p, T, \mu)} \quad ; \quad \frac{1}{\xi_{\perp}} \equiv \frac{1}{\xi_{\perp}(\delta p, T, \mu)}$$

This should be compared with the notation which was previously introduced to represent the I.C.L.'s of the pure, one-dimensional system viz:

$$K_{//}^{(d=1)} \; ; \; K_{\perp}^{(d=1)}$$

Using the results (4.d.9) and similar arguments to those initially presented to treat the pure, two-dimensional model in Chapter 3, the I.C.L.'s of the dilute model may be expressed as:

$$\frac{1}{\xi_{//}} \equiv \Theta \Phi_{//}^{\lessgtr}\left(\frac{t}{\Theta}, \frac{|\delta p|^{\nu_p}}{\Theta}\right) \qquad (4.d.10)$$

$$\frac{1}{\xi_{\perp}} \equiv \Theta \Phi_{\perp}^{\lessgtr}\left(\frac{t}{\Theta}, \frac{|\delta p|^{\nu_p}}{\Theta}\right) \qquad (4.d.11)$$

with the superscript $>$ ($<$) denoting behaviour for values of the bond concentration greater (less) than percolation threshold. Our reasons for distinguishing between the two regimes will become clearer as we proceed.

We firstly consider the behaviour of the I.C.L.'s for a model in which the bond concentration lies below the critical value. In this case we have:

$$\frac{1}{\xi_{//}} = \Theta \Phi_{//}^{<}\left(\frac{t}{\Theta}, \frac{|\delta p|^{\nu_p}}{\Theta}\right) \; ; \; \frac{1}{\xi_{\perp}} = \Theta \Phi_{\perp}^{<}\left(\frac{t}{\Theta}, \frac{|\delta p|^{\nu_p}}{\Theta}\right)$$

within such a concentration regime, no transition to L.R.O occurs in the dilute model, even at absolute zero temperature. By taking the limits:

(i) $\Theta \to 0^{+}$ Isotropic Heisenberg

(ii) $\Theta \to \infty$ Ising

and exploiting the absence of a phase transition we obtain:

$$\frac{1}{\xi_{//}} \sim \frac{1}{\xi_{\perp}} \sim |\delta p|^{\nu_p} \left| \top \right|^{<}\left(\frac{t}{|\delta p|^{\nu_p}}\right) \; : \; \left(\frac{t}{\Theta}, \frac{|\delta p|^{\nu_p}}{\Theta} \to \infty\right) \qquad (4.d.12)$$

$$\frac{1}{\xi_{//}} \sim |\delta p|^{\nu_p} \Big|\Big|_{//}^{<}\left(\frac{t}{|\delta p|^{\nu_p}}\right) \qquad \left(\frac{t}{\Theta}, \frac{|\delta p|^{\nu_p}}{\Theta} \longrightarrow 0^{+}\right) \quad (4.d.13)$$

By working at asymptotically low temperatures and demanding that the transverse I.C.L. remain finite we have:

$$\frac{1}{\xi_{\perp}} \sim \Theta\, G_{\perp}^{<}\left(\frac{|\delta p|^{\nu_p}}{\Theta}\right) \qquad (t \ll \Theta) \qquad (4.d.14)$$

Considering equations (4.d. 12) and (4.d. 13) in the limits of

$$(i)\ \frac{t}{|\delta p|^{\nu_p}} \gg 1 \quad ; \quad (ii)\ \frac{t}{|\delta p|^{\nu_p}} \ll 1$$

results in the limiting forms:

$$\frac{1}{\xi_{//}} \sim \frac{1}{\xi_{\perp}} \sim t \sim [K_{//}^{(d=1)}]^{\nu_{HEIS}} \qquad \left(\frac{t}{\Theta}, \frac{|\delta p|^{\nu_p}}{\Theta} \gg 1 ; \frac{t}{|\delta p|^{\nu_p}} \gg 1\right) \quad (4.d.15)$$

$$\frac{1}{\xi_{//}} \sim \frac{1}{\xi_{\perp}} \sim |\delta p|^{\nu_p} \qquad \left(\frac{t}{\Theta}, \frac{|\delta p|^{\nu_p}}{\Theta} \gg 1 ; \frac{t}{|\delta p|^{\nu_p}} \ll 1\right)$$

$$\frac{1}{\xi_{//}} \sim t \sim [K_{//}^{(d=1)}]^{\nu_p} \qquad \left(\frac{t}{\Theta}, \frac{|\delta p|^{\nu_p}}{\Theta} \ll 1 ; \frac{t}{|\delta p|^{\nu_p}} \gg 1\right) \quad (4.d.16)$$

$$\frac{1}{\xi_{//}} \sim |\delta p|^{\nu_p} \qquad \left(\frac{t}{\Theta}, \frac{|\delta p|^{\nu_p}}{\Theta} \ll 1 ; \frac{t}{|\delta p|^{\nu_p}} \ll 1\right)$$

The limiting behaviour of the transverse I.C.L. may be determined in a similar manner. For example, by imposing the finiteness of $1/\xi_{\perp}$ at percolation threshold one obtains:

$$\frac{1}{\xi_{\perp}} \sim \Theta \sim K_{\perp}^{(d=1)} \quad : \quad \left(\frac{t}{\Theta} \ll 1 \; ; \; \delta p = 0\right) \quad (4.d.17)$$

The forms obtained above are already sufficient to suggest that the

weakly dilute model is capable of displaying a far wider range of crossover behaviour than its pure analogue. Well above the crossover temperature of the corresponding one-dimensional model the behaviour is characteristically Heisenberg-like, well below the model crosses over to Ising-like behaviour and, unless one works precisely at the critical concentration, there is a crossover to purely geometric behaviour as absolute zero temperature is approached. We now turn our attention to the behaviour of models in which the bond concentration is greater than the critical value.

Above percolation threshold, our expression (4.d. 10) for the longitudinal I.C.L. becomes:

$$\frac{1}{\xi_{\parallel}} = \Theta \, \Phi_{\parallel}^{>}\left(\frac{t}{\Theta}, \frac{|\delta p|^{\nu_p}}{\Theta} \right)$$

Except in the Isotropic Heisenberg limit, our model will now undergo a transition to L.R.O. at some non-zero temperature $T_c(\delta p, \Theta)$. Thus, working at finite temperature, but not at the critical temperature itself, and considering the limits of $\Theta \to 0, \infty$ (so that the I.C.L. remains finite and non-zero) we obtain:

$$\frac{1}{\xi_{\parallel}} \sim |\delta p|^{\nu_p} \, g_{\parallel}^{>}\left(\frac{t}{|\delta p|^{\nu_p}} \right) \quad \left(\frac{t}{\Theta}, \frac{|\delta p|^{\nu_p}}{\Theta} \ll 1 ; T \neq T_c(\delta p, \Theta) \right) \qquad (4.d.18)$$

$$\frac{1}{\xi_{\perp}} \sim |\delta p|^{\nu_p} \, h_{\parallel}^{>}\left(\frac{t}{|\delta p|^{\nu_p}} \right) \quad \left(\frac{t}{\Theta}, \frac{|\delta p|^{\nu_p}}{\Theta} \gg 1 ; T \neq T_c(\delta p, \Theta) \right) \qquad (4.d.19)$$

Provided that the transition to L.R.O is continuous, the longitudinal I.C.L. will have a zero at $T_c(\delta p, \Theta)$. Thus, the functions $g_{\parallel}^{>}(z)$ and $h_{\parallel}^{>}(x)$ must also have a zero at some critical value of their argument viz:

$$g_{\parallel}^{>}(z_c) = 0 \; ; \; h_{\parallel}^{>}(x_c) = 0$$

where:

$$z_c = \frac{a_1 t(T_c[\delta p,\Theta])}{|\delta p|^{\nu_p}} \; ; \; x_c = \frac{a_2 t(T_c[\delta p,0])}{|\delta p|^{\nu_p}} = 0$$

and a_1, a_2 are both of order one [$O(1)$].

In the neighbourhood of these critical values, the (possibly non-analytic) functions $g_{//}^{>}$ and $h_{//}^{>}$ may be expanded as:

$$g_{//}^{>}(z) \sim \begin{cases} (z - z_c)^{\beta^{+}_{ISING}} \; ; \; z > z_c \\ \\ |(z - z_c)|^{\beta^{-}_{ISING}} \; ; \; z < z_c \end{cases} \qquad |z - z_c| \ll 1$$

(4.d. 20)

$$h_{//}^{>}(x) \sim x^{\beta_{HEIS}} \qquad x \ll 1.$$

where $\beta^{\pm}_{ISING}$ and β_{HEIS} are the exponents associated with the Ising and Heisenberg limits of our model respectively. Hence, the behaviour of the longitudinal I.C.L. on approaching a finite temperature transition is:

$$\frac{1}{\xi_{//}} \sim |\delta p|^{\nu_p} \left| \frac{t - t_c(\delta p,\Theta)}{|\delta p|^{\nu_p}} \right|^{\beta^{\pm}_{ISING}} \qquad \left(t, |\delta p|^{\nu_p} \ll \Theta \; ; \; \frac{|t - t_c|}{|\delta p|^{\nu_p}} \ll 1 \right)$$

$$\frac{1}{\xi_{//}} \sim |\delta p|^{\nu_p} \left| \frac{t}{|\delta p|^{\nu_p}} \right|^{\beta_{HEIS}} \qquad \left(t, |\delta p|^{\nu_p} \gg \Theta \; ; \; \frac{t}{|\delta p|^{\nu_p}} \ll 1 \right)$$

(4.d.21)

Equations (4.d. 19) et sequens allow us to determine the dependence of the weakly anisotropic model's critical temperature on concentration and anisotropy since the limits:

$$t \gg \Theta \; ; \; t \ll \Theta$$

correspond to being well above or below the crossover temperature of the corresponding one-dimensional system, respectively. Hence, for a weakly anisotropic system sufficiently close to percolation threshold that the phase transition takes place below the one-dimensional crossover temperature, the critical condition reduces to:

$$K_{//}^{(d=1)}[T_c(\delta p, \Theta), \Theta] = a_o \delta p$$

or

$$T_c(\delta p, \Theta) \sim \frac{J}{k_B} \frac{2\Theta}{\ln 1/|\delta p|} \quad \{t_c, |\delta p|^{\nu_p} << \Theta\} : (4.d.22)$$

Similar methods to those outlined above may be used to determine the limiting forms of both longitudinal and transverse I.C.L.'s in various other limits. However, we leave our discussion of the I.C.L.'s here and move on to consider the behaviour of the wavevector dependent susceptibilities for the dilute model.

iv) The Wavevector Dependent Susceptibility Behaviour At Low Temperatures Near Pc.

Employing equations (4.d.9) and arguments completely analagous to those introduced to treat the W.D.S's of the pure two-dimensional

model in Chapter 3 (section (ii)), we may express the longitudinal and transverse W.D.S.'s of the dilute model as:

$$\chi_{//,\perp} = \Theta^{-\gamma} \Gamma^{>}_{//,\perp}\left(\frac{t}{\Theta}, \frac{|\delta p|^{\nu_p}}{\Theta}, \frac{q_\nu}{\Theta}\right) \qquad (4.d.26)$$

where, as in the last section, the superscript $>$ ($<$) refers to behaviour above (below) percolation threshold. For the sake of brevity we restrict our attention to the longitudinal W.D.S. but similar results to those presented here, and in the previous section, may be used to obtain results for the transverse W.D.S.

For a model in which the concentration of bonds is less than the critical value, p_c, equation (4.d. 26) becomes:

$$\chi_{//} = \Theta^{-\gamma} \Gamma^{<}_{//}\left(\frac{t}{\Theta}, \frac{|\delta p|^{\nu_p}}{\Theta}, \frac{q_\nu}{\Theta}\right) \qquad (4.d.27)$$

Since we expect there to be no transition to L.R.O. in such a concentration regime, the W.D.S.'s should remain finite at non-zero temperature and/or wavevector. This property may be exploited by taking the limit of $\Theta \to \infty$ in (4.d. 27) and imposing the condition that $\chi_{//}$ remain finite in this limit. Thus:

$$\chi_{//} \sim t^{-\gamma_{ISING}} G^{<}\left(\frac{|\delta p|^{\nu_p}}{t}, \frac{q_\nu}{t}\right) \qquad (4.d.28)$$

$$[\, t, |\delta p|^{\nu_p}, q_\nu \ll \Theta \,]$$

Furthermore, the W.D.S. should remain finite if the percolation threshold is approached at finite temperature and/or q_ν so that:

$$\chi_{//} \sim t^{-\gamma_{ISING}} g^{<}\left(\frac{q_\nu}{t}\right) \quad [|\delta p|^{\nu_p} \ll t, q_\nu \ll \Theta]$$

By further restricting our attention to the regime in which:

$$q \ll t$$

we may expand the function $g^{<}(x)$ to obtain:

$$\chi_{//} \sim t^{-\gamma_{ISING}} \left\{ a_0 - \beta q_{//}^2 / t^2 + O\left(q_{//}^4 / t^4\right) \right\}$$

whence we have:

$$\chi_{//} \sim \frac{a_0 t^{2-\gamma_{ISING}}}{t^2 + \beta_0 q_{//}^2} : [|\delta p|^{\nu_p} \ll q \ll t \ll \Theta] \qquad (4.d.29)$$

By using the methods of Chapter 3, it is possible to show that the exponent, γ_{ISING} in (4.d. 28) et seq. is that characteristic of the dilute Ising model. In a similar fashion, by considering the limit of temperature tending to absolute zero in (4.d. 28) at finite $|\delta p|^{\nu_p}$ and q we obtain:

$$\chi_{//} \sim |\delta p|^{-\gamma_{ISING}\nu_p} f^{<}\left(\frac{q_{//}}{|\delta p|^{\nu_p}}\right) \qquad [t \ll |\delta p|^{\nu_p}, q \ll \Theta]$$

and hence:

$$\chi_{//} \sim \frac{a_0 |\delta p|^{(2-\gamma_{ISING})\nu_p}}{|\delta p|^{2\nu_p} + \beta_0 q_{//}^2} \qquad [t \ll q \ll |\delta p|^{\nu_p} \ll \Theta] \qquad (4.d.30)$$

Above percolation threshold we expect the dilute model to undergo a finite temperature transition to a state of L.R.O. Within this concentration regime (4.d. 26) becomes:

$$\chi_{//} = \Theta^{-\gamma} \Gamma_{//}^{>}\left(\frac{t}{\Theta}, \frac{|\delta p|^{\nu_p}}{\Theta}, \frac{q_{//}}{\Theta}\right) \qquad (4.d.31)$$

By working away from the critical temperature, $T_c(\delta p, \Theta)$, taking the limit of $\Theta \to \infty$ and noting that $\chi_{//}$ should remain finite in such a limit we obtain:

$$\chi_{//} \sim |\delta p|^{-\gamma\nu_p} G^{>}_{//}\left(\frac{t}{|\delta p|^{\nu_p}}, \frac{q}{|\delta p|^{\nu_p}}\right) \qquad (4.d.32)$$

$$[t, |\delta p|^{\nu_p}, q << \Theta : T \neq T_c(\delta p, \Theta)]$$

From our work on the I.C.L.'s in the previous section we know that the dilute system above percolation threshold undergoes a second order transition when:

$$\frac{t_c(\delta p)}{|\delta p|^{\nu_p}} \equiv Z_c$$

In order to investigate the limiting behaviour of the longitudinal W.D.S. near this transition, it is useful to consider the inverse of the function viz:

$$\frac{1}{\chi_{//}} \sim |\delta p|^{\gamma\nu_p} B^{>}_{//}\left(\frac{t}{|\delta p|^{\nu_p}}, \frac{q}{|\delta p|^{\nu_p}}\right) \qquad (4.d.35)$$

$$[t, |\delta p|^{\nu_p}, q << \Theta : T \neq T_c(\delta p, \Theta)]$$

Since this function is expected to have a zero at $t_c(\delta p), q = 0$ we have:

$$B^{>}_{//}(Z_c, 0) = 0 \qquad (4.d.36)$$

It therefore seems plausible that:

$$\frac{1}{\chi_{//}} \sim |\delta p|^{\gamma_{ISING}\nu_p} \left|\frac{t - t_c(\delta p)}{|\delta p|^{\nu_p}}\right|^{\sigma^{I}_{ISING}} : \begin{pmatrix} t, |\delta p|^{\nu_p} << \Theta : q = 0 \\ |t - t_c(\delta p)| << |\delta p|^{\nu_p} \end{pmatrix} \qquad (4.d.37)$$

where we have expanded the possibly non-analytic function $B^{>}_{//}(Z,0) \equiv f^{>}_{//}(Z)$ about its zero, and introduced the new exponents

$$\{\sigma^{I}_{ISING}\}$$

corresponding to behaviour above and below the critical temperature, to characterise the function's decay.

Precisely at the critical concentration, p_c, equations (4.d.27) and (4.d.31) become:

$$\chi_{//} = \Theta^{-\gamma} \Gamma_{//}^{\gtrless}\left(\frac{t}{\Theta}, 0, \frac{q_\nu}{\Theta}\right) \equiv \Theta^{-\gamma}\,\Phi\left(\frac{t}{\Theta}, \frac{q_\nu}{\Theta}\right) \qquad (4.d.38)$$

so that by considering the limits of $\Theta \to 0^{+}$ and $\Theta \to \infty$ we have:

$$\chi_{//} \sim \frac{a_0 t^{2-\gamma_{HEIS.}}}{t^2 + b_0 q_\nu^2} \qquad [p = p_c ;\ t \gg q_\nu \gg \Theta] \qquad (4.d.39)$$

$$\chi_{//} \sim \frac{a_0 t^{2-\gamma_{ISING}}}{t^2 + b_0 q_\nu^2} \qquad [p = p_c ;\ q_\nu \ll t \ll \Theta] \qquad (4.d.40)$$

where γ_{HEIS} and γ_{ISING} refer to the exponents relevant to the isotropic Heisenberg and Ising models at percolation threshold, respectively.

Until now we have only considered the behaviour of the dilute, two-dimensional anisotropic Heisenberg model near percolation threshold. Below, we briefly show how the binary or 'first moment matching' approximation may be used to investigate the qualitative behaviour of the same model near its pure limit.

e) Behaviour Of The Dilute, Anisotropic Heisenberg Model Near The Pure Limit

Near the pure ($p = 1$) limit, our scaling equations (4.b.7-9) may be treated within the binary approximation to give:

$$\delta p' = 0 \qquad (4.e.1(a))$$

$$\Theta' = 2\Theta \qquad (4.e.1(b))$$

$$h' = 2(1 - 2\delta p)(h - \tfrac{1}{2}.\ln 2.\tanh\Theta) \qquad (4.e.1(c))$$

where we have used h as the thermal parameter and terms of second or higher order in the small variable:

$$\delta p = 1 - p$$

have been discarded. The resulting set of equations (4.e. 1) may be used to determine the form of the critical surface near both the Ising and Isotropic Heisenberg fixed points.

i) The Form Of The Critical Surface In The Vicinity Of The Pure Isotropic Heisenberg Fixed Point

Near an Isotropic Heisenberg fixed point, the anisotropy scaling in (4.e. 1(b)) may be re-expressed in terms of the variable:

$$x \equiv \frac{1}{\cosh \mu}$$

as:

$$x' \simeq 2x(1-x^2) \quad : \quad (x \to 0^+) \qquad (4.e.2)$$

Thus, multiplying through both sides of (4.e. 1(c)) by $(1/x')$ we obtain the thermal variable scaling near the pure Isotropic Heisenberg fixed point as

$$K' \simeq (1-2\delta p)(K - \tfrac{1}{2}\ln 2) \qquad (4.e.3)$$

where we have discarded terms of order two or higher in the small variables δp and x. In the vicinity of this fixed point there are two relevant parameters. One is the anisotropy parameter viz:

$$\Theta' = 2\Theta$$

the other is obtained from (4.e. 3) as:

$$\omega' = e^{-2K'(1-2\delta p') + 2\ln 2 . \delta p'} \equiv e^{-2K(1-2\delta p) + 2\ln 2 . \delta p + \ln 2}$$

$$= 2\omega \qquad (4.e.4)$$

The critical condition near this fixed point is therefore:

$$\omega = a_0 \Theta \qquad (4.e.4(a))$$

which, using (4.e. 4) gives the dependence of critical temperature on anisotropy and concentration as:

$$\frac{k_B T_c(\cosh\mu, p)}{J} = \frac{2[2p - 1 + O(1/\cosh^2\mu)]}{\ln(1/a_0.\cosh\mu)} \qquad (4.e.5)$$

and, hence:

$$\left.\frac{1}{T_c}\frac{dT_c}{dp}\right|_{p=1} = 2(1 + O[1/\cosh^2\mu]) \qquad (4.e.6)$$

The expression (4.e. 5) is in good agreement with the corresponding result obtained by Stinchcombe (1981) using the Suzuki-Takano method.

The form for the logarithmic derivative (4.e. 6) in the isotropic limit agrees exactly with that of McGurn (1979) obtained from a random phase approximation treatment of the model.

ii) The Form Of The Critical Surface In The Vicinity Of The Pure Ising Fixed Point

Near the pure Ising fixed point, equation (4.e. 1(b)) for the anisotropy parameter scaling may be re-expressed in terms of the variable $\cosh\mu$ as:

$$\cosh\mu' \simeq \cosh\mu\left(1 - \frac{\mu^2}{2}\right) \qquad (4.e.7)$$

where terms of fourth or higher order in the variable μ have been discarded. Multiplying through both sides of (4.e. 1(c)) by $\cosh\mu'$ we have:

$$K' = 2(1 - 2\delta p - \mu^2/2).(K - \tfrac{1}{2}.\ln 2) \qquad (4.e.8)$$

Near this fixed point, the only relevant scaling variable is:

$$\omega \equiv K[1-2\delta p-\mu^2/2] + \ln 2.\delta p + \tfrac{1}{4}.\ln 2.\mu^2 - \ln 2 \qquad (4.e.9)$$

In the same limit, the form of the critical surface is given by:

$$\omega \equiv 0$$

Hence, we obtain the dependence of the critical temperature upon anisotropy and concentration in this limit as:

$$\frac{k_B T_c}{J}(\mu, p) \simeq \frac{1}{\ln 2}\left(p-\frac{\mu^2}{4}\right) \qquad (4.e.10)$$

so that:

$$\frac{1}{T_c}\frac{dT_c}{dp}\bigg|_{p=1} \simeq \left(1+\frac{\mu^2}{4}\right) \qquad (4.e.11)$$

Our final expression (4.e.11) for the logarithmic derivative at the pure limit compares badly with the result:

$$\frac{1}{T_c}\frac{dT_c}{dp}\bigg|_{p=1} \simeq 1.329$$

obtained by Harris (1974) using perturbation theory at the Ising limit. The dependence of (4.e.11) on anisotropy is, however, in qualitative agreement with Stinchcombe (1981).

This completes our treatment of the dilute, two-dimensional, anisotropic system. In Chapter 6 we will discuss the results obtained in more detail and their relevance to the interpretation of experimental data such as that obtained by Birgeneau et al. (1980).

In the next chapter, we apply our analysis to the pure and dilute three-dimensional model.

Chapter 5

The Three-Dimensional System

a) Introduction

In this chapter we extend our treatment of the anisotropic Heisenberg model to include the pure and dilute three-dimensional systems.

In section (b) we direct our attention to the inverse correlation length (I.C.L.), transition temperature and wavevector dependent susceptibility (W.D.S.) behaviour in the pure, three-dimensional system. The methods of analysis we employ are completely analagous to those used in Chapter 3 to probe the behaviour of the corresponding two-dimensional systems.

In section (c) we consider the effects of bond dilution on the three-dimensional model. In particular, we determine various limiting forms for the I.C.L.'s and W.D.S.'s of the dilute model near percolation threshold. The analysis employed is, again, a straightforward extension of that previously used to investigate the two-dimensional model.

In the final section of this chapter, section (d), we give a brief discussion of the dilute, three-dimensional anisotropic model near the pure limit.

b) The Pure Three-Dimensional System

In Chapter 3 we introduced the Migdal/Kadanoff (M-K) bond moving scheme and showed how the scheme could be applied to the pure, two-dimensional model to obtain approximate transformation equations for the anisotropy and thermal parameters under a dilation of the

underlying length scales of the system by a factor b. As discussed therein (Chapter 3, section (b)), the length dilation operation, within the M-K scheme, is built up from two basic combinations of bond movement (bond combination 'in parallel') and accompanying decimation: one along each of the basic lattice vector directions. In order to extend the applicability of the scheme to include the three-dimensional model, we have merely to carry out the bond combination 'in parallel'/decimation operations along all three basic lattice vector directions. This procedure is illustrated graphically in figure (14) for one bond combination/decimation operation along a single basic lattice vector direction of a simple cubic cluster. For the infinite simple cubic lattice, the operation is repeated along all three basic lattice vector directions in order to dilate the underlying length scales by a factor b = 2. From our results in Chapter 2 on the pure one-dimensional model, we may obtain the infinitesimal limit of the thermal and anisotropy parameter scalings in the three-dimensional model as; (cf. equations (3.c.1) and (2.b.11))

$$\Theta' = (1+\epsilon)\Theta = b\Theta \qquad (5.b.1)$$

$$h' = (1+2\epsilon)h - \frac{\epsilon}{2}\tanh\Theta \qquad (5.b.2)$$

under a length dilation by a factor:

$$b = 1+\epsilon \quad ; \quad \epsilon \to 0^{+}$$

In equations (5.b.1/2) we have omitted terms of second or higher order in the small quantity, ϵ . As pointed out in Chapter 3, taking the infinitesimal limit of this operation removes certain commutation difficulties.

Equation (5.b.1) immediately implies that the anisotropy parameter, Θ , is a scaling variable. In order to obtain a second scaling variable, we define:

$$u \equiv u(h,\Theta) \equiv \left\{ h - \frac{\Theta^2}{2} \int_{\Theta}^{\infty} \frac{\tanh x}{x^3}\, dx \right\}^{1/2} \qquad (5.b.3)$$

so that our final transformation equations become:

$$\Theta' = (1+\epsilon)\Theta = b\Theta$$
$$u' = (1+\epsilon)u = bu \qquad (5.b.4)$$

We now use the forms (5.b.4) to obtain details of the limiting behaviour of the inverse correlation lengths (I.C.L.'s) and wavevector dependent susceptibilities (W.D.S.'s) of the pure, three-dimensional model.

Under the length dilation operation the I.C.L.'s of the system scale as:

$$K_{//,\perp}(\Theta,u) \longrightarrow K'_{//,\perp}(\Theta,u) \equiv bK_{//,\perp}(\Theta,u)$$
$$= K_{//,\perp}(\Theta',u')$$

where, in the last equality, we have interpreted the change in length scale as a change in the parameters Θ ,u. Using (5.b.4) in the above we obtain:

$$K_{//,\perp}(\Theta,u) \equiv \Theta\, \Phi_{//,\perp}(u/\Theta) \qquad (5.b.5)$$

In order to determine the functional form of $\Phi_{//,\perp}(x)$ we consider the Ising and Isotropic Heisenberg limits of (5.b.5).

At the Ising limit, the anisotropy scaling variable, Θ ,

diverges and the second scaling variable, u, defined in (5.b.3) becomes:

$$u \sim [K - K_c^{ISING}]^{1/2} \quad : \quad K_c^{ISING} \equiv 1/4 \qquad (5.b.6)$$

We may immediately deduce the form of $\Phi_{//}(x)$ for small x by noting that the longitudinal I.C.L. of the Ising model should be finite and non-zero except, possibly, at a second order phase transition whence:

$$\Phi_{//}(x) \sim |x| \quad : \quad (|x| \rightarrow 0^+) \qquad (5.b.7)$$

Our analysis therefore predicts that the longitudinal I.C.L. of the three-dimensional Ising model tends to zero as:

$$K_{//}^{ISING} \sim |K - K_c^{ISING}|^{\nu_2} \qquad (5.b.8)$$

near the critical temperature;

$$T_c^{ISING} = \frac{4J}{k_B} \qquad (5.b.9)$$

At the Isotropic Heisenberg limit of (5.b.3), where Θ tends to zero, the variable u becomes:

$$u \sim \Theta^{1/2}[K - K_c^{HEIS.}]^{1/2} \qquad (\Theta \rightarrow 0^+)$$

$$K_c^{HEIS.} = 1/2 \qquad (5.b.10)$$

In order that the longitudinal and transverse I.C.L.'s be equal and share a single zero in this limit, the behaviour of the functions $\Phi_{//,\perp}(x)$ must be such that:

$$\Phi_{//}(x) \sim \Phi_{\perp}(x) \sim |x|^2 \quad : \quad (|x| \rightarrow \infty) \qquad (5.b.11)$$

In this case, the I.C.L. behaviour of the Isotropic Heisenberg model

is predicted as:

$$K_{//}^{HEIS.} = K_{\perp}^{HEIS.} \sim |K - K_c^{HEIS.}| \qquad (5.b.12)$$

with a non-zero temperature phase transition occuring at:

$$T_c^{HEIS.} = \frac{2J}{k_B} \qquad (5.b.13)$$

The forms (5.b.7) and (5.b.11) now enable us to make various predictions about the behaviour of the two I.C.L.'s for systems with arbitrary anisotropy values. In particular, we may investigate the I.C.L. forms for the weakly anisotropic system in which:

$$\Theta \ll 1$$

As a first step in this direction we re-express equation (5.b.3) for the second scaling variable, u, as:

$$u \equiv [h - h_c(\Theta)]^{1/2} \qquad (5.b.14)$$

where:

$$h_c(\Theta) \equiv \frac{\Theta^2}{2}\int_{\Theta}^{\infty} dx \cdot \frac{\tanh x}{x^3}$$

By inspection of equations (5.b.7) and (5.b.11) we see that the behaviour of the longitudinal I.C.L. will depend on whether the variable;

$$x \equiv \frac{u}{\Theta}$$

is much greater than or much less than unity. In the former case viz:

$$x = \frac{u}{\Theta} \gg 1$$

the longitudinal and transverse I.C.L.'s are given by:

$$K_{//} \sim K_{\perp} \sim \frac{1}{\Theta}|h - h_c(\Theta)| \; : \; (u \gg \Theta) \qquad (5.b.15)$$

In the latter case viz:

$$x = \frac{u}{\Theta} \ll 1.$$

the form for the longitudinal I.C.L. may be obtained from (5.b.7) as:

$$K_{//} \sim |h - h_c(\Theta)|^{1/2} \qquad (5.b.16)$$

This last form predicts that the weakly anisotropic model in three dimensions undergoes a second order phase transition at a non-zero temperature, $T_c(\Theta)$, where:

$$\frac{J}{k_B T_c(\Theta)} = \frac{\cosh \mu . \Theta}{2} \int_{\Theta}^{\infty} \frac{\tanh x}{x^3} \, dx \qquad (5.b.17)$$

$$\sim \frac{1}{2} + O(\Theta) \; : \; (\Theta \to 0^+)$$

The full dependence of critical temperature upon anisotropy is illustrated in figure (15).

In order to determine the form of the transverse I.C.L. when the critical temperature is approached, we have merely to note that the I.C.L. should remain finite in this limit whence:

$$\Phi_{\perp}(x) \sim c_0, \quad \text{a constant} \quad (|x| \to 0) \qquad (5.b.18)$$

Thus:

$$K_{\perp} \sim c_0 \Theta \quad : \; (\Theta \ll 1 ; \; u \ll \Theta) \qquad (5.b.19)$$

In summary, the weakly anisotropic model in three dimensions displays typically Heisenberg-like behaviour when the variable:

$$|X| = \left| \frac{u}{\Theta} \right| = \left| \frac{h - h_c(\Theta)}{\Theta} \right|^{1/2}$$

is much greater than unity, but Ising-like behaviour when it is much

less than unity. This allows us to estimate the characteristic crossover temperature, $T_x(\Theta)$, of the system through the relationship:

$$|h - h_c(\Theta)|_{T_x(\Theta)} \sim \Theta^2 \qquad (5.b.20)$$

For the weakly anisotropic system this reduces to:

$$T_x(\Theta \ll 1) \sim \frac{2J}{k_B}(1 - a_o\Theta)$$

where

$$a_o = O(1)$$

Having shown how various limiting forms may be obtained for both the longitudinal and transverse I.C.L.'s in the anisotropic model, we now turn our attention to the wave vector dependent susceptibility (W.D.S.) behaviour.

Under a length dilation operation the susceptibility scales as:

$$\chi_{//,\perp}(\Theta, u, q) \rightarrow \chi'_{//,\perp}(\Theta, u, q) = b^{-\gamma}\chi_{//,\perp}(\Theta, u, q)$$

$$= \chi_{//,\perp}(\Theta', u', q')$$

where u' and Θ' are given by (5.b.4) and:

$$q' = (1+\epsilon)q = bq$$

This last expression results from the fact that the wavevector q, defines a new, relevent, inverse length in the system. By combining the scaling equations for $\chi_{//,\perp}$ and q with equations (5.b.4) we obtain:

$$\chi_{//,\perp}(\Theta, u, q) = \Theta^{-\gamma}\Gamma_{//,\perp}\left(\frac{u}{\Theta}, \frac{q}{\Theta^{\nu}}\right) \qquad (5b.21)$$

We recognise the first variable in $\Gamma_{//,\perp}$ viz:

$$\times \equiv \frac{u}{\Theta}$$

as the crossover variable which arose in our investigation of the I.C.L. behaviour.

By considering the Ising limit of (5.b.21) away from the critical temperature and at finite wavevector we obtain:

$$\chi_{//}^{ISING} \sim u^{-\gamma_{ISING}} G_{//}\left(\frac{q_v}{u}\right) \sim \left(K_{//}^{ISING}\right)^{-\gamma_{ISING}} G_{//}\left(q_v / K_{//}^{ISING}\right)$$

and:

$$\Gamma_{//}(x,y) \sim |x|^{-\gamma_{ISING}} G_{//}\left(\frac{y}{x \equiv}\right) \quad : (x,y \to 0^{+}) \qquad (5.b.22)$$

The expressions above allow us to identify γ_{ISING} in equations (5.b.22) as the critical exponent of the three-dimensional Ising model.

By taking the Isotropic Heisenberg limit of equation (5.b.21) we obtain:

$$\chi_{\perp}^{HEIS.} = \chi_{//}^{HEIS.} \sim \left(K_{//,\perp}^{HEIS}\right)^{-\gamma_{HEIS.}} H_{//,\perp}\left(q / K_{//,\perp}^{HEIS.}\right) : (5.b.23)$$

and:

$$\Gamma_{//,\perp}(x,y) \sim |x|^{-2\gamma_{HEIS.}} H_{//,\perp}(y/x^{2}) \qquad (x,y \to \infty)$$

We now identify $\gamma_{HEIS.}$ in equations (5.b.23) as being the susceptibility exponent of the three-dimensional Isotropic Heisenberg model. Equations (5.b.22/23) suggest that, as in the two-dimensional model, the critical exponent γ is crossover-dependent viz:

$$\gamma \sim \begin{cases} \gamma_{ISING} : |x| \to 0 \\ \\ \gamma_{HEIS.} : |x| \to \infty \end{cases} \qquad (5.b.24)$$

As in the case of the I.C.L's previously considered, forms such as (5.b.22/23) enable us to predict various limiting forms for the W.D.S's for intermediate values of the anisotropy parameter, Θ. Thus, for the weakly anisotropic model well above crossover we may use (5.b.23) to obtain:

$$\chi_{//} \sim \chi_{\perp} \sim (K_{//,\perp})^{-\gamma_{HEIS.}} H(q/K_{//,\perp}) : \begin{cases} x >> 1 \\ q >> \Theta \end{cases}$$

and, therefore

$$\chi_{//} \sim \chi_{\perp} \sim \frac{(K_{//,\perp})^{2-\gamma_{HEIS.}}}{(K_{//,\perp})^2 + \alpha_0 q^2} : (\Theta << q << K_{//,\perp}) \qquad (5.b.25)$$

Similarly, well below crossover, equation (5.b.22) may be used to obtain:

$$\chi_{//} \sim |h - h_c(\Theta)|^{-\gamma_{ISING}/2} G(q/|h-h_c(\Theta)|^{1/2})$$

$$\sim (K_{//})^{-\gamma_{ISING}} G(q/K_{//}) : (x << 1)$$

and, hence:

$$\chi_{//} \sim \frac{K_{//}^{2-\gamma_{ISING}}}{(K_{//})^2 + \beta_0 q^2} : (q << K_{//} << \Theta) \qquad (5.b.26)$$

In order to determine the form of the transverse W.D.S. well below crossover, we note that if the susceptibility is to remain finite as the critical temperature is approached we must have:

$$\Gamma_{\perp}(x,y) \sim a_0, \text{ a constant} : (|x| \to 0) \qquad (5.b.27)$$

and;

$$\chi_{\perp} \sim \frac{a_0 \Theta^{2-\gamma_{ISING}}}{\Theta^2 + \epsilon_0 q^2} \quad : (K_{\parallel} \ll q \ll \Theta) \qquad (5.b.28)$$

As in the previous chapter we note that the behaviour of both the transverse and longitudinal W.D.S. may be determined in various other limits by similar means although we have not done so explicitly here.

In the following section we turn our attention to the diluted system and, in particular, the behaviour of such a system in the neighbourhood of the percolation threshold.

c) The Dilute, Three-Dimensional Model Near Percolation Threshold

In Chapter 4 we showed how the two-dimensional, dilute system with magnetic interaction concentration, p, close to the critical value, p_c, could be treated within the framework of the Migdal/Kadanoff bond moving scheme. In particular, we pointed out that our treatment of the dilute system necessitated the introduction of a probability distribution for the thermal parameter, u, in sharp contrast to the pure model in which a single value of this variable was sufficient to characterise the entire system. Furthermore, provided we started from a system in which all bonds had the same anisotropy value, it was shown in Appendix 2 that it was always possible to parameterise the anisotropy of the resultant system after a length dilation operation, by another unique anisotropy value. In fact (see Appendix 2) this decoupling of the anisotropy variable scaling occurs in arbitrary dimensionality within the M-K scheme. Below, we demonstrate how the ideas and methods introduced in Chapter 4 may be adapted to treat the dilute, three-dimensional system near the critical concentration (p_c).

The dilute, three-dimensional system may be modelled as a network of spins whose interaction parameters $\{u_i\}$ are random variables distributed according to some probability distribution, $P(u_i)$ viz:

$$P(u_i) = (1-p)\delta(u_i) + p\delta(u_i - u) \qquad (5.c.1)$$

The system may therefore be characterised in terms of the anisotropy parameter (Θ), the concentration of interactions present (p) and the probability distribution (p.d.) $P(u_i)$

As in the analagous two-dimensional model, the length scaling transformation in three dimensions results in the p.d. for the interaction parameters losing its binary form under even a single interaction. In general, however, the probability distribution obtained after n iterations of the length scaling transformation, $P^{(n)}(u_i)$, is of the form:

$$P^{(n)}(u_i) = (1-p^{(n)})\delta(u_i) + p^{(n)}Q^{(n)}(u_i) \qquad (5.c.1(a))$$

The distribution (5.c.1) corresponding to a real, dilute system may be seen as a special case of (5.c.1(a)) with:

$$Q^{(0)}(u_i) = \delta(u_i - u)$$

Under the operations of the M-K bond moving scheme, as discussed for the three-dimensional case in section (b), the various parameters and distribution transform as:

$$\Theta' = 2\Theta = b\Theta$$

$$p' = 1 - (1-p^2)^4$$

$$p'Q'(u) = 4p^2(1-p^2)^3 \int du_1 \int du_2 Q(u_1) Q(u_2) \delta[u - D(u_1, u_2)]$$
$$+ 6p^4(1-p^2)^2 \prod_{i=1}^{4} \left\{ \int du_i Q(u_i) \right\} \delta[u - L\{D(u_1,u_2); D(u_3,u_4)\}]$$
$$+ 4p^6(1-p^2) \prod_{i=1}^{6} \left\{ \int du_i Q(u_i) \right\} \delta[u - L\{D(u_1,u_2); D(u_3,u_4); D(u_5,u_6)\}]$$
$$+ p^8 \prod_{i=1}^{8} \left\{ \int du_i Q(u_i) \right\} \delta[u - L\{D(u_1,u_2); D(u_3,u_4); D(u_5,u_6); D(u_7,u_8)\}]$$

(5.c.2)

where we have used the notation:

$$D(x,y)$$

to denote the thermal variable obtained on taking a trace over a spin connecting bonds with thermal variable x and y as in figure(11 (b)), and:

$$L\{a,b,c,\ldots\}$$

to denote the thermal variable obtained on combining bonds with thermal variables a,b,c,.... in parallel as illustrated in figure(11(b)).

The fixed point values of the concentration and anisotropy parameters may be obtained directly from (5.c.2) as:

$$\Theta^* = 0, \infty \qquad (5.c.3)$$

$$p^* = 0, p_c, 1 \qquad (5.c.4)$$

where p_c is the real solution of:

$$p^6 + p^5 - 3p^4 - 3p^3 + 3p^2 + 3p - 1 = 0$$

which satisfies:

$$0 < p_c < 1$$

From numerical work we have:

$$p_c \simeq 0.28$$

We now focus our attention on the probability distribution scaling

precisely at percolation threshold i.e. $p = p_c$, where the transformation (5.c.2) takes the form:

$$Q^{(n+1)}(u) \equiv R_2\{Q^{(n)}(u)\} \qquad (5.c.5)$$

$$\equiv a_0(p_c)\int du_1 \int du_2\, Q^{(n)}(u_1)\, Q^{(n)}(u_2)\, \delta[u - D(u_1,u_2)]$$

$$+ a_1(p_c)\prod_{i=1}^{4}\left\{\int du_i Q^{(n)}(u_i)\right\}\delta[u - L\{D(u_1,u_2); D(u_3,u_4)\}]$$

$$+ a_2(p_c)\prod_{i=1}^{6}\left\{\int du_i Q^{(n)}(u_i)\right\}\delta[u - L\{D(u_1,u_2); D(u_3,u_4); D(u_5,u_6)\}]$$

$$+ a_3(p_c)\prod_{i=1}^{8}\left\{\int du_i Q^{(n)}(u_i)\right\}\delta[u - L\{D(u_1,u_2); D(u_3,u_4); D(u_5,u_6); D(u_7,u_8)\}]$$

with:

$$a_0(p_c) \equiv 4p_c(1-p_c^2)^3 \equiv 4p_c/(1+p_c) \qquad (5.c.6)$$

$$a_1(p_c) \equiv 6p_c^3(1-p_c^2)^2$$

$$a_2(p_c) \equiv 4p_c^5(1-p_c^2)$$

$$a_3(p_c) \equiv p_c^7$$

In order to parameterise the distribution, $Q^{(n)}(u)$, we introduce the set of moments $\{m_\alpha^{(n)}\}$ defined through:

$$m_\alpha^{(n)} \equiv \int du\, Q^{(n)}(u).u^\alpha \qquad (5.c.7)$$

The fixed point distribution, $Q^*(u)$, then corresponds to the set $\{m_\alpha^*\}$ which remain invariant under the length dilation operation. In general it is extremely difficult to obtain the fixed point distribution, $Q^*(u)$, explicitly. However, following the

arguments first presented in Chapter 4 for the two-dimensional model, we are able to obtain the qualitative behaviour of the probability distribution scaling at percolation threshold by means of the binary approximation.

Below we treat both the Ising and Isotropic Heisenberg limits of our model precisely at p_c using the binary approximation.

A) The Three-Dimensional Ising Model At Percolation Threshold Using The Binary Approximation

For the Ising limit of our model at percolation threshold we again use the thermal variable

$$u \equiv e^{-2K}$$

which was introduced in the previous chapter (cf. Young & Stinchcombe (1976)). In this case, a single iteration of equation (5.c.2) from the initial distribution:

$$Q^{(0)}(u) = \delta(u - u^{(0)}) \qquad (5.c.8)$$

yields:

$$Q^{(1)}(u) = a_0(p_c)\,\delta(u - 2u^{(0)}) + a_1(p_c)\,\delta(u - O(u^{(0)2}))$$
$$+ a_2(p_c)\,\delta(u - O(u^{(0)3})) + a_3(p_c)\,\delta(u - O(u^{(0)4}))$$
$$\sim \delta(u - u^{(1)}) \qquad (5.c.9)$$

The quantity $u^{(1)}$ is determined by preservation of the first moment of the distribution as:

$$u^{(1)} = 2a_0(p_c)u^{(0)} + O(u^{(0)2}) \qquad (5.c.10)$$

and, hence, the thermal variable scaling at asymptotically low temperatures is, within the binary approximation, given by,

$$u' = \lambda_u^{ISING} u \qquad (5.c.11)$$

$$\lambda_u = 2a_0(p_c) = \frac{8p_c}{1+p_c} \sim 1.76 \qquad (5.c.12)$$

The relevant fixed point value of the thermal variable is therefore:

$$u^* = 0$$

corresponding to absolute zero temperature.

B) The Three Dimensional Isotropic Heisenberg Model At Percolation Threshold Using The Binary Approximation

For the Isotropic Heisenberg limit of our model at percolation threshold we use the thermal variable:

$$u \equiv 1/K$$

as previously introduced in Chapter 4. In this case, the scaling equation for the probability distribution $Q(u)$ starting from an initial distribution:

$$Q^{(')}(u) = \delta(u - u^{(')})$$

is given by:

$$Q^{(n+1)}(u) = a_0(p_c)\,\delta(u - 2u^{(n)}) + a_1(p_c)\,\delta(u - u^{(n)})$$
$$+ a_2(p_c)\,\delta(u - \tfrac{2}{3}u^{(n)}) + a_3(p_c)\,\delta(u - \tfrac{1}{2}u^{(n)})$$
$$\sim \delta(u - u^{(n+1)})$$

The quantity $u^{(n+1)}$ is determined via first moment matching as:

$$U^{(n+1)} = \left\{ 2a_0(p_c) + a_1(p_c) + 2/3 \cdot a_2(p_c) + 1/2 \cdot a_3(p_c) \right\} U^{(n)}$$

$$= \lambda_u^{HEIS.} U^{(n)}$$

with:

$$\lambda_u^{HEIS} \equiv \frac{8p_c}{1+p_c} + 6p_c^3(1-p_c^2)^2 + \frac{8}{3} p_c^5(1-p_c^2) + p_c^7$$

$$\simeq 1.88 \qquad (5.c.14)$$

Again the fixed point structure of $Q^*(u)$ is given by:

$$Q^*(u) = \delta(u)$$

and, hence, corresponds to absolute zero temperature.

In terms of the anisotropy parameter , Θ , the concentration parameter, p, and the set of moments $\{m_\alpha\}$ of the thermal variable probability distribution, the binary approximation gives the fixed points of the three-dimensional system at percolation threshold as:

$$i)\ \Theta \to \infty\ ;\ m_\alpha = 0, \forall\alpha\ ;\ u \equiv e^{-2K} \qquad : [\ \text{Ising}\ ]$$

$$ii)\ \Theta = 0\ ;\ m_\alpha = 0, \forall\alpha\ ;\ u \equiv 1/K \qquad : [\ \text{Iso. Heis.}\ ]$$

The fact that these fixed points occur at absolute zero temperature can be shown directly from (5.c.5) without the use of the binary approximation.

We now look for the 'shape-invariant' functions $\{f_j(u-u^*)\}$ and associated set $\{\lambda_j\}$ such that under the operation R_2 in (5.c.5) we have:

$$R_2\{f_j(u-u^*)\} = \frac{1}{\lambda_j} f_j\left(\frac{u-u^*}{\lambda_j}\right)$$

(compare the discussion leading to (4.c.3)).

In particular, we require the maximum value of the set $\{\lambda_j\}$

$$\lambda_{max} = \max\{\lambda_j\}$$

which, after many iterations, gives the unique scaling of the thermal parameter under a length dilation by a factor b = 2 as:

$$(u - u^*)' = \lambda_{max}(u - u^*) \qquad (5.c.15)$$

In order to determine λ_{max} we have first to decide upon a thermal variable, u, for systems with arbitrary anisotropy intermediate between the limiting Ising and Isotropic Heisenberg values. Motivated by our analysis of the two-dimensional model, we choose u to be the longitudinal I.C.L. of the corresponding one-dimensional model. That is:

$$u \equiv K_{//}^{(d=1)}(h, \Theta) \qquad (5.c.16)$$

where, h and Θ are taken to refer to a particular bond of the system. Of course, the particular choice of thermal variable employed is immaterial to our final results provided we solve the problem exactly. However, if we intend to use an approximation scheme such as the binary approximation, the choice of thermal variable becomes crucial if we are to obtain qualitatively meaningful results. In this respect our reasons for making the choice (5.c.16) are the same as those outlined earlier for the two-dimensional model: that in the Ising and Isotropic Heisenberg limits, the variable u simplifies to the usual choice of variable.

Three-Dimensional Anisotropic Heisenberg Model Near Percolation Threshold

In the following subsections we investigate the scaling of the

thermal parameter, u, for the anisotropic system precisely at percolation threshold using the binary approximation.

i) Binary Approximation For System Well Above Crossover (All bonds have $h \ll 1$)

For a dilute system in which all bonds have a value of the variable:

$$h \ll 1$$

and, hence, an associated thermal parameter:

$$u = K_{//}^{(d=1)}(h,\Theta) \sim \frac{1}{K}$$

the binary approximation results in the scaling (compare (5.c.13))

$$(u-u^*)' = \lambda_u^{HEIS}(u-u^*) \qquad (5.c.17)$$

with:

$$\lambda_u^{HEIS} = \frac{8p_c}{1+p_c} + 6p_c^3(1-p_c^2)^2 + \frac{8}{3}p_c^5(1-p_c^2) + p_c^7$$

ii) Binary Approximation For System Well Below Crossover (All bonds have $h \gg 1$)

For a dilute system in which all bonds have a value of the variable:

$$h \gg 1$$

and, hence, an associated thermal parameter:

$$u = K_{//}^{(d=1)}(h,\Theta) \sim \begin{cases} 16h\Theta e^{-2h} : \Theta \ll 1 \\ 8k\ln k\, e^{-2k} : \Theta \to \infty \end{cases}$$

the binary approximation results in the scaling (compare (5.c.10)):

$$(u-u^*)' = \lambda_u^{ISING}(u-u^*) \qquad (5.c.18)$$

where:

$$\lambda_u^{ISING} = \frac{8p_c}{1+p_c}$$

In fact, by using the small-width perturbation scheme, introduced for the two-dimensional dilute model, it is possible to show that the result (5.c.18) is exact within the Migdal/Kadanoff approximation.

Our results so far have been concerned with scaling transformations obtained precisely at the critical concentration, p_c. We now show how these results may be extended to treat dilute models whose bond concentration is close to the critical value, p_c.

iii) Binary Approximation For A System Near The Percolation Threshold

Linearising equations (5.c.2) around the fixed point values:

$$p^* = p_c$$

$$u^* = 0$$

applying the binary approximation and discarding terms of higher than first order in the assumed small variables:

$$\delta p = p - p_c \,,\, u$$

we obtain:

$$\Theta' = 2\Theta = b\Theta$$

$$\delta p' = \lambda_p \delta p = b^{1/\nu_p}\delta p \qquad (5.c.19)$$

$$(u-u^*)' = \lambda_u (u-u^*) = b^{1/\nu_u}(u-u^*) \qquad (5.c.20)$$

where:

$$\lambda_p = 8p_c(1-p_c^2)^3 \qquad (5.c.21)$$

$$\lambda_u \sim \begin{cases} \lambda_p & ; h \gg 1 \\ \lambda_u^{HEIS.} & ; h \ll 1 \end{cases} \qquad (5.c.22)$$

and $\lambda_u^{HEIS.}$ was previously defined in (5.c.17). Equations (5.c.19-22)

also imply:

$$\nu_p = \frac{\ln b}{\ln \lambda_p} \qquad (5.c.23)$$

$$\nu_u \begin{cases} \dfrac{\ln b}{\ln \lambda_p} = \nu_p \; ; \; h \gg 1 \\ \\ \dfrac{\ln b}{\ln \lambda_u^{HEIS.}} = \nu_u^{HEIS.} \; ; \; h \ll 1 \end{cases} \qquad (5.c.24)$$

and, therefore, that the three scaling variables for the three-dimensional anisotropic Heisenberg model near percolation threshold are:

$$\Theta, \delta p^{\nu_p}, u^{\nu_u}$$

i.e.

$$\left.\begin{aligned} \Theta' &= b\Theta \\ \delta p'^{\nu_p} &= b\,\delta p^{\nu_p} \\ u'^{\nu_u} &= b\,u^{\nu_u} \end{aligned}\right\} \qquad (5.c.25)$$

Equations (5.c.25) express our final scaling transformations which we will later use to obtain limiting forms for the I.C.L.'s and W.D.S.'s of the dilute model. Before we do so, however, a few remarks are in order.

The analysis which led to equations (5.c.19) et seq. was based upon the binary approximation. However, by using the 'small-width' perturbation scheme it is possible to show that the results obtained within the regime where all bonds have $h \gg 1$ are exact to first order in the variables u, δp . For the regime in which all bonds have $h \ll 1$ one should really extend the work of Stinchcombe & Watson (1976) to obtain the exact three-dimensional eigenvalue, λ_u^{HEIS} , within the M-K scheme. Nevertheless, we believe our results from

the binary approximation to be qualitatively correct.

Below, we consider the implications of equations (5.c.25) for the I.C.L.'s of the dilute, three-dimensional model near p_c.

iv) Inverse Correlation Length (I.C.L.) Behaviour In The Dilute, Three-Dimensional , Anisotropic Heisenberg Model Near Percolation Threshold

Equations (5.c.25) imply the following functional forms for the longitudinal and transverse I.C.L.'s of the three-dimensional, anisotropic Heisenberg model near percolation threshold:

$$\frac{1}{\xi_{//,\perp}} = \Theta \, \Phi^{\zeta}_{//,\perp} \left(\frac{\delta p}{\Theta}^{\nu_p}, \frac{u}{\Theta}^{\nu_u} \right) \qquad (5.c.26)$$

Hereafter, we use the notation:

$$\frac{1}{\xi_{//}} , \frac{1}{\xi_{\perp}}$$

to represent the I.C.L.'s of the dilute, three- dimensional system and reserve the symbols

$$K_{//}, K_{\perp}$$

to represent the I.C.L.'s of the corresponding one-dimensional model.

Below we show how the functional forms (5.c.26) and the scaling variables $\delta p^{\nu_p}, \Theta, u^{\nu_u}$ obtained in the previous subsection (cf. 5.c.25) may be combined to obtain the behaviour of both the longitudinal and transverse I.C.L. in the dilute system near p_c.

For the sake of clarity, the following discussion is divided into two main subsections. In the first we consider the behaviour of a system in which the interaction or bond concentration lies below the critical value, p_c. For such a system we find a crossover from Heisenberg-like to Ising-like behaviour at the crossover temperature

of the corresponding one-dimensional model, followed by a crossover to purely geometric behaviour at asymptotically low temperatures. In the second subsection we consider systems in which the bond concentration is greater than the critical value. In this case, the crossover from Heisenberg-like to Ising-like behaviour is further complicated by a transition to a state of long range order at a finite critical temperature T_c.

a) I.C.L. Behaviour For Systems With Bond Concentration Below Percolation Threshold

For systems with bond concentration, p, less than the critical value, p_c, equation (5.c.26) became:

$$\frac{1}{\xi_{\parallel}} = \Theta \, \Phi\left(\frac{|\delta p|^{\nu_p}}{\Theta}, \frac{u^{\nu_u}}{\Theta}\right)$$

$$\frac{1}{\xi_{\perp}} = \Theta \, \Phi\left(\frac{|\delta p|^{\nu_p}}{\Theta}, \frac{u^{\nu_u}}{\Theta}\right)$$

Within the present concentration regime ($p < p_c$) both I.C.L.'s are expected to be finite and non-zero except at the Ising limit where $1/\xi_{\perp}$ is undefined. Hence, by considering the limits of vanishing and divergent anisotropy parameter, Θ, in the forms above we obtain:

$$\frac{1}{\xi_{\parallel}} \sim |\delta p|^{\nu_p} G_{\parallel}^{<}\left(\frac{u^{\nu_u}}{|\delta p|^{\nu_p}}\right) : (|\delta p|^{\nu_p}, u^{\nu_u} \ll \Theta) \qquad (5.c.27)$$

$$\frac{1}{\xi_{\parallel}} \sim \frac{1}{\xi_{\perp}} \sim |\delta p|^{\nu_p} H_{\parallel,\perp}^{<}\left(\frac{u^{\nu_u}}{|\delta p|^{\nu_p}}\right) : (|\delta p|^{\nu_p}, u^{\nu_u} \gg \Theta) \qquad (5.c.28)$$

Since the I.C.L.'s should remain finite as percolation threshold is

approached at non-zero temperature we have:

$$\frac{1}{\xi_{\parallel}} \sim u^{\nu_u} \quad : \quad (|\delta p|^{\nu_p} \ll u^{\nu_u} \ll \Theta) \qquad (5.c.29)$$

$$\frac{1}{\xi_{\parallel}} \sim \frac{1}{\xi_{\perp}} \sim u^{\nu_u} \quad : \quad (u^{\nu_u} \gg |\delta p|^{\nu_p} \gg \Theta) \qquad (5.c.30)$$

For equations (5.c.29) and (5.c.30) to be consistent, the variable u must have a different form depending on whether u^{ν_u} is greater or less than Θ . In the former case the thermal variable is of Heisenberg type whereas in the latter case it is of the Ising type and, hence:

$$\frac{1}{\xi_{\parallel}} \sim u^{\nu_u} \sim \{K_{\parallel}^{(d=1)}\}^{\nu_p} \quad : \quad (|\delta p|^{\nu_p} \ll u^{\nu_u} \ll \Theta)$$

$$\frac{1}{\xi_{\parallel}} \sim \frac{1}{\xi_{\perp}} \sim u^{\nu_u} \sim \{K_{\parallel}^{(d=1)}\}^{\nu_{HEIS.}} \quad : \quad (u^{\nu_u} \gg |\delta p|^{\nu_p} \gg \Theta)$$

On approaching the critical concentration from below at non-zero temperature and finite anisotropy, our original forms for $1/\xi_{\parallel}$ and $1/\xi_{\perp}$ yield:

$$\frac{1}{\xi_{\parallel}} \sim \Theta A^{<}\left(\frac{u^{\nu_u}}{\Theta}\right) \quad : \quad (u^{\nu_u}, \Theta \gg |\delta p|^{\nu_p}) \qquad (5.c.32)$$

$$\frac{1}{\xi_{\perp}} \sim \Theta B^{<}\left(\frac{u^{\nu_u}}{\Theta}\right) \quad : \quad (u^{\nu_u}, \Theta \gg |\delta p|^{\nu_p}) \qquad (5.c.33)$$

Thus, be allowing Θ to diverge or vanish in (5.c.31) we obtain:

$$\frac{1}{\xi_{\parallel}} \sim u^{\nu_u} \sim \{K_{\parallel}^{(d=1)}\}^{\nu_p} \quad : \quad (u^{\nu_u} \gg \Theta \gg |\delta p|^{\nu_p}) \qquad (5.c.33(a))$$

$$\frac{1}{\xi_{\parallel}} \sim u^{\nu_u} \sim \{K_{\parallel}^{(d=1)}\}^{\nu_{HEIS.}} \quad : \quad (\Theta \gg u^{\nu_u} \gg |\delta p|^{\nu_p})$$

Finally, on imposing that both I.C.L.'s remain finite as absolute zero temperature is approached in (5.c.27) and (5.c.28) we have:

$$\frac{1}{\xi_{\parallel}} \sim |\delta p|^{\nu_p} \quad : \quad (u^{\nu_u} \ll |\delta p|^{\nu_p})$$

Our results show that the I.C.L.'s of the dilute, three-dimensional, anisotropic model display a series of crossovers in behaviour. Below we consider the special situation

$$|\delta p|^{\nu_p} \ll \Theta \ll 1$$

since it is in this case that successive crossovers occur in an explicit and easily describable way.

Equations (5.c.29),(5.c.33) and (5.c.34) show that the weakly anisotropic model with interaction/bond concentration, p, within a small neighbourhood of percolation threshold defined by:

$$|\delta p|^{\nu_p} \ll \Theta \ll 1$$

crosses over from isotropic Heisenberg-like behaviour viz:

$$\frac{1}{\xi_{//}} \sim u^{\nu_u} \sim \left(\frac{1}{h}\right)^{\nu_{HEIS.}} : \begin{matrix}(h \ll 1) \\ (u^{\nu_u} \gg |\delta p|^{\nu_p})\end{matrix}$$

to Ising-like behaviour, viz:

$$\frac{1}{\xi_{//}} \sim u^{\nu_u} \sim [\coth\Theta e^{-2h}]^{\nu_p} \quad \begin{matrix}(h \gg 1) \\ (u^{\nu_u} \gg |\delta p|^{\nu_p})\end{matrix}$$

and finally to purely geometric behaviour viz:

$$\frac{1}{\xi_{//}} \sim |\delta p|^{\nu_p} \quad : \quad (u^{\nu_u} \ll |\delta p|^{\nu_p})$$

as the temperature of the system is lowered. The thermal crossover from Heisenberg-like to Ising-like behaviour takes place at the crossover temperature of the corresponding one-dimensional model, i.e:

$$T_x \sim \frac{J}{k_B} \cdot \frac{1}{\cosh\mu}$$

In the next subsection we discuss the I.C.L. behaviour for systems with bond/interaction concentration, p, above the critical value, p_c.

b) I.C.L. Behaviour For Systems With Bond Concentration Above Percolation Threshold

For a system with a bond concentration, p, greater than the critical value, p_c, equations (5.c.26) become:

$$\frac{1}{\xi_{//}} = \Theta \, \Phi^{>}_{//}\left(\frac{|\delta p|^{\nu_p}}{\Theta}, \frac{U^{\nu_u}}{\Theta} \right)$$

$$\frac{1}{\xi_{\perp}} = \Theta \, \Phi^{>}_{\perp}\left(\frac{|\delta p|^{\nu_p}}{\Theta}, \frac{U^{\nu_u}}{\Theta} \right)$$

For the sake of brevity we will consider only the longitudinal I.C.L. in the following discussion, although similar arguments to those presented below and in previous chapters can equally well be applied to the transverse I.C.L.

Above the critical concentration, the dilute anisotropic Heisenberg model is expected to undergo a second order phase transition to a state of long range order at some finite temperature, $T_c(\delta p, \mu)$. By working at finite temperature, but away from the critical value, and considering the cases of divergent and vanishing anisotropy parameter, Θ , in the above form for the longitudinal I.C.L. we obtain:

$$\frac{1}{\xi_{//}} \sim |\delta p|^{\nu_p} \, g^{>}_{//}\left(\frac{U^{\nu_u}}{|\delta p|^{\nu_p}} \right) \quad : \quad (|\delta p|^{\nu_p}, U^{\nu_u} \ll \Theta : T \neq T_c(\delta p, \mu)) \qquad (5.c.35)$$

$$\frac{1}{\xi_{//}} \sim |\delta p|^{\nu_p} \, h^{>}_{//}\left(\frac{U^{\nu_u}}{|\delta p|^{\nu_p}} \right) \quad : \quad (|\delta p|^{\nu_p}, U^{\nu_u} \gg \Theta : T \neq T_c(\delta p, \mu)) \qquad (5.c.36)$$

Provided that the transition is continuous, the functions $g^{>}_{//}$ and $h^{>}_{//}$ are expected to have a single zero at some critical value

of their arguments i.e.

$$g_{//}^{>}(z_c) = 0 \quad ; \quad h_{//}^{>}(x_c) = 0 \qquad (5.c.37)$$

Equations (5.c.37) then give an implicit relationship between the critical temperature of a system and its concentration and anisotropy parameters viz:

$$u(T_c, \mu) = a_o \, \delta p^{\phi} \qquad (5.c.38)$$

where:

$$\phi \equiv \nu_p / \nu_u$$

and a_o , although possibly crossover dependent, is of order one. [O(1)] . For the weakly anisotropic system asymptotically close to percolation threshold where the transition takes place below the crossover temperature of the corresponding one-dimensional system, equation (5.c.38) reduces to:

$$T_c(\Theta, \delta p) \sim \frac{J}{k_B} \cdot \Theta \cdot \frac{1}{\ln(1/|\delta p|)} \qquad (h \gg 1 \, ; \, |\delta p|^{\nu_p} \ll \Theta \ll 1) \qquad (5.c.39)$$

Away from percolation threshold, where the transition takes place well above the crossover temperature, the dependence of the weakly anisotropic model's critical temperature on anisotropy and concentration takes the form:

$$T_c(\Theta, \delta p) \sim \frac{J}{k_B} \cdot \delta p^{\phi_{HEIS}} \qquad (h \ll 1 \, ; \, 1 \gg |\delta p|^{\nu_p} \gg \Theta) \qquad (5.c.40)$$

where:

$$\phi_{HEIS.} \equiv \nu_p / \nu_{HEIS}$$

Close to their respective zeroes, both $g_{//}^{>}(z)$ and $h_{//}^{>}(x)$ may be expanded as:

$$g_{//}^{>}(z) \sim \begin{cases} (z-z_c)^{\sigma^{+}_{ISING}} & : z > z_c \\ & \quad |z-z_c| \ll 1 \\ |z-z_c|^{\sigma^{-}_{ISING}} & : z < z_c \end{cases}$$

$$h_{//}^{>}(x) \sim \begin{cases} (x-x_c)^{\sigma^{+}_{ISING}} & : x > x_c \\ & \quad |x-x_c| \ll 1 \\ |x-x_c|^{\sigma^{-}_{HEIS.}} & x < x_c \end{cases}$$

where $\sigma^{\pm}_{ISING}$ and $\sigma^{\pm}_{HEIS}$ are the exponents associated with the Ising and isotropic Heisenberg limits of our model respectively.

Combining the above expansions with equations (5.c.35) and (5.c.36), we obtain the longitudinal I.C.L. behaviour near a phase transition occuring below or above the crossover temperature of the corresponding one-dimensional model respectively, as:

$$\frac{1}{\xi_{//}} \sim |\delta p|^{\nu_p} \left| \frac{U^{\nu_u}(T,\Theta) - U^{\nu_u}(T_c\{\Theta,\delta p\},\Theta)}{|\delta p|^{\nu_p}} \right|^{\sigma^{\pm}_{ISING}} \qquad (5.c.41)$$

$$-\left(|\delta p|^{\nu_p}, U^{\nu_u} \ll \Theta\,;\, |U^{\nu_u}(T,\Theta) - U^{\nu_u}(T_c,\Theta)| \ll |\delta p|^{\nu_p}\right)$$

$$\frac{1}{\xi_{//}} \sim |\delta p|^{\nu_p} \left| \frac{U^{\nu_u}(T,\Theta) - U^{\nu_u}(T_c\{\Theta,\delta p\},\Theta)}{|\delta p|^{\nu_p}} \right|^{\sigma^{\pm}_{HEIS.}} \qquad (5.c.42)$$

$$\left(|\delta p|^{\nu_p}, U^{\nu_u} \gg \Theta\,;\, |U^{\nu_u}(T,\Theta) - U^{\nu_u}(T_c,\Theta)| \ll |\delta p|^{\nu_p}\right)$$

This completes our discussion of the longitudinal I.C.L. behaviour in the anisotropic, three-dimensional Heisenberg model near percolation threshold. To summarise:

i) Both below and above percolation threshold, the inverse, longitudinal correlation length shows a marked crossover from characteristically Heisenberg-like to Ising-like behaviour at the crossover temperature of the corresponding one-dimensional system.

ii) Above percolation threshold, the model undergoes a continuous

phase transition to a state of long range order (L.R.O.) at finite temperature. Below the critical concentration, no such transition takes place. Precisely at p_c, the transition to L.R.O. occurs at absolute zero temperature.

iii) Above the critical concentration, the exponents characterising the longitudinal I.C.L.'s behaviour near the finite temperature transition are the same as those of the corresponding isotropic Heisenberg and Ising models: depending on whether the transition takes place above or below the one-dimensional crossover temperature respectively.

In the following two subsections we determine the behaviour of the wavevector dependent susceptibilities (W.D.S.) of the anisotropic, three-dimensional Heisenberg model near percolation threshold.

c) W.D.S. Behaviour For Systems With Bond Concentration Below Percolation Threshold

By combining the susceptibility and wavevector scaling (cf. 3.c. (ii)) with equations (5.c.25) of this chapter, we obtain the W.D.S's dependence on temperature, anisotropy and concentration as:

$$\chi_{//,\perp} = \Theta^{-\gamma} \Gamma^{<}_{//,\perp}\left(\frac{|\delta p|^{\nu_p}}{\Theta}, \frac{\mu^{\nu_u}}{\Theta}, \frac{q}{\Theta} \right) \qquad (5.c.43)$$

where γ is, as yet, an undetermined exponent. Below percolation threshold, our system exhibits no transition to L.R.O. so that the W.D.S.'s are expected to remain finite throughout this regime. Thus, by taking the limits:

$$\Theta \to \infty; \ \Theta \to 0^{+}$$

in (5.c.43) at finite temperature and wavevector we have:

$$\chi_{//} \sim |\delta p|^{-\gamma_{ISING}\cdot\nu_p} \Phi^{>}_{//}\left(\frac{u^{\nu_u}}{|\delta p|^{\nu_p}}, \frac{q_{\nu}}{|\delta p|^{\nu_p}}\right) : \{|\delta p|^{\nu_p}, u^{\nu_u}, q_{\nu} \ll \Theta\} \qquad (5.c.44)$$

$$\chi_{//} \sim |\delta p|^{-\gamma_{HEIS}\cdot\nu_p} Z_{//}\left(\frac{u^{\nu_u}}{|\delta p|^{\nu_p}}, \frac{q_{\nu}}{|\delta p|^{\nu_p}}\right) : \{|\delta p|^{\nu_p}, u^{\nu_u}, q_{\nu} \gg \Theta\} \qquad (5.c.45)$$

where γ_{ISING} and γ_{HEIS} are the exponent characteristic of the Ising and isotropic Heisenberg limits of our model respectively. Hence, at asymptotically low temperatures (where $u \to 0^{+}$) we obtain:

$$\chi_{//} \sim \frac{|\delta p|^{(2-\gamma_{ISING})\nu_p}}{|\delta p|^{2\nu_p} + \beta_0 q_{\nu}^{2}} : (u^{\nu_u} \ll q_{\nu} \ll |\delta p|^{\nu_p} \ll \Theta) \qquad (5.c.46)$$

$$\chi_{//} \sim \frac{|\delta p|^{(2-\gamma_{HEIS})\nu_p}}{|\delta p|^{2\nu_p} + \beta_0 q_{\nu}^{2}} : (q_{\nu} \ll |\delta p|^{\nu_p} : \Theta = 0) \qquad (5.c.47)$$

By first approaching the critical concentration from below at finite temperature and then taking the limit of:

$$\Theta \to 0^{+}$$

in (5.c.43) we have:

$$\chi_{//} \sim \frac{u^{(2-\gamma_{HEIS})\nu_u}}{u^{2\nu_u} + c_0 q_{\nu}^{2}} : (|\delta p|^{\nu_p} \ll \Theta \ll q_{\nu} \ll u^{\nu_u}) \qquad (5.c.48)$$

whereas approaching the critical concentration from below in (5.c.44) gives:

$$\chi_{//} \sim \frac{u^{(2-\gamma_{ISING})\nu_u}}{u^{2\nu_u} + d_0 q_{\nu}^{2}} : (|\delta p|^{\nu_p} \ll q_{\nu} \ll u^{\nu_u} \ll \Theta) \qquad (5.c.49)$$

Equations (5.c.46),(5.c.48) and (5.c.49) again illustrate the way in which the three-dimensional, dilute weakly anisotropic system crosses firstly from Heisenberg- to Ising-like behaviour at the crossover temperature of the corresponding one-dimensional model, and then to purely geometric behaviour as the temperature of the system is

lowered still further.

We next consider the W.D.S. behaviour above the critical concentration.

d) W.D.S. Behaviour For Systems With Bond Concentration Above Percolation Threshold

Above percolation threshold, our functional expression for the longitudinal W.D.S. becomes:

$$\chi_{//} = \Theta^{-\gamma} \Gamma_{//}^{>}\left(\frac{|\delta p|^{\nu_p}}{\Theta}, \frac{U^{\nu_u}}{\Theta}, \frac{q}{\Theta} \right) \qquad (5.c.50)$$

Thus, working away from the critical temperature and allowing the anisotropy variable to diverge or vanish we obtain:

$$\chi_{//} \sim |\delta p|^{-\gamma_{ISING}\nu_p} S_{//}^{>}\left(\frac{U^{\nu_u}}{|\delta p|^{\nu_p}}, \frac{q}{|\delta p|^{\nu_p}} \right) : \left\{ \begin{matrix} |\delta p|^{\nu_p}, U^{\nu_u}, q \ll \Theta \\ T \neq T_c\,(\delta p, \Theta) \end{matrix} \right\} \qquad (5.c.51)$$

$$\chi_{//} \sim |\delta p|^{-\gamma_{HEIS.}\nu_p} R_{//}^{>}\left(\frac{U^{\nu_u}}{|\delta p|^{\nu_p}}, \frac{q}{|\delta p|^{\nu_p}} \right) : \left\{ \begin{matrix} |\delta p|^{\nu_p}, U^{\nu_u}, q \gg \Theta \\ T \neq T_c\,(\delta p, \Theta) \end{matrix} \right\} \qquad (5.c.52)$$

From our previous work on the longitudinal I.C.L. in this concentration regime (5.c.(b)) we know that a transition to L.R.O. occurs at:

i) $U^{\nu_u}/|\delta p|^{\nu_p} \equiv z_c$ below crossover: $(h \gg 1)$

ii) $U^{\nu_u}/|\delta p|^{\nu_p} \equiv x_c$ above crossover: $(h \ll 1)$

and so we expect the functions $S_{//}^{>}$ and $R_{//}^{>}$ to behave as:

$$1/S_{//}^{>}(z_c, 0) \equiv 0 \; ; \; 1/R_{//}^{>}(x_c, 0) \equiv 0$$

By expanding these two, possibly non-analytic, functions about their poles we obtain the zero wavevector dependence of the W.D.S. near the

transition as:

$$\chi_{\substack{\parallel \\ q=0}} \sim |\delta p|^{-\gamma_{ISING}\nu_p} \left| \frac{U^{\nu_u}(T,\Theta) - U^{\nu_u}(T_c\{\Theta,p\},\Theta)}{|\delta p|^{\nu_p}} \right|^{-\eta^{\pm}_{ISING}} \quad (5.c.53)$$

below crossover and:

$$\chi_{\substack{\parallel \\ q=0}} \sim |\delta p|^{-\gamma_{HEIS}\nu_p} \left| \frac{U^{\nu_u}(T,\Theta) - U^{\nu_u}(T_c\{\Theta,p\},\Theta\}}{|\delta p|^{\nu_p}} \right|^{-\eta^{\dagger}_{HEIS.}} \quad (5.c.54)$$

where $\eta^{\dagger}_{ISING}$ and $\eta^{\dagger}_{HEIS.}$ characterise the zero wavevector divergence in the corresponding Ising and isotropic Heisenberg limits of our model.

Having illustrated some of the methods by which limiting forms may be obtained for the I.C.L.'s and W.D.S.'s of the dilute, three-dimensional anisotropic Heisenberg model near percolation threshold, the next section briefly investigates the nearly pure limit of the same model.

d) The Dilute Three-Dimensional Model Near The Pure Limit.

In this section we show how the scaling equations (5.c.2.) may be investigated using the binary approximation in order to determine the critical surface structure asymptotically close to both the Ising and Isotropic Heisenberg pure fixed points.

Linearising (5.c.2) about $p = 1$ and using the first moment matching approximation we obtain:

$$\delta p' = 0 \quad (5.d.1)$$

$$\Theta' = 2\Theta \quad (5.d.2)$$

$$h' = 4(1-2\delta p)(h - \tfrac{1}{2}.\ln 2.\tanh\Theta) \quad (5.d.3)$$

where h has been used as the thermal variable in the moment matching process, and terms of second or higher order in the small parameter.

$$\delta p = 1 - p$$

have been discarded. We now consider the behaviour of equations (5.d.2)

and (5.d.3) near the Ising and isotropic Heisenberg limits respectively.

i) Critical Surface Structure Near The Pure Ising Fixed Point

Near the Ising limit, equation (5.d.2) gives the scaling of the anisotropy parameter $\cosh\mu$ as:

$$\cosh\mu' \simeq \cosh\mu\left(1-\frac{\mu^2}{2}\right) \qquad (5.d.4)$$

Multiplying through both sides of (5.d.3) with (5.d.4) we obtain:

$$K' \doteq 4\,(1-2\delta p-\tfrac{1}{2}.\mu^2)(K-\tfrac{1}{2}\ln 2) \qquad (5.d.5)$$

The only relevant scaling variable near this fixed point is:

$$S = \{K(1-2\delta p-\tfrac{1}{2}.\mu^2)+\ln 2\,(\delta p+\tfrac{1}{4}.\mu^2-\tfrac{2}{3})\}^{1/2} \qquad (5.d.6)$$

The critical condition near this fixed point is, therefore:

$$S\equiv 0$$

or

$$K_c(\mu,\delta p) = \frac{\ln 2.(\frac{2}{3}-\delta p-\mu^2/4)}{(1-2\delta p-\frac{1}{2}\mu^2)}$$

Thus, the critical temperature of the nearly pure, strongly anisotropic model is given by:

$$T_c(\mu,p) \simeq \frac{J}{k_B}.\frac{3}{4\ln 2}.(1+p-\mu^2/4) \quad : \qquad (5.d.7)$$

Hence:

$$\frac{1}{T_c}\frac{dT_c}{dp}\bigg|_{p=1} \simeq \frac{1}{2}\left(1+\frac{\mu^2}{8}\right) \quad : \qquad (5.d.8)$$

The value of (5.d.8) evaluated precisely at the Ising limit (viz. $\frac{1}{2}$) does not compare well with the value

$$\frac{1}{T_c}\cdot\frac{dT_c}{dp}\bigg|_{p=1}^{ISING} \doteq 1.067$$

obtained by Harris (1974) and Thorpe & Beeman(1975) using perturbation theory. However, the expression:

$$T_c(\mu, p) \doteq T_c(0,1)\left[1 - a_0\delta p - b_0\mu^2\right] \;:\; (a_0 = \tfrac{1}{2};\; b_0 = \tfrac{1}{8})$$

obtained from (5.d.8) is in qualitative agreement with the corresponding result of Stinchcombe (1981) who, using the Suzuki-Takano method, found

$$a_c \simeq 1.04$$
$$b_0 \simeq 0.12$$

ii) Critical Surface Structure Near The Pure, Isotropic Heisenberg Fixed Point

Near the Isotropic Heisenberg limit, equation (5.d.2) gives the scaling of the anisotropy parameter $\cosh\mu$ as:

$$\cosh\mu' \simeq \frac{1}{2}\cosh\mu\left(1 + \frac{1}{\cosh^2\mu}\right) \qquad (5.d.9)$$

Multiplying through both sides of (5.d.3) with (5.d.9) we obtain:

$$K' \simeq 2K\left(1 - 2\delta p + \frac{1}{\cosh^2\mu}\right)(K - \tfrac{1}{2}\ln 2)$$

Near the pure Isotropic Heisenberg fixed point there are two relevant variables. The first is the anisotropy parameter, Θ , appearing in (5.d.2). The second is the variable:

$$\omega = K\left(1 - 2\delta p - \tfrac{1}{3}\cdot\frac{1}{\cosh^2\mu}\right) - \ln 2\,.\left(1 - \delta p + \tfrac{1}{6}\,\frac{1}{\cosh^2\mu}\right) \qquad (5.d.10)$$

The critical condition in this case is therefore:

$$\omega \equiv a_0\,\Theta$$

Equation (5.d.11) gives the dependence of the nearly pure, weakly anisotropic system's critical temperature upon concentration and

anisotropy as:

$$T_c(p,\cosh\mu) \simeq \frac{J}{k_B}\cdot\frac{1}{\ln 2}\cdot\left(p - \frac{1}{\ln 2.\cosh\mu}\right) : (5.d.12)$$

and, hence:

$$\frac{1}{T_c}\frac{dT_c}{dp}\bigg|_{p=1} \simeq \left(1 + \frac{1}{\ln 2.\cosh\mu}\right) : (5.d.13)$$

This should be compared with the values

$$\frac{1}{T_c}\frac{dT_c}{dp}\bigg|_{p=1}^{\text{ISO. HEIS.}} = \frac{3}{2}$$

obtained by McGurn (1979) at the Isotropic Heisenberg limit using an R.P.A. method, and:

$$\frac{1}{T_c}\frac{dT_c}{dp}\bigg|_{p=1}^{\text{ISO. HEIS.}} \simeq 1.22$$

obtained by Stinchcombe (1981) using the Suzuki-Takano method and the Migdal/Kadanoff bond moving scheme.

The expression

$$\frac{T_c(p,1/\cosh\mu)}{T_c(1,0)} \simeq 1 - \delta p - \frac{1}{\ln 2.\cosh\mu}$$

obtained from (5.d.12) is in qualitative agreement with the corresponding result of Stinchcombe (1981) viz:

$$\frac{T_c(p,1/\cosh\mu)}{T_c(1,0)} \doteq 1 - a_0\delta p + c\left(\frac{1}{\cosh\mu}\right)^{1/\phi}$$

with:

$$a_0 \simeq 1.22$$
$$c = O(1)$$
$$\phi \simeq 1.56$$

In this chapter we have shown how limiting forms may be obtained for the inverse correlation lengths, wavevector dependent susceptibilities and critical temperature of both the dilute and pure, three-dimensional

anisotropic Heisenberg model. In the next, and final, chapter we discuss the connection between our present results, those of previous chapters and experimental work which has been carried out on pure and dilute Heisenberg systems.

Chapter 6

Conclusions

In this, the final, chapter we represent some of our results from the text and discuss their applicability to real, dilute magnetic systems. In particular, we draw a comparison between the functional forms which we derived for the inverse correlation lengths (I.C.L.'s) and wavevector dependent susceptibilities (W.D.S's) of our two-dimensional, dilute anisotropic model, and those employed by Birgeneau et al. (1980) in their analysis of data obtained from experiments on the $Rb_2Mn_pMg_{1-p}F_4$ systems discussed in Chapter 1.

A brief review and comparison of existing theoretical work is included, and possible extensions of the present analysis are outlined.

a) Overview Of Results

In the first five chapters of this thesis, we considered the behaviour of pure and dilute anisotropic Heisenberg models in one, two and three dimensions. Below we briefly set out some of the major results from this analysis and consider the effects of dilution and anisotropy within each dimensionality in turn.

i) The One-Dimensional Model

The pure one-dimensional isotropic Heisenberg model was found to undergo a transition to long range order (L.R.O.) at absolute zero temperature with an accompanying correlation length divergence given by the inverse of the absolute temperature. The presence of an arbitrarily small uniaxial anisotropy in the exchange interaction did not alter the transition temperature but caused the resulting model to

exhibit a drastic crossover in behaviour from that characteristic of the isotropic Heisenberg model to a form somewhat reminiscent of the one-dimensional Ising model at an anisotropy dependent cross-over temperature, $T_x^{(d=1)}$, given approximately by:

$$T_x^{(d=1)} \sim \frac{J}{k_B . \cosh \mu}$$

where the anisotropy parameter, μ , was introduced in equation (2.a.1) of Chapter 2.

The introduction of dilution into the one-dimensional model removed the transition to L.R.O. at absolute zero temperature for all values of the uniaxial anisotropy. In this particularly simple case, the I.C.L. of the dilute model was found to be the sum of a thermal and purely geometric contribution viz: (cf. equation (2.g.2) of Chapter 2).

$$\frac{1}{\xi^{(d=1)}_{\text{dilute system}}} \equiv \frac{1}{\xi^{(d=1)}_{\text{pure system}}} + \frac{1}{\xi^{(d=1)}_{\text{geometric}}}$$

with:

$$\frac{1}{\xi^{(d=1)}_{\text{geometric}}} \equiv \ln (1/p)$$

ii) The Two-Dimensional Model

As in its one-dimensional analogue, the pure, two-dimensional, isotropic Heisenberg model undergoes a transition to L.R.O. at absolute zero temperature. In contrast to the one-dimensional case, however, the introduction of uniaxial exchange anisotropy into the two-dimensional model lifts the transition temperature to a finite, anisotropy dependent value. In the limit of weak anisotropy, our expression for this critical temperature reduces to:

$$T_c^{(d=2)} \simeq \frac{2J}{k_B . \ln (\cosh \mu)} \quad : \quad (\cosh \mu \gg 1)$$

(cf. equation [3.c.24] of Chapter 3)

The I.C.L and W.D.S. behaviours well away from the critical temperature of the weakly anisotropic model are characteristic of the isotropic Heisenberg limit, but, within a small temperature regime around the critical temperature, $T_c^{(d=2)}$, the transverse fluctuations of the model are substantially damped and, as a result, the behaviour of the thermodynamic functions becomes increasingly Ising-like. For the weakly anisotropic system, the temperature, $T_x^{(d=2)}$, at which such crossover effects become important is given approximately by:

$$\left| \frac{1}{T_x^{(d=2)}} - \frac{1}{T_c^{(d=2)}} \right| \sim \frac{k_B}{J} \quad : \quad (\cosh\mu \gg 1)$$

(cf. equation (3.c.29) of Chapter 3.)

As an example of such crossover behaviour, and a useful precursor to our discussion of the dilute, anisotropic model, the I.C.L. behaviour in the pure, isotropic Heisenberg model is given by:

$$K_{//}^{HEIS\ (d=2)} = K_{\perp}^{HEIS\ (d=2)} = a_0 e^{-2K}$$

whereas in the pure Ising model:

$$K_{//}^{ISING\ (d=2)} = a_0 |K - K_c|$$

cf. equations (3.c.20) and (3.c.18) of Chapter 3).

However, for the pure model with weak, uniaxial exchange anisotropy, the corresponding I.C.L. behaviour is:

$$K_{//}^{(d=2)} \simeq K_{\perp}^{(d=2)} \sim a_1 \frac{e^{-2|K - K_c(\cosh\mu)|}}{\cosh\mu} \quad : \quad (|K - K_c| \gg 1)$$

$$K_{//}^{(d=2)} \simeq a_1 \frac{|K - K_c(\cosh\mu)|}{\cosh\mu} \quad : \quad (|K - K_c| \ll 1)$$

$$K_{\perp}^{(d=2)} \simeq \beta_1/\cosh\mu \quad : \quad (|K - K_c(\cosh\mu)| \ll 1)$$

cf. equations (3.c.23), (3.c.25(a)) and (3.c.28)]

where the former expression relates to behaviour 'above crossover' and the latter pair to 'below crossover'.

We now consider the effects of dilution upon the weakly anisotropic system.

When a fraction (1-p) of the magnetic sites (bonds) are removed from the weakly anisotropic model, the critical temperature is depressed from its pure value. When the fraction, p, of remaining sites(bonds) reaches a critical value, p_c, the transition to L.R.O. in the system takes place at absolute zero temperature. Upon further dilution (i.e. $p < p_c$) no such transition to L.R.O. is observed; even at absolute zero temperature. The phase diagram for such a dilute, weakly anisotropic, two-dimensional Heisenberg model is sketched in figure (16). Asymptotically close to the critical concentration p_c, the dependence of the weakly anisotropic model's critical temperature upon anisotropy and concentration is given by:

$$T_c^{(d=2)}(\delta p, \mu) \sim a_0 \frac{J}{k_B} \cdot \frac{1}{\cosh\mu} \cdot \frac{1}{\ln|1/\delta p|} \quad : \quad \left\{ \begin{matrix} |\delta p|^{\nu_p} \ll \frac{1}{\cosh\mu} \ll 1 \\ h \gg 1 \end{matrix} \right\}$$

(cf. equation 4.d.22).

The weakly anisotropic system with site (bond) concentration close to the critical value, p_c, shows a striking crossover in behaviour from isotropic Heisenberg-like above, to Ising-like below the crossover temperature of the corresponding one-dimensional model given by:

$$T_x^{(d=1)}(\mu) \sim \frac{J}{k_B} \cdot \frac{1}{\cosh\mu}$$

Provided the system is below percolation threshold, a second crossover to purely geometric behaviour takes place at asymptotically low temperatures. In particular, for weakly anisotropic systems sufficiently close to the critical concentration that:

$$|\delta p|^{\nu_p} \ll \Theta \ll 1$$

the methods of chapters 4 and 5 give the longitudinal I.C.L. behaviour in this region as:

$$\frac{1}{\xi}_{//} \sim \frac{1}{\xi}_{\perp} \sim \{K_{//}^{(d=1)}\}^{\nu_{HEIS.}^{(d=2)}} \quad : \left\{ \begin{array}{l} T > T_x^{(d=1)} \\ (K_{//}^{(d=1)})^{\nu_{HEIS.}^{(d=2)}} \gg |\delta p|^{\nu_p^{(d=2)}} \end{array} \right\}$$

$$\frac{1}{\xi}_{//} \sim \{K_{//}^{(d=1)}\}^{\nu_p^{(d=2)}} \quad : \quad [T < T_x^{(d=1)} : K_{//}^{(d=1)} \gg |\delta p|]$$

$$\frac{1}{\xi}_{//} \sim |\delta p|^{\nu_p^{(d=2)}} \quad [T < T_x^{(d=1)} : K_{//}^{(d=1)} \ll |\delta p|]$$

In the present, approximate Migdal calculation, the exponents are:

$$\nu_{HEIS.}^{(d=2)} \simeq 1.2 \quad ; \quad \nu_p^{(d=2)} \simeq 1.6$$

but more precise values from scaling and series methods are:

$$\nu_{HEIS.}^{(d=2)} \simeq 0.92 \qquad [\text{Coniglio (1981)}]$$

$$\nu_p^{(d=2)} \simeq 1.33 \qquad [\text{Blöte et al. (1981), Dunn et al. (1975)}]$$

iii) The Three-Dimensional Model

The pure, three-dimensional Heisenberg models were found to undergo finite temperature transitions for all values of the uniaxial exchange anisotropy including (compare the one-and two-dimensional analogues) the Isotropic model. Once again, the weakly anisotropic model displays a marked crossover from isotropic-like to somewhat more Ising-like behaviour on passing through a temperature, $T_x^{(d=3)}$,

given approximately by:

$$\left| \frac{1}{T_x^{(d=3)}} - \frac{1}{T_c^{(d=3)}} \right| \sim \frac{k_B}{J.\cosh\mu}$$

(cf. equation [5.b.20] of Chapter 5)

where $T_c^{(d=3)}$ is the critical temperature of the same model.

As an example of this crossover behaviour, our analysis leads to a low temperature I.C.L. behaviour in the Isotropic limit of:

$$K_{//}^{HEIS.(d=3)} = K_{\perp}^{HEIS(d=3)} \sim |K - K_c^{HEIS}| \quad : \quad K_c^{HEIS} = 1/2$$

whereas for the Ising model:

$$K_{//}^{ISING(d=3)} \sim |K - K_c^{ISING}|^{1/2} \quad : \quad K_c^{ISING} = 1/4$$

(cf. equations [5.b.8] and [5.b.12] of Chapter 5.)

For the weakly anisotropic model, however, we find:

$$K_{//}^{(d=3)} \sim K_{\perp}^{(d=3)} \sim |K - K_c(\Theta)|$$

(cf. equation [5.b.15] of Chapter 5)

well above the crossover temperature, but, as the critical temperature is approached from above:

$$K_{//}^{(d=3)} \sim \{ |K - K_c(\Theta)| / \cosh\mu \}^{1/2}$$

$$K_{\perp}^{(d=3)} \sim 1/\cosh\mu$$

(cf. equations[5.b.16/19] of Chapter 5)

We now consider the effects of dilution upon the weakly anisotropic, three-dimensional model.

As in the two-dimensional case, dilution of the three-dimensional, weakly anisotropic model depresses the critical temperature of the model from its pure value until the fraction of remaining bonds (sites) reaches the critical value, p_c. Precisely at p_c, the model only

undergoes a transition to L.R.O. at absolute zero. Further dilution removes the transition. The phase diagram for a dilute, weakly anisotropic, three-dimensional Heisenberg model is sketched in figure (17).

For a weakly anisotropic system sufficiently close to percolation threshold that the phase transition takes place below the crossover temperature of the corresponding one-dimensional model, the critical temperature takes the form:

$$T_c^{(d=3)} \sim a_1 \frac{J}{k_B \cdot \cosh\mu} \cdot \frac{1}{\ln(1/|\delta p|)}$$

(cf. equation [5.c.39])

Near the critical concentration, p_c, the system again demonstrates a crossover in behaviour from that characteristic of the isotropic Heisenberg model to a form more reminiscent of the Ising model at the crossover temperature $T_x^{(d=1)}$ of the corresponding one-dimensional model. In particular, for a weakly anisotropic system below percolation threshold but sufficiently close that $|\delta p|^{\nu_p} \ll \Theta \ll 1$, the results of chapter 5 give the longitudinal I.C.L. behaviour as:

$$\frac{1}{\xi_{//}} \sim \frac{1}{\xi_{\perp}} \sim \left\{ K_{//}^{(d=1)} \right\}^{\nu_{HEIS}^{(d=3)}} : \left\{ T \gg T_x^{(d=1)} : \left(K_{//}^{(d=1)}\right)^{\nu_{HEIS}^{(d=3)}} \gg |\delta p|^{\nu_p^{(d=3)}} \right\}$$

$$\frac{1}{\xi_{//}} \sim \left\{ K_{//}^{(d=1)} \right\}^{\nu_p^{(d=3)}} : \left\{ T \ll T_x^{(d=1)} : \left(K_{//}^{(d=1)}\right)^{\nu_p^{(d=3)}} \gg |\delta p|^{\nu_p^{(d=3)}} \right\}$$

$$\frac{1}{\xi_{//}} \sim |\delta p|^{\nu_p^{(d=3)}} : \left\{ T \ll T_x^{(d=1)} : \left(K_{//}^{(d=1)}\right)^{\nu_p^{(d=3)}} \ll |\delta p|^{\nu_p^{(d=3)}} \right\}$$

Our present approximate, Migdal calculation gives the exponents as:

$$\nu_{HEIS}^{(d=3)} \simeq 1.1$$

$$\nu_p^{(d=3)} \simeq 1.2$$

but more precise values from scaling and series methods are:

$$\nu_{HEIS.}^{(d=3)} \simeq 0.7 \qquad \text{[Coniglio (1981)]}$$

$$\nu_{p}^{(d=3)} \simeq 0.8 \qquad \text{[Dunn et al. (1975)]}$$

Having very briefly reviewed the results of the last four chapters we now turn our attention to the approximations, both in the models and in the methods of analysis, which have been used to obtain them.

b) Qualifications

In the introduction to this thesis we stated that in order to make any progress on this problem we had to treat the spins of our model magnetic systems as classical. That is, we had neglected all the commutation relationships which any real spins obey. As we also pointed out at that time, the use of classical spins had removed the possibility of our detecting any crossover to essentially quantum mechanical behaviour which may occur in any real experimental system. From the work of Young (1975) and of Hertz (1976) we expect that our classical approximation will lead to qualitatively correct results in the neighbourhood of the finite temperature transitions which we have considered but that it may be completely inadequate for certain situations in which the critical temperature tends to absolute zero. As an example of the latter, the approximation may be a particularly poor one for some dilute two- and three-dimensional models precisely at percolation threshold. Perhaps even more worrying is the possibility that if such quantum mechanical effects occur, they would be expected throughout some low temperature regime. Unfortunately it is difficult to see how to improve considerably on this, probably our most severe,

approximation.

One aim of the present work has been a comparison of our final results with those of experiments on the $Rb_2Mn_pMg_{1-p}F_4$ range of quasi-two-dimensional systems. These materials are antiferromagnets whereas the models we have introduced have all been ferromagnets. Nevertheless, as we first pointed out in the introductory preamble, we expect that the static critical behaviour of the classical ferro- and antiferromagnet in the absence of an external field and on lattices without frustration will be the same.

The Migdal-Kadanoff approximation scheme which was used to treat the two- and three-dimensional models, was employed for three main reasons. Firstly, it is known to give qualitatively correct results for both the Ising and isotropic Heisenberg limits of our models near their respective lower critical dimensionalities and, as such, is a natural candidate for treating the intermediate case. Secondly, it is a relatively simple process to carry out, and lastly, it allows the effects of dilution to be introduced into the problem in a natural and straightforward manner. Despite these qualities, however, the accuracy of the scheme is difficult to quantify and difficult to improve upon (though Martinelli and Parisi (1981) have recently suggested a new means of interpretation of the scheme which may allow improvements to be made). These difficulties may, to some extent, be sidestepped by employing field theoretic techniques, but for investigating the properties of model systems such as ours throughout their phase diagrams with a minimum of mathematical machinery, the real space renormalisation group methodology coupled with the Migdal-Kadanoff bond moving scheme certainly seems to represent one of the optimal means available at the present time.

In the course of our investigations into the effects of dilution upon our two- and three-dimensional models, it turned out to be far easier to treat the case of bond-dilution than site-dilution. Unfortunately, real dilute systems are obtained from the corresponding pure systems by site dilution so that, at first sight, the replacement of site- by bond-dilution may appear to be both a drastic and unphysical approximation. However, universality arguments suggest that quantities such as critical exponents and amplitudes will be the same for both types of dilution, although properties of a lower universality class, such as the critical value for the concentration, will, in general, differ. In fact, the critical concentration for the bond-diluted square lattice is known to be exactly $\frac{1}{2}$, whereas its value for the site diluted case is ~ 0.59. From the former value we see that our estimate of p_c in Chapter 4 for the bond-diluted square lattice is a fairly poor one, but that it lies fortuitously close to the corresponding site-dilution value. Thus, universality arguments and the value of p_c obtained suggest that this approximation is a fairly good one near criticality.

A further approximation which requires some explanation is concerned with the dimensionality of the models we have considered. In particular, we have tried to model the $Rb_2Mn_pMg_{1-p}F_4$ system by means of a two-dimensional model whereas the system itself is manifestly three-dimensional. In the introduction to this thesis we argued that data from neutron scattering experiments on the pure system showed that as the critical temperature was approached from above, there was no observable build up of macroscopic L.R.O. along one of the crystal axis until the transition occurred. Moreover, the characteristics of the ordered state itself seemed to suggest that the system's magnetism was largely due to interactions lying within planes. We suggested therefore, that it was

entirely reasonable to model this behaviour by treating the system as if it were truly two-dimensional.

Similar arguments were presented for the dilute systems although here it was noted that there was experimental evidence for some degree of interplanar correlation near criticality: suggesting that in this case, the presence of interplaner interactions was more important than in the pure model.

Although we expect this 'dimensionality approximation' to be acceptable within the experimentally probed temperature regime, we are well aware that, along with next-nearest-neighbour interactions, such effects become increasingly important as the temperature of the system is lowered. In particular, the critical concentration for the $Rb_2Mn_pMg_{1-p}F_4$ system would occur well below the value predicted in our naive approximation, as illustrated in figure (18), and would display further crossover behaviour associated with further neighbour interactions within the plane, and finally, interplanar interactions. Mujeeb & Stinchcombe (1982) have studied effects such as these in the dilute two- and three-dimensional, weakly coupled layer/chain Ising systems. We will not, however, pursue this point any further here.

One of the last two points we wish to bring up here concerns our scaling of the anisotropy parameter, Θ, in the dilute system. In appendix 2, where we derived the transformation equations for both thermal and anisotropy parameters under a length scaling in the dilute system, we assumed that the model had all interaction anisotropies the same. Since it is by no means clear that this assumption is true of any real system, it should be viewed with some concern. Ideally, we would have liked to have considered an arbitrary initial distribution for the bond anisotropy since by neglecting deviations from the delta-

function form of the Θ distribution we may be missing some further aspects of the problem. Indeed, recent work (Imry & Ma (1975), Grinstein (1976),Aharony, Imry & Ma (1976), Young (1977) Pelcovits, Pytte & Rudnick (1978), Parisi & Sourlas (1979))has shown the presence of random anisotropy or fields in magnetic materials to have the effect of lowering the effective dimensionality of a system and this is possibly relevant to the interpretation of certain experimental data as we will discuss in a later section.

Having pointed out some of the approximations which were made in our analysis, we now proceed to compare our results for the two- and three-dimensional models with those of experiments.

c) Comparison With Experiments

In this section we compare the results of our investigation of the dilute, anisotropic Heisenberg model with those obtained from recent experiments. In particular we consider the functional forms employed by Birgeneau et al. (1980) and Cowley et al(1977(a)) in the interpretation of data from neutron scattering experiments on the $Rb_2Mn_pMg_{1-p}F_4$ and $Mn_pZn_{1-p}F_2$ families of systems and discuss their applicability with respect to the analagous functional forms which were derived in Chapters 4/5. To begin with, however, we consider the results of experiments carried out on the pure, quasi-two-dimensional system Rb_2MnF_4.

i) Experiments Carried Out On Rb_2MnF_4

On the basis of susceptibility experiments, Breed (1967) suggested that crystalline samples of Rb_2MnF_4 undergo a phase transition at a critical temperature

$$T_c^{(BREED)} \simeq 38.5 \text{ K}$$

Later neutron scattering experiments by Birgeneau et al. (1970)

confirmed Breed's results, finding a transition to long range order at a critical temperature:

$$T_c^{[BIRG.]} \simeq 38{\cdot}4\,K$$

with a sublattice magnetisation exponent close to that of the two-dimensional Ising model viz:

$$\beta \simeq 0{\cdot}16 \quad : \{\, |1 - T/T_c| \lesssim 0{\cdot}1 \,\}$$

compared with the Ising value:

$$\beta^{ISING} = 1/8$$

From our own treatment of the pure, two-dimensional model and the exchange values quoted by Birgeneau et al. we are able to predict the critical temperature for Rb_2MnF_4 as being:

$$T_c \sim 40\ K$$

Furthermore, our estimate for the crossover temperature of the pure system, T_x , (cf. equation 3.c.27) suggests that the temperature regime:

$$\left| 1 - \frac{T}{T_c} \right| < 0{\cdot}1$$

is 'well below crossover' and, as such, the measured value of β **should** be the same as that for the two-dimensional Ising model. Thus, our results for the pure, two-dimensional, weakly anisotropic system seem to be in good qualitative and quantitave agreement with the experiments of both Breed and Birgeneau et al.

Having investigated the pure, quasi-two-dimensional Rb_2MnF_4 system, Birgeneau et al. (1980) went on to carry out a series of neutron scattering experiments on the diluted system $Rb_2Mn_pMg_{1-p}F_4$. Below, we summarise their results, discuss their interpretation of the data acquired and compare both with our own analysis.

ii) Experiments Carried Out On $Rb_2Mn_pMg_{1-p}F_4$

Experiments were carried out on three crystalline samples of $Rb_2Mn_pMg_{1-p}F_4$ with nominal magnetic ion concentrations of $p = 0.54$, 0.57 and 0.60. These values straddle the critical concentration for the site diluted square lattice which is believed to be ~ 0.59. The quasi-elastic scattering from all three samples was measured over a broad temperature range. The $p = 0.60$ sample was found to undergo a transition to a state of two-dimensional long range order within the layers of the system and with finite correlations along the third crystal axis at $\sim$ 8K. No such transition was seen in the other two samples.

In the absence of theoretical work on the expected forms for the scattering functions, Birg. et al. assummed the behaviour:

$$S_{\perp}(q) + S_{//}(q) \simeq \frac{a_o^{\lessgtr}\,(1/\xi_{//})^{\gamma}}{(1/\xi_{//})^{2} + q^{2}} \quad : \quad \begin{matrix} a_o^{<} \Leftrightarrow T < 10\,K \\ a_o^{>} \Leftrightarrow T > 15\,K \end{matrix} \qquad 6(a)$$

for the interpretation of their data from the $p = 0.54$, 0.57 samples, where the I.C.L. $1/\xi_{//}$ is defined through the relationship:

$$\frac{1}{\xi_{//}}(p, T, \mu) \cong \frac{1}{\xi_{//}}(p, T=0, \mu) + \left[K_{//}^{(d=1)}\right]^{\nu_t} \qquad 6(b)$$

That is, the longitudinal I.C.L. of the dilute system was taken to be the algebraic sum of the I.C.L. at $T = 0$ and the longitudinal I.C.L. of the analagous one-dimensional system raised to the power of an exponent ν_t. From fitting the experimental data to the form 6(a), the value of the exponent ν_t was found to be:

$$\nu_t = 0.90 \pm 0.05$$

this value for ν_t resulted in the experimentally obtained crossover exponent being:

$$\phi = \nu_p / \nu_t = 1.56 \pm 0.15$$

for the system.

From our own analysis, we associate the absence of a transition to a state of long range order in the p = 0.54, 0.57 samples with their magnetic ion concentrations being below the critical value, $p_c \simeq 0.59$. For the p = 0.60 specimen, equation (4.d.22) of the text would seem to provide an implicit estimate of the transition temperature via:

$$K_{/\!/}^{(d=1)} \left[T_c(\delta p, \mu), \mu \right] \simeq a_o \delta p$$

but, unfortunately, we do not know the value of the constant, a_o However, the fact that the critical temperature of a system lying a distance:

$$\delta p \sim O(10^{-2})$$

from percolation threshold is already one-fifth (1/5) that of the pure system seems to lend credence to our postulated inverse logarithmic dependence of $T_c(\delta p)$ upon δp in equation (4.d.22). Equations 6(a) and 6(b), which were used in the analysis of data obtained from the p = 0.54, 0.57 samples, are certainly consistant with the results of our own analysis provided the exponent, ν_t, in 6(b) is interpreted, not as a constant but as a temperature dependent quantity with limiting behaviour:

$$\nu_t \sim \begin{cases} \nu_p^{(d=2)} & : \quad T \ll J / k_B \cosh\mu \\ \nu_{HEIS}^{(d=2)} & : \quad T \gg J / k_B \cosh\mu \end{cases}$$

Under these circumstances, 6(b) appears as an expansion of equation (4.d.10) of the text viz:

$$\frac{1}{\xi_{//}} \equiv \Theta \, \Phi_{//}\left(\frac{t}{\Theta}\cdot\frac{|\delta p|^{\nu_p}}{\Theta}\right) \sim t + |\delta p|^{\nu_p}$$

The latter form seems to agree with various limits of the longitudinal I.C.L.'s behaviour which we have considered. As an example, precisely at percolation threshold ($\delta p \equiv 0$) our analysis suggets that:

$$\frac{1}{\xi_{//}} \sim \{K_{//}^{(d=1)}\}^{\nu_t} \qquad (\delta p = 0)$$

with ν_t defined as above. Similarly, the limiting expressions (4.d.15) and (4.d.16) of the text are in complete agreement with this form of expansion. Certainly within the framework of our analysis, the assumed form for the longitudinal I.C.L, in the two-dimensional, dilute, weakly, anisotropic Heisenberg system near percolation threshold, is expected to be a very good interpolation form linking the various limiting cases discussed above and in the text.

For the specific case of $Rb_2Mn_pMg_{1-p}F_4$, the samples investigated with concentration less than the critical value, p_c, are expected to show a crossover in behaviour at a characteristic temperature:

$$T_x^{(d=2)} = \frac{J}{k_B \cosh\mu} \sim 9K$$

In terms of this new variable, our expression for the thermal exponent becomes:

$$\nu_t \sim \begin{cases} \nu_p^{(d=2)} & : T \ll T_x \\ \nu_{HEIS}^{(d=2)} & : T \gg T_x \end{cases}$$

Referring back to equations 6(a) we see that the two temperature regimes in which these forms were used correspond to being well below or above crossover. In the former case, $S_{//}(q)$ is expected to

dominate the combination of scattering functions in 6(a), whereas in the latter instance we expect:

$$S_{/\!/}(q) \simeq S_{\perp}(q)$$

so that within either temperature regime the approximation:

$$S_{/\!/}(q) + S_{\perp}(q) \sim \frac{a_o \left\{ K_{/\!/}^{(d=1)} \right\}^{2-\gamma}}{\left\{ K_{/\!/}^{(d=1)} \right\}^{2} + q^2}$$

seems entirely reasonable and is certainly consistent with our own analysis if γ is interpreted as being a function of temperature and anisotropy such that:

$$\gamma \sim \begin{cases} \gamma_{ISING} : T \ll T_x^{(d-2)} \\ \gamma_{HEIS} : T \gg T_x^{(d-2)} \end{cases}$$

where γ_{ISING} and γ_{HEIS} are the corresponding exponents for the Ising and isotropic Heisenberg models at p_c respectively . Under these circumstances, equations 6(a) can be viewed as an expansion of the function:

$$\chi_{/\!/}(q, t, \mu) = \Theta \prod_{/\!/}^{<} \left(\frac{t}{\Theta}, \frac{|\delta p|^{\nu_p}}{\Theta}, \frac{q}{\Theta} \right)$$

which certainly agrees with our own limiting expressions such as (4.d.29) and (4.d.30) in the text.

In conclusion, the results of our present analysis suggest that the functional forms employed by Birgeneau et al. in the interpretation of their neutron scattering experiments on crystalline samples of $Rb_2Mn_pMg_{1-p}F_4$ with $p < p_c$ are consistent with those obtained from a scaling approach provided exponents such as ν_t, γ are interpreted as crossover dependent quantities. In this case, the present analysis suggests the limiting forms:

$$\phi \sim \begin{cases} \phi_I = \nu_p^{(d=2)} / \nu_{ISING}^{(d=2)} & : T \ll T_x \\ \phi_H = \nu_p^{(d=2)} / \nu_{HEIS}^{(d=2)} & : T \gg T_x \end{cases}$$

for the crossover exponent defined by Birgeneau et al. Using the best estimates of $\nu_p^{(d=2)}$ and $\nu_{HEIS}^{(d=2)}$ quoted in 6.a.(ii) and the exact result of Wallace and Young (1978) we obtain:

$$\phi \sim \begin{cases} 1 \quad ; \quad T \ll T_x \\ \\ 1.43 \; ; T \gg T_x \; [\text{Coniglio. 1981}] \end{cases}$$

In figure (19) we give a plot of the expected longitudinal I.C.L. behaviour for systems with the same concentrations as those investigated by Birgeneau et al. (1980) using the interpolation form 6(b) viz:

$$\frac{1}{\xi_{//}}(p,T,\mu) = \frac{1}{\xi_{//}}(p,T=0,\mu) + [K_{//}^{(d=1)}]^{\nu_t}$$

Experimental data is also shown.

In the next section we review the experimental data from neutron scattering experiments on the three-dimensional $Mn_pZn_{1-p}F_2$ system.

(iii) Experiments Carried Out On $Mn_pZn_{1-p}F_2$

Cowley et al.(1977(a))have carried out a series of neutron scattering experiments on the dilute, anisotropic, three-dimensional Heisenberg antiferromagnet $Mn_pZn_{1-p}F_2$. The crystal sample used was found to have a concentration gradient along its length so that it was possible to investigate the scattering as a function of concentration and temperature by masking off small slices of the specimen.

Near to percolation threshold, the experimental data was fitted to the Lorentzian forms:

$$\chi_{\perp}(q) = \frac{A_{\perp}}{K_{\perp}^2 + q^2}$$

$$\chi_{//}(q) = \frac{A_{//}}{K_{//}^2 + q^2}$$

which are consistent with our results (5.c.48) and (5.c.49) for the W.D.S. behaviour in the dilute three-dimensional model below the critical concentration. The exchange constants quoted by Cowley et al. imply an anisotropy parameter, Θ , for the system of:

$$\Theta \simeq 0.3$$

Hence, the crossover temperature of the corresponding one-dimensional system, T_x, is:

$$T_x^{(d=1)} = \frac{J}{k_B \cosh\mu} \sim 10\,K$$

We would therefore expect the I.C.L. forms obtained from fitting the scattering data to the susceptibility expressions above to show a crossover from isotropic Heisenberg-like to Ising-like behaviour near this temperature. This crossover is observed, both above and below percolation threshold, at the temperature, T_x, above.

Below the critical concentration, no transition to L.R.O. occurs and the longitudinal inverse correlation length is finite at absolute zero temperature in agreement with equation (5.c.34) of this thesis, viz:

$$\frac{1}{\xi_{//}} \sim |\delta p|^{\nu_p} \quad : \quad (T=0)$$

However, above percolation threshold, the experimental data would seem to suggest that the longitudinal correlation length does not diverge at the observed, finite temperature phase transition. This behaviour conflicts drastically with the results of our own analysis which predict a continuous transition for samples within this

concentration regime ($p > p_c$). This behaviour may be due to configuration fluctuations giving rise to an effective random anisotropy field. Such a field could reduce the effective dimensionality of the system (Pelcovits, Pytte, Rudnick (1978)). Since we have excluded the possibility of an anisotropy distribution in our original model, our analysis would not be expected to reproduce such behaviour.

For completeness, however, we have included a plot (Figure (20)) of the I.C.L.;

$$\frac{1}{\xi_{//}} = \frac{1}{\xi_{//}}(T=0) + [K_{//}^{(d=1)}]\,\nu_t^{(d=3)}$$

for a model with the exchange constant quoted by Cowley et al. (1977) using the results of our own analysis combined with exponent values obtained from series and scaling methods. Also included on this plot is the corresponding curve for a model in which the anisotropy has been enhanced by a factor of six.

This completes the comparison of our theoretical results with those of experiments. In the following section we briefly review some of the theoretical work which has been carried out on models similar to our own.

d) Comparison With Existing Theoretical Work

In this penultimate section we briefly review some of the theoretical work which has been published on dilute, anisotropic Heisenberg models in two and three dimensions and compare, where possible, with the results of our present analysis.

Stinchcombe (1981) has treated the dilute, anisotropic Heisenberg model within a framework first introduced for the pure case by Suzuki

and Takano (1979) and Barma et al. (1979). This approximation scheme was introduced in order to deal with the case of finite spin ($S = 1/2$) and, hence, quantum effects in the analysis of the Heisenberg model. Unfortunately, in addition to the expected fixed points an additional spurious fixed point occurs very close to the percolation fixed point, due to the combination of the Suzuki-Takano approximation with the binary distribution moment matching approximation. As a result no discussion of the dilute model with magnetic ion concentration close to percolation threshold was possible. However, the results obtained for the dependence of the critical temperature on anisotropy and dilution near the pure limit of the two- and three-dimensional models were in qualitative agreement with those of our present work. In particular, for the limits of strong ($\mu \to 0^+$) and weak ($\Theta \to 0^+$) anisotropy, equations (4.b.45), (4.d.50), (5.d.8) and (5.d.12) of the text give:

i) Two Dimensions

a) Strong Anisotropy ($\mu \to 0^+$)

$$T_c(\delta p, \mu) \doteq T_c(0.0)[1 - \delta p - C_0 \mu^2]$$

$$C_0 = 0.25 \quad \text{cf.} \quad C_0^{\text{STINCHCOMBE}} \simeq 0.32$$

b) Weak Anisotropy ($\Theta \to 0^+$)

$$T_c(\Theta) = C_1 \cdot \left(\frac{J}{k_B}\right) \cdot \frac{1}{\ln(1/\Theta)} \quad : C_1 = 2 \quad \text{cf. } C_1^{\text{STINCHCOMBE}} \sim 5$$

ii) Three Dimensions

a) Strong Anisotropy ($\mu \to 0^+$)

$$T_c(\delta p, \mu) \doteq T_c(0.0)[1 - a_0 \delta p - C_0 \mu^2]$$

$$a_0 = 1/2 \,, \; C_0 = 1/8 \quad \text{cf. } a_0^{\text{STINCHCOMBE}} \sim 1.04 \,, \; C_0^{\text{STINCHCOMBE}} \sim 0.12$$

b) Weak Anisotropy ($\Theta \to \dot{O}$)

$$T_c(\Theta, \delta p) = T_c(0,0)[1 - a_0 \delta p + c_0 \Theta^{1/\phi}]$$

$$a_0 = 1,\ c_0 = 1/\ln 2,\ \phi = 1 \quad \text{cf. } \phi^{\text{STINCHCOMBE}} = 1.56,\ a_0^{\text{STINCHCOMBE}} \approx 1.22$$

Following the investigations outlined above, Stinchcombe (1980(a), 1980(b)), published a series of papers in which he treated the dilute, classical, anisotropic Heisenberg model within a framework similar to our own: a simple decimation procedure in the one-dimensional model and subsequent use of the Migdal/Kadanoff bond moving scheme to obtain results relevant to systems of higher dimensionalities. Although somewhat similar, our expressions for the thermal scaling variables near p_c in two and three dimensions differ from those of Stinchcombe.

In particular, Stinchcombe suggests the following form for the thermal scaling variable:

$$u^{\text{STINCHCOMBE}} = [K_{//}^{(d=1)}]^{\nu_t^{(d)}} \cdot \cosh\mu^{\phi_H^{(d)}-1}$$

whereas our own analysis suggests

$$u = [K_{//}^{(d=1)}]^{\nu_t^{(d)}}$$

The two expressions differ away from the Ising limit (where $\cosh\mu = 1$). Nevertheless, his results for the I.C.L. and transition temperature behaviour of the weakly anisotropic system are in qualitative agreement with our own. It must be stressed that both analyses agree on the qualitative behaviour to be expected from the dilute system near percolation threshold, predicting a crossover from isotropic Heisenberg to Ising and finally geometric behaviour as the temperature of the system is reduced.

More recently, Kumar,Pandy and Barma (1981) have considered the

problem of the weakly anisotropic system near percolation threshold from three different viewpoints. Firstly, following the ideas put forward by Stanley et al. (1976), they have shown that the Lorentzian form for the longitudinal scattering function viz:

$$S_{//}(q) \sim \frac{K_{//}^{2-\gamma}}{K_{//}^{2} + q^{2}}$$

and the form:

$$K_{//} = 1/\xi_{percolation} + \left\{K_{//}^{(d=1)}\right\}^{\nu_t}$$

for the longitudinal I.C.L. of the dilute, anisotropic two-dimensional model near percolation threshold may be derived from the hypotheses that:

i) the spin-spin correlation function, C(r), for the dilute system near p_c may be factored into the form:

$$C(r) = C_1(r) \cdot C_p(r)$$

where $C_1(r)$ is the correlation function on a one-dimensional chain and $C_p(r)$ is a purely geometric factor.

ii) correlations in the dilute system near p_c propagate along one-dimensional paths, and that these paths are effectively self avoiding walks. (SAW's).

In this case, the thermal exponent, ν_t, which appears in the expression for $K_{//}$, is found to be temperature and anisotropy independent in contrast to our own analysis.

In their second approach, Kumar et al. derived approximate but analytic expressions for the I.C.L.'s of the associated one-dimensional model, somewhat akin to our own. They then assumed that the correct scaling variable for this system was the longitudinal I.C.L. of the

one-dimensional model, $K_{//}^{(d=1)}$, raised to some power, $\nu_{\perp}$, and used the usual scaling arguments to predict the analytic form of the critical surface for the two- and three-dimensional models as:

$$K_{//}^{(d=1)}\left(T_c(\delta p,\mu),\mu\right) = a_0\,\delta p^{\phi}$$

This result is again in agreement with our own provided the crossover exponent, ϕ, is taken to be crossover dependent.

Lastly, Kumar et al. used the previously mentioned Suzuki-Takano/Barma approximation scheme together with a slightly different form of distribution matching to that employed by Stinchcombe (1981) in order to obtain numerical plots of the flow diagrams for the anisotropic system in two and three dimensions, and, hence, to obtain phase diagrams for such. These latter plots show a sharp increase in critical temperature with concentration near p_c in qualitative agreement with the results of our own analysis in this regime.

Coniglio (1981) has recently presented an analysis of both the Ising and Isotropic Heisenberg limits of our model near percolation threshold which, like that of Kumar et al., assumes that correlations in the dilute system near p_c propagate along one-dimensional paths. In contrast to the work of Kumar et al., however, Coniglio suggests that it is only the singly connected 'backbone' bonds of the incipient infinite cluster which limit the spread of correlations in the dilute system near p_c.

In the last section, we discuss some of the ways in which the present work may be extended.

e) Possible Extensions

Having explained the methods of analysis we have adopted, reviewed

the results we have obtained and briefly set both in the context of other contemporary work on the subject, we feel that a few, final words are in order on some of the ways in which we consider our work might be extended.

Firstly, we feel that it would be worthwhile calculating the form of the scaling variable, t, throughout the entire temperature range investigated for a given value of the anisotropy. In our present work we have merely indicated the limiting forms for this variable whereas a more complete knowledge of its behaviour would allow more detailed predictions to be made about properties such as the I.C.L.'s , W.D.S's and the phase diagram of the model.

As regards the Migdal/Kadanoff approximation scheme, the recent work of Martinelli and Parisi (1981) seems to open up the possibility of improving on the bond moving scheme in a well controlled manner and, as such, may prove to be particularly useful for the evaluation of the thermal to percolative crossover exponent in the isotropic Heisenberg model in two dimensions.

At a rather more fundamental level, we feel that the effects of concentration fluctuations in $Rb_2Mn_pMg_{1-p}F_4$ and $Mn_pZn_{1-p}F_4$ should be included in our basic models of the experimental systems: especially in the light of recent work by Imry and Ma (1975), Grinstein (1976), Imry and Ma (1976), Young (1977), Pelcovits, Pytte and Rudnick (1978), Parisi and Sourlas (1979) on the effects of random fields and random anisotropy in magnetic systems. In particular, such effects may help to explain the data obtained from the $Mn_pZn_{1-p}F_4$ system.

Lastly, there is the whole question of quantum effects and, in particular, how to include them in our present model. Regretfully we are unable to suggest how such a modeification could be carried out,

at present, but we stress the the inclusion of non-commutation effects into the treatment of dilute, anisotropic Heisenberg systems at or near percolation thresholds could result in qualitatively new behaviour.

Appendix 1

The Iteration Scheme Formalism and Exact Results

The purpose of this appendix is to explain and derive some of the results which, for the sake of brevity, are merely quoted in the main text. In particular, we show how both exact and approximate analytic forms may be obtained for the eigenfunctions $\{\varphi_{pm}\}$ and eigenvectors $\{\lambda_{pm}\}$ of the transfer integral

$$\int_{\Omega_i} \frac{d^2\underline{\sigma}_i}{4\pi} e^{\beta J[\tanh\mu(\sigma_i^x\sigma_j^x + \sigma_i^y\sigma_j^y) + \sigma_i^z\sigma_j^z]} \varphi_{pm}(\hat{\underline{\sigma}}_i|\beta J,\mu)$$

$$= \lambda_{pm}(\beta J,\mu)\,\varphi_{pm}(\hat{\underline{\sigma}}_j|\beta J,\mu) \qquad (A.1.1)$$

which appears as equation (2.b. 4) of chapter two.

The eigenfunctions $\{\varphi_{pm}\}$ and eigenvectors $\{\lambda_{pm}\}$ above are known to be the spheroidal wave functions and radial functions respectively [Joyce (1967), Morse & Feshbach (1953)] . Their explicit forms are:

$$\varphi_{pm}(\hat{\underline{\sigma}}|\beta J,\mu) \equiv \left\{\frac{2}{\Lambda_{pm|}(-ih)}\right\}^{1/2} S_{pm|}(-ih,\cos\theta)\, e^{im\varphi} \qquad [\text{cf. (2.b.10)}]$$

$$\lambda_{pm}(\beta J,\mu) \equiv i^p j e_{pm|}(-ih,\cosh\mu) \qquad [\text{cf.(2.b.12)}]$$

where

$$h \equiv \frac{\beta J}{\cosh\mu}$$

and the polar angles (θ,φ). have been introduced to parameterise the unit spins. Substituting the above forms into our integral

equation and simplifying we obtain:

$$\lambda_{p,o}(h,1).S_{p,o}(-ih,x)=\frac{1}{2}\int_{-1}^{1}dt.e^{hxt}.S_{p,o}(-ih,t) \qquad (A.1.2)$$

Noting that $S_{oo}(-ih,x)$ and $S_{1o}(-ih,x)$ are even and odd under $x\rightarrow -x$ we have:

$$\lambda_{oo}(h,1).S_{oo}(-ih,x)=\int_{o}^{1}dt.\cosh hxt\,.\,S_{oo}(-ih,t) \qquad (A.1.3)$$

$$\lambda_{1o}(h,1).S_{1o}(-ih,x)=\int_{o}^{1}dt.\sinh hxt\,.\,S_{1o}(-ih,t) \qquad (A.1.4)$$

Equations (A.1.3) and (A.1.4) are already sufficient to obtain the exact forms of $S_{oo}(-ih,x)$, $S_{1o}(-ih,x)$, $\lambda_{oo}(h,1)$ and $\lambda_{1o}(h,1)$ as $h\rightarrow 0^{+}$ by expressing the eigenfunctions as a power series in h and x and equating coefficients. These two expressions appear as equations (2.c. 8) and (2.c. 9) of the main text. In order to determine the more general form of $\lambda_{oo}(h,\cosh\mu)$ and $\lambda_{1o}(h,\cosh\mu)$ in the same limit (viz $h\rightarrow 0^{+}$) we put $\cos\theta = 1$ and $m=0$ in (A.1.1) and simplify to obtain:

$$\lambda_{po}(h,\cosh\mu).S_{po}(-ih,1)=\int_{-1}^{1}dx.e^{hx\cosh\mu}S_{po}(-ih,x) \qquad (A.1.5)$$

or:

$$\lambda_{oo}(h,\cosh\mu)=\frac{1}{S_{oo}(-ih,1)}\int_{o}^{1}dx.\cosh(h.\cosh\mu.x).S_{oo}(-ih,x) \qquad (A.1.6)$$

$$\lambda_{1o}(h,\cosh\mu)=\frac{1}{S_{1o}(-ih,1)}\int_{o}^{1}dx.\sinh(h.\cosh\mu.x).S_{1o}(-ih,x) \qquad (A.1.7)$$

By substituting the forms for $S_{oo}(-ih,x)$ and $S_{1o}(-ih,x)$ obtained from equations (A.1.3) and (A.1.6) and (A.1.7) we can

evaluate λ_{oo} and λ_{1o} to arbitrary precision in this limit. Equations (A.1.6) and (A.1.7) appear as (2.c. 11) and (2.c. 12) in the main text.

When the variable h becomes large, the methods outlined above are inapplicable. However, following the discussion in 2 (c) of the text we expect λ_{oo}, λ_{1o} and λ_{11} to completely dominate the eigenvalue spectrum of the transfer integral in this regime ($h \gg 1$). This property may be exploited by using an iterative process to project out these three eigenvalues in this limit.

Consider the general symmetric 'seed' function $S^{(o)}_{oo}(-ih,x)$ which we may expand in the complete set $\{S_{\rho,o}(-ih,x)\}$ as:

$$S^{(o)}_{o,o}(-ih,x) = \sum_{\rho=0}^{\infty} a_{2\rho}\, S_{2\rho,o}(-ih,x) \qquad (A.1.8)$$

Substituting this form into the right-hand side of (A.1.3) in place of $S_{o,o}(-ih,x)$ we obtain:

$$S^{(1)}_{o,o}(-ih,x) \equiv \int_o^1 dt.\cosh hxt\; S^{(o)}_{oo}(-ih,t) \qquad (A.1.9)$$

$$= \sum_{\rho=0}^{\infty} a_{2\rho} \int_o^1 dt.\cosh hxt.\, S_{2\rho,o}(-ih,t)$$

$$= \sum_{\rho=0}^{\infty} a_{2\rho}\, \lambda_{2\rho,o}(h,1).\, S_{2\rho,o}(-ih,x)$$

where the last step follows from the symmetric nature of $S_{2\rho,o}(-ih,x)$ under $x \to -x$ and (A.1.2).

Repeating the process (n + 1) time we have:

$$S^{(n+1)}_{o,o}(-ih,x) = [\,\lambda_{oo}(h,1)]^{n+1} \sum_{\rho=0}^{\infty} a_{2\rho}\left[\frac{\lambda_{2\rho,o}(h,1)}{\lambda_{o,o}(h,1)}\right]^{n+1} S_{2\rho,o}(-ih,x)$$

In the limit of large h, the ratio

$$\left[\frac{\lambda_{2\rho,0}(h,1)}{\lambda_{0,0}(h,1)}\right]^{n+1} \sim \delta_{\rho,0} \qquad \begin{pmatrix} n\to\infty \\ h \gg 1 \end{pmatrix}$$

since $\cosh\mu = 1$ corresponds to the Ising limit of the anisotropic model. Thus, in this same limit we have:

$$S_{oo}^{(n)}(-ih,x) \sim S_{oo}(-ih,x)$$

so that successive approximations to the eigenfunction $S_{oo}(-ih,x)$ may be obtained by iterating equation (A.1.9) in the more general form:

$$S_{oo}^{(n+1)}(-ih,x) = \int_0^1 dt.\cosh hxt.\, S_{oo}^{(n)}(-ih,t) \qquad (A.1.10)$$

This is equation (2.c. 2) of the main text.

Replacing $S_{oo}(-ih,x)$ by $S_{oo}^{(n)}(-ih,x)$ in the r.h.s. of (A.1.6) and using (A.I.5) we have:

$$\frac{1}{S_{oo}^{(n)}(-ih,1)}\int_0^1 dx.\cosh(h.\cosh\mu.x)\, S_{oo}^{(n)}(-ih,x)$$

$$= \lambda_{oo}(h,\cosh\mu)\left\{\frac{\sum_{\rho=0}^{\infty} a_{2\rho}\left(\frac{\lambda_{2\rho,0}(h,1)}{\lambda_{0,0}(h,1)}\right)^n \cdot \frac{\lambda_{2\rho,0}(h,\cosh\mu)}{\lambda_{0,0}(h,\cosh\mu)} S_{2\rho,0}(-ih,1)}{\sum_{\rho=0}^{\infty} a_{2\rho}\left(\frac{\lambda_{2\rho,0}(h,1)}{\lambda_{0,0}(h,1)}\right)^n S_{2\rho,0}(-ih,1)}\right\}$$

$$\equiv \lambda_{oo}^{(n)}(h,\cosh\mu) \sim \lambda_{oo}(h,\cosh\mu) \qquad (n\to\infty)$$

so that successive estimates to the eigenvalue λ_{oo} may be obtained from:

$$\lambda^{(n)}(h,\cosh\mu) = \frac{1}{S_{oo}^{(n)}(-ih,1)}\int_0^1 dx.\cosh[h.\cosh\mu.x].S_{oo}^{(n)}(-ih,x) \qquad (A.1.11)$$

This is equation (2.c. 5) of the main text. In a similar fashion, equation (2.c. 6) may be derived by using an antisymmetric seed

function.

In order to determine the form of $S_{11}(-ih,x)$ and $\lambda_{11}(h,\cosh\mu)$ we firstly put $r = m = 1$ in (A.1.1) to obtain:

$$\lambda_{11}(h,\cosh\mu).S_{11}(-ih,\cos\theta) = \int_0^{2\pi}\frac{d\varphi}{4\pi}.e^{i\varphi}\int_0^{\pi}d\theta'.\sin\theta'. \tag{A.1.12}$$
$$e^{h.\sinh\mu.\sin\theta\sin\theta'\cos\varphi + h.\cosh\mu.\cos\theta\cos\theta'}\,S_{11}(-ih,\cos\theta')$$

Taking the partial derivative of (A.1.12) w.r.t. μ at constant h and allowing $\mu \to 0^+$ we have:

$$\frac{\partial}{\partial\mu}.\lambda_{11}(h,\cosh\mu)\Big|_{\substack{h\\ \cosh\mu\to 1}}.S_{11}(-ih,\cos\theta) =$$
$$h.\sin\theta.\left\{\int_0^{2\pi}\frac{d\varphi}{4\pi}.e^{i\varphi}.\cos\varphi.\right\}.\int_0^{\pi}d\theta'\sin^2\theta.e^{h.\cos\theta\cos\theta'}\,S_{11}(-ih,\cos\theta')$$

By substituting:

$$S_{11}(-ih,\cos\theta) = f_{11}(-ih,\cos\theta).\sin\theta$$

we obtain

$$\frac{\partial}{\partial\mu}\lambda_{11}(h,\cosh\mu)\Big|_{\mu\to 0^+}.f_{11}(-ih,x) = \frac{h}{2}.\int_0^1 dt.(1-t^2).\cosh hxt.f_{11}(-ih,t) \tag{A.1.13}$$

For $\mu = 0$, all the $\{\lambda_{r,m\neq 0}\}$ are identically zero. [Put $\mu = 0$ in (A.1.1)]. However, for arbitrarily small μ, we expect the $|r|=|m|=1$ eigenvalue to be the largest element of the set

$$\{\lambda_{r,m}|\ m\neq 0\}$$

It therefore seems plausible that as $h \to \infty$:

$$\frac{\partial}{\partial\mu}\lambda_{\shortparallel}(h,\cosh\mu)\Big|_{\mu\to 0^+}$$

is the largest element of the set

$$\left\{\frac{\partial}{\partial\mu}\lambda_{rm}(h,\cosh\mu)\Big|_{\mu\to 0^+}\;\middle|\; m\neq 0\right\}$$

Hence, equation (A.1.13) is analagous to (A.1.2). It is therefore, a straightforward extension of our previous analysis to use (A.1.13) to obtain f(-ih,x) as a power series in h and x for h small as in (2.c. 10). In order to obtain $\lambda_{\shortparallel}$ in the same limit we take the limit of $\Theta\to 0^+$ in (A.1.12) to obtain:

$$\lambda_{\shortparallel}(h,\cosh\mu)=\frac{1}{\int_{\shortparallel}(-ih,1)}\cdot\frac{K.\tanh\mu}{2}\cdot\int_0^1 dx.(1-x^2).\cosh Kx\cdot\int_{\shortparallel}(-ih,x) \qquad (A.1.14)$$

This is equation (2.c. 13) of the text.

For large values of h, we may iterate an initial 'seed' function,

$$\int_{\shortparallel}^{(0)}(-ih,x)$$

in the r.h.s. of (A.1.13) to obtain successive estimates of f(-ih,x) through:

$$\int_{\shortparallel}^{(n+1)}(-ih,x)=\int_0^1 dt.(1-t^2).\cosh hxt.\int_{\shortparallel}^{(n)}(-ih,t)$$

and, hence, from the definition of $\int_{\shortparallel}$:

$$S_{\shortparallel}^{(n+1)}(-ih,x)=(1-x^2)^{1/2}\int_0^1 dt\,(1-t^2)^{1/2}.\cosh hxt.S_{\shortparallel}^{(n)}(-ih,t) \qquad (A.1.15)$$

This is equation (2.c. 4) of the text.

Equation (A.1.14) may be used to obtain successive estimates of the eigenvalue $\lambda_{\shortparallel}(h,\cosh\mu)$ from:

$$\lambda_{\parallel}^{(n)}(h,\cosh\mu) = \frac{1}{\oint^{(n)}(-ih,1)} \cdot \frac{K.\tanh\mu}{2} \cdot \int_0^1 dx\,(1-x^2)\cosh Kx \cdot \oint^{(n)}(-ih,x) \qquad (A.1.16)$$

with

$$\lambda_{\parallel}^{(n)}(h,\cosh\mu) \sim \lambda_{\parallel}(h,\cosh\mu) \qquad (n\to\infty)$$

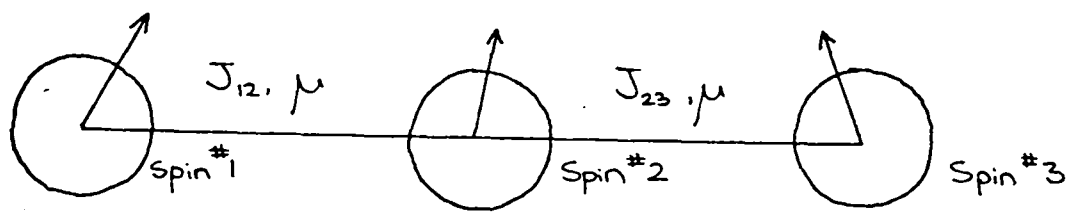
(A.1.16) is equation (2.c. 7) of the text.

Appendix 2

Bond Combination And Decimation In Dilute Systems

In this appendix we derive some of the results which for the sake of brevity, were simply quoted in the text. In particular, we outline and discuss the explicit means by which the bond combination and decimation operations arising in the Migdal/Kadanoff bond moving scheme are carried out. From the outset we restrict our attention to dilute magnetic systems in which all interactions between nearest neighbour spins have the same anisotropy value.

To begin with, we consider taking a trace over the central spin in the cluster illustrated below.



This operation is entirely analagous to the trace which was taken over spins B or E in figures 11(a), (b) and, as discussed in the text, is one of the basic procedures from which the bond moving scheme is built up.

The Hamiltonian, H_{12}, for the interaction between spins # 1 and # 2 may be expressed as:

$$e^{-\beta H_{12}} = e^{K_{12}\left[\tanh\mu\left(\sigma_1^x\sigma_2^x + \sigma_1^y\sigma_2^y\right) + \sigma_1^z\sigma_2^z\right]} \qquad (A.2.1)$$

where:

$$K_{12} \equiv \frac{J_{12}}{k_B T} \equiv \beta J_{12}$$

and we have used the notation formerly introduced in Chapter 2 of the text (eqn. 2.a.1) to parameterise the interaction strength and

anisotropy.

Alternatively, equation (A.2.1) may be re-expressed in terms of the spheroidal wavefunctions:

$$\{ S_{p,|m|}(-ih, \cos\Theta) \}$$

, which were discussed at length in Chapter 2, as:

$$e^{-\beta H_{12}} = \sum_{p,m} \alpha_{p|m|}(h_{12})\, \lambda_{p,m}(h_{12},\mu)\, S_{p|m|}(-ih_{12}, \cos\Theta_1)\, e^{im(\varphi_1-\varphi_2)}\, S^{*}_{p|m|}(-ih_{12}, \cos\Theta_2) \quad : (A.2.1(a))$$

with:

$$h_{12} \equiv \frac{\beta J_{12}}{\cosh\mu}$$

This latter expansion allows the trace over spin # 2 in our original diagram to be re-phrased as:

$$e^{-\beta H_{13}} = \int \frac{d^2\sigma_2}{4\pi} \cdot e^{-\beta H_{12}} \cdot e^{-\beta H_{23}}$$

$$= \sum_{\substack{p,q \\ m}} \alpha_{p|m|}(h_{12})\, \alpha_{q|m|}(h_{23})\, \lambda_{pm}(h_{12},\mu)\, \lambda_{qm}(h_{23},\mu)$$

$$S_{p|m|}(-ih_{12}, \cos\Theta_1)\, S^{*}_{q|m|}(-ih_{23}, \cos\Theta_3)\, e^{im(\varphi_1-\varphi_3)}$$

$$\left\{ \frac{1}{2} \int_{-1}^{1} dx \cdot S_{p|m|}(-ih_{12}, x)\, S^{*}_{q|m|}(-ih_{23}, x) \right\} \quad : (A.2.2)$$

Having obtained the expansion (A.2.2) for the new Hamiltonian, H_{13}, we proceed to show how this expression simplifies in the limits of large or small values for the thermal variables $\{ h_{ij} \}$.

i) Both h_{12} and h_{23} much greater than unity

In this regime, as discussed in Chapter 2, the eigenvalue spectrum:

$$\{ \lambda_{p,m}(h,\mu) \}$$

for the anisotropic Heisenberg model is dominated by just three members viz:

$$\lambda_{00}, \lambda_{10}, \lambda_{11} \; (= \lambda_{1,-1})$$

As a result, (A.2.2) may be asymptotically approximated as:

$$e^{-\beta H_{13}} \sim \sum_{\substack{p,q=0 \\ m \le \min(p,q)}} \alpha_{p|m|}(h_{12})\, \alpha_{q|m|}(h_{23})\, \lambda_{p,m}(h_{12},\mu)\, \lambda_{q,m}(h_{23},\mu)\, S_{p|m|}(-ih_{12},\cos\Theta_1)\, S^{*}_{q|m|}(-ih_{23},\cos\Theta_3)\, e^{im(\varphi_1-\varphi_3)} \left\{ \frac{1}{2}\int_{-1}^{1} dx\, S_{p|m|}(-ih_{12},x)\, S^{*}_{q|m|}(-ih_{23},x) \right\}$$

By using the functional forms for S_{00}, S_{10} and S_{11} which were obtained from the iteration scheme, in Chapter 2, this expression may be further reduced to the same form as (2.A.1(a)) viz:

$$e^{-\beta H_{13}} \sim \sum_{\substack{p=0 \\ m \le p}}^{1} \alpha_{p|m|}(h')\, \lambda_{pm}(h',\mu')\, S_{p|m|}(-ih',\cos\Theta_1)\, S^{*}_{p|m|}(-ih',\cos\Theta_3)\, e^{im(\varphi_1-\varphi_3)}$$

where the transformed parameters

$$h', \mu'$$

are implicitly defined through the relationships:

$$\frac{\lambda_{10}(h',\mu')}{\lambda_{00}(h',\mu')} = \frac{\lambda_{10}(h_{12},\mu)}{\lambda_{00}(h_{12},\mu)} \cdot \frac{\lambda_{10}(h_{23},\mu)}{\lambda_{00}(h_{23},\mu)} \qquad (A.2.4)$$

$$\frac{\lambda_{11}(h',\mu')}{\lambda_{00}(h',\mu')} = \frac{\lambda_{11}(h_{12},\mu)}{\lambda_{00}(h_{12},\mu)} \cdot \frac{\lambda_{11}(h_{23},\mu)}{\lambda_{00}(h_{23},\mu)} \qquad (A.2.5)$$

By taking the logarithm of (A.2.4/5) and using equations

(2.b.17-18) in the text for the I.C.L. of the one-dimensional anisotropic model, the transformation equations may be re-written as:

$$K_{//}^{(d=1)}(h',\mu') = K_{//}^{(d=1)}(h_{12},\mu) + K_{//}^{(d=1)}(h_{23},\mu) \quad : (A.2.6)$$

$$K_{\perp}^{(d=1)}(h',\mu') = K_{\perp}^{(d=1)}(h_{12},\mu) + K_{\perp}^{(d=1)}(h_{23},\mu) \quad : (A.2.7)$$

where $K_{//}^{(d=1)}(h,\mu)$ and $K_{\perp}^{(d=1)}(h,\mu)$ are to be interpreted as the longitudinal and transverse I.C.L. of a one-dimensional chain in which all bonds have the same thermal and anisotropy value, viz. h,μ.

Before we discuss the explicit transformations for h and μ we consider the second regime:

ii) Both h_{12} and h_{23} much less than unity

In this case we may use the exact result:

$$\lim_{h_{12},h_{23}\to 0^+} \frac{1}{2}\int_{-1}^{1} dx\, S_{p|m|}(-ih_{12},x)\, S_{q|m|}(-ih_{23},x) = \delta_{qp}$$

which follows from the fact that in this limit, the $S_{p,|m|}$, become Legendre Polynomials in the variable x. As a result, our expression (A.2.2) again simplifies to the form (2.A.1(a)) with transformed thermal and anisotropy parameters h, μ given implicitly by:

$$\frac{\lambda_{10}(h',\mu')}{\lambda_{00}(h',\mu')} \qquad \frac{\lambda_{10}(h_{12},\mu)}{\lambda_{00}(h_{12},\mu)} \cdot \frac{\lambda_{10}(h_{23},\mu)}{\lambda_{00}(h_{23},\mu)}$$

$$\frac{\lambda_{11}(h',\mu')}{\lambda_{00}(h',\mu')} \qquad \frac{\lambda_{11}(h_{12},\mu)}{\lambda_{00}(h_{12},\mu)} \cdot \frac{\lambda_{11}(h_{23},\mu)}{\lambda_{00}(h_{23},\mu)}$$

These are the same transformation equations as previously obtained in the regime where

$$h_{12}, h_{23} \gg 1$$

(cf. equations (A.2.4/5)).

Again, by taking their logarithm they may be expressed in terms of the I.C.L.'s of the associated one-dimensional, anisotropic model as:

$$K_{\parallel}^{(d=1)}(h',\mu') = K_{\parallel}^{(d=1)}(h_{12},\mu) + K_{\parallel}^{(d=1)}(h_{23},\mu)$$

$$K_{\perp}^{(d=1)}(h',\mu') = K_{\perp}^{(d=1)}(h_{12},\mu) + K_{\perp}^{(d=1)}(h_{23},\mu)$$

We now consider the explicit transformation equations

$$h' = h'(h,\mu)$$
$$\mu' = \mu'(h,\mu)$$

and how they may be obtained from our results above in particular limiting cases.

a) The Weakly Anisotropic System ($\mu \gg 1$) With h_{12}, $h_{23} \gg 1$

In this limit equations (2.f.3-4) of the text may be substituted into equations (A.2.6/7) to obtain:

$$\left.\begin{aligned} \Theta' &= 2\Theta \\ h' &= h_{min} - \tfrac{1}{2}\ln\left(\frac{1+e^{-2\Delta h}}{2}\right) \end{aligned}\right\} \quad (A.2.8)$$

where Θ was defined in equation (3.c.1) of the text and:

$$h_{min} = \min(h_{12}, h_{23})$$
$$\Delta h = |h_{12} - h_{23}|$$

In the limit of $h_{12} = h_{23} = h$ we regain the pure one-dimensional(below crossover) scaling results:

$$\Theta' = 2\Theta$$
$$h' = h$$

b) Weakly Anisotropic System ($\mu \gg 1$) With h_{12}, $h_{23} \ll 1$.

By using equations (2.f.1-2) in the text, the transformations for h and Θ become:

$$\left.\begin{aligned} \Theta' &= 2\Theta \\ \frac{1}{h'} &= \left(\frac{1}{h_{12}} + \frac{1}{h_{23}}\right)\cdot\frac{1}{2} \end{aligned}\right\} \quad (A.2.9)$$

c) The Ising Limit: $\mu = 0$; $h_{12}, h_{23} \gg 1$

From equation (2.d.1) in the text we have:

$$h' = h - \tfrac{1}{2} \ln\left(1 + e^{-2\Delta h}\right) \qquad (A.2.10)$$

which, in the limit $h_{12} = h_{23} = h$ becomes the usual result for scaling of the Ising chain viz:

$$h' = h - \tfrac{1}{2} \ln 2$$

d) The Isotropic Heisenberg Limit: $\frac{1}{\mu} = 0$; $h_{12}, h_{23} \longrightarrow 0^{+}$

In this limit, equations (2.e.1) of the text give the resultant scaling for $K = h/\Theta$ as:

$$\frac{1}{K} = \frac{1}{K_{12}} + \frac{1}{K_{23}} \qquad (A.2.11)$$

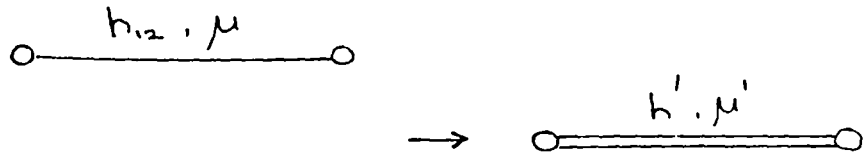
In summary, our results (A.2.8-11) show that if we start from a dilute system in which all bonds have the same anisotropy, μ, the first step of the M-K scheme, decimation, leaves us with a new unique value for the anisotropy, μ', given by:

$$\frac{\cosh\mu' + 1}{\cosh\mu' - 1} = \left(\frac{\cosh\mu + 1}{\cosh\mu - 1}\right)^{2}$$

or, in terms of the variable Θ defined in (3.c.1):

$$\Theta' = 2\Theta$$

The second step of the bond moving scheme combines bonds 'in parallel'. If both bonds have the same initial anisotropy value, μ, the resultant bond formed by bond combination will have the same anisotropy value, but its interaction strength will be the algebraic sum of the two constituent bond strength combined. This process is shown schematically below:



$$h' = h_{12} + h_{23}$$
$$\mu' = \mu$$

As a direct result of combining the above two processes, decimation and bond combination 'in parallel', any dilute system which starts with a well defined anisotropy value, μ , for all bonds can be seen to retain this property under the operation of the M-K bond moving scheme. Moreover, the anisotropy scaling decouples from the associated thermal parameter scaling and is given, in arbitrary dimensionality by the transformation

$$\Theta' = b\Theta \qquad (A.2.12)$$

under a length dilation by a factor b.

REFERENCES

Aharony, A., Imry, Y., Ma, S.-K., 1976, Phys. Rev. Lett. 37, 1364.

Balz, D., Plieth, K., 1955, Z. Electrochemie 59, 545.

Barma, M., Kumar, K., Pandey, R. P., 1979, J. Phys. C12, L283.

Belavin, A. A., Polyakov, A. M., 1975, JETP Lett. 22, 245.

Birgeneau, R. J., Guggenheim, H. J., Shirane, G, 1970, Phys. Rev. B1, 2211.

Birgeneau, R. J., Dingle, R., Hutchings, M. T., Shirane, G., Holt, S. L., 1971, Phys. Rev. Lett. 26, 718.

Birgeneau, R. J., Cowley, R. A., Shirane, G., Guggenheim, H. J., 1976, Phys. Rev. Lett. 37, 940.

Birgeneau, R. J., Cowley, R. A., Shirane, G., Tarvin, J. A., Guggenheim, H. J., 1980, Phys. Rev. B21, 317.

Blote, H. W. J., Nightingale, M. P., Derrida, B., 1981, J. Phys. A14, L45.

Blume, M., Heller, P., Lurie, N. A., 1975, Phys. Rev. B11, 4483.

Breed, D. J., 1967, Physica 37, 35.

Breed, D. J., Gilijamse, K., Sterkenburg, J. W. E., Miedema, A. R., 1973, Physica 68, 303.

Coniglio, A., 1981, Phys. Rev. Lett. 46, 250.

Cowley, R. A., Shirane, G., Birgeneau, R. J., Guggenheim, H. J., 1977, Phys. Rev. B15, 4292.

Cowley, R. A., Shirane, G., Birgeneau, R. J., Svensson, E. C., 1977(a), Phys. Rev. Lett. 39, 894.

Davies, M. R., Harris, C. K., Stinchcombe, R. B., 1981, J. Phys. A14, 459.

Domb, C., 1960, Adv. Phys. 9, 149.

Dunn, A. G., Essam, J. W., Ritchie, D. S., 1975, J. Phys. C8, 4219.

Elliott, R. J., Heap, R. B., Morgan, D. J., Rushbrooke, G. S., 1960, Phys. Rev. Lett. 5, 366.

Essam, J. W., in 'Phase Transitions and Critical Phenomena , Vol 2', 1972, eds. C. Domb & M. S. Green (London: Academic Press), 1972.

Faria, A. C., Pires, A. S. T., 1979, J. Phys. C12, 2637.

Feigel'man, M. V., 1976, Sov. Phys. Solid State 18, 1434.

Fisher, M. E., 1964, Am. J. Phys. 32, 343.

Griffiths, R. B., 1965, J. Chem. Phys. 43, 1958.

Grinstein, G., 1976, Phys. Rev. Lett. 37, 944.

Grinstein, G., Luther, A., 1976, Phys. Rev. B13, 1329.

Harris, A. B., 1974, J. Phys. C7, 1671.

Hertz, J. A., 1976, Phys. Rev. B14, 1165.

Imry, Y., Ma, S-K., 1975, Phys. Rev. Lett. 35, 1399.

de Jongh, L. J., Miedema, A. R., 1974, 'Experiments On Simple Magnetic Model Systems', (Taylor & Francis).

Joyce, G. S., 1967, Phys. Rev. Lett. 19, 581.

Joyce, G. S., 1967(a), Phys. Rev. 155, 478.

Kadanoff, L. P., 1966, Physics 2, 263.

Kadanoff, L. P., 1976, Annals of Physics 100, 359.

Kirkpatrick, S., 1977, Phys. Rev. B15, 1533.

Kumar, D., Pandey, R. B., Barma, M., 1981, Phys. Rev. B23, 2269.

Loveluck, J. M., Lovesey, S. W., Aubry, S., 1975, J. Phys. C8, 3841.

Lubensky, T. C., 1975, Phys. Rev. B9, 3573.

Lubensky, T. C., 1977, Phys. Rev. B15, 311.

Ma, S-K., 1976, 'Modern Theory of Critical Phenomena', (W. A. Benjamin Inc.).

Martinelli, G., Parisi, G., 1981, Nucl. Phys. B (Netherlands) 180. [FS2] , 201.

McGurn, A. R., Scalapino, D. J., 1975, Phys. Rev. B11, 2552.

McGurn, A. R., 1979, J. Phys. C12, 3523.

Migdal, 1976, Sov. Phys. JETP 42, 743.

Montrell, E. W., Potts, R. B., Ward, J. C., 1963, J. Math. Phys. 4, 308.

Morse, P. M., Feshbach, H., 1953, 'Methods of Theoretical Physics, Part II', (McGraw-Hill).

Mujeeb, A., Stinchcombe, R. B., 1982, J. Phys. C15, 3163.

Nakamura, K., Sasada, T., 1978, J. Phys. C11, 331.

Niemeijer, Th., Van Leeuwen, J. M. J., 1976, in 'Phase Transitions and Critical Phenomena, Part 6' eds. C. Domb and M. S. Green (London: Academic Press).

Onsager, L., 1944, Phys. Rev. 65, 117.

Parisi, G., Sourlas, N., 1979, Phys. Rev. Lett. 43, 744.

Pelcovits, R. A., Pytte, E., Rudnick, J., 1978, Phys. Rev. 40, 476.

Pfeuty, P., Toulouse, G., 1977, 'Introduction to the Renormalisation Group and to Critical Phenomena', (Wiley-Interscience).

Polyakov, A. M., 1975, Phys. Lett. 59B, 79.

Rae, J., 1974, J. Phys. A7, 1349.

Riedel, E., Wegner, F., 1969, Z. Phys. 225, 195.

Riedel, E. K., 1971, J. Appl. Phys. 42, 1383.

Satija, I., 1980, Phys. Rev. B22, 1362.

Sneddon, L., Stinchcombe, R. B., 1978, J. Phys. C11, 4037.

Stanley, H. E., 1971, 'Introduction To Phase Transitions And Critical Phenomena' (Clarendon Press, Oxford).

Stanley, H. E., Birgeneau, R. J., Reynolds, P. J., Nicoll, J. F., 1976, J. Phys. C9, L553.

Stauffer, D., 1975, Z. Phys. B22, 161.

Stinchcombe, R. B., Watson, B. P., 1976, J. phys. C9, 3221.

Stinchcombe, R. B., 1979, J. Phys. C12, L41.

Stinchcombe, R. B., 1980, J. Phys. C13, L133.

Stinchcombe, R. B., 1980(a), J. Phys. C13, 3713.

Stinchcombe, R. B., 1980(b), J. Phys. C13, 3723.

Stinchcombe, R. B., 1981, J. Phys. C14, 397.

Suzuki, M., Takano, H., 1979, Phys. Lett. 69A, 426.

Tahir-Kheli, R.A., Ter Haar, D., 1962, Phys Rev. 127, 88,95

Thompson, C. J., 1968, J. Math. Phys. 9, 241.

Thorpe, M. F., 1975, J. Phys. (Paris) 36, 1177.

Thorpe, M. F., Beeman, 1975, Phys. Rev. B14, 188.

Wallace, D. J., Young, A. P., 1978, Phys. Rev. B17, 2384.

Widom, B., 1965, J. Chem. Phys. 43, 3892, 3898.

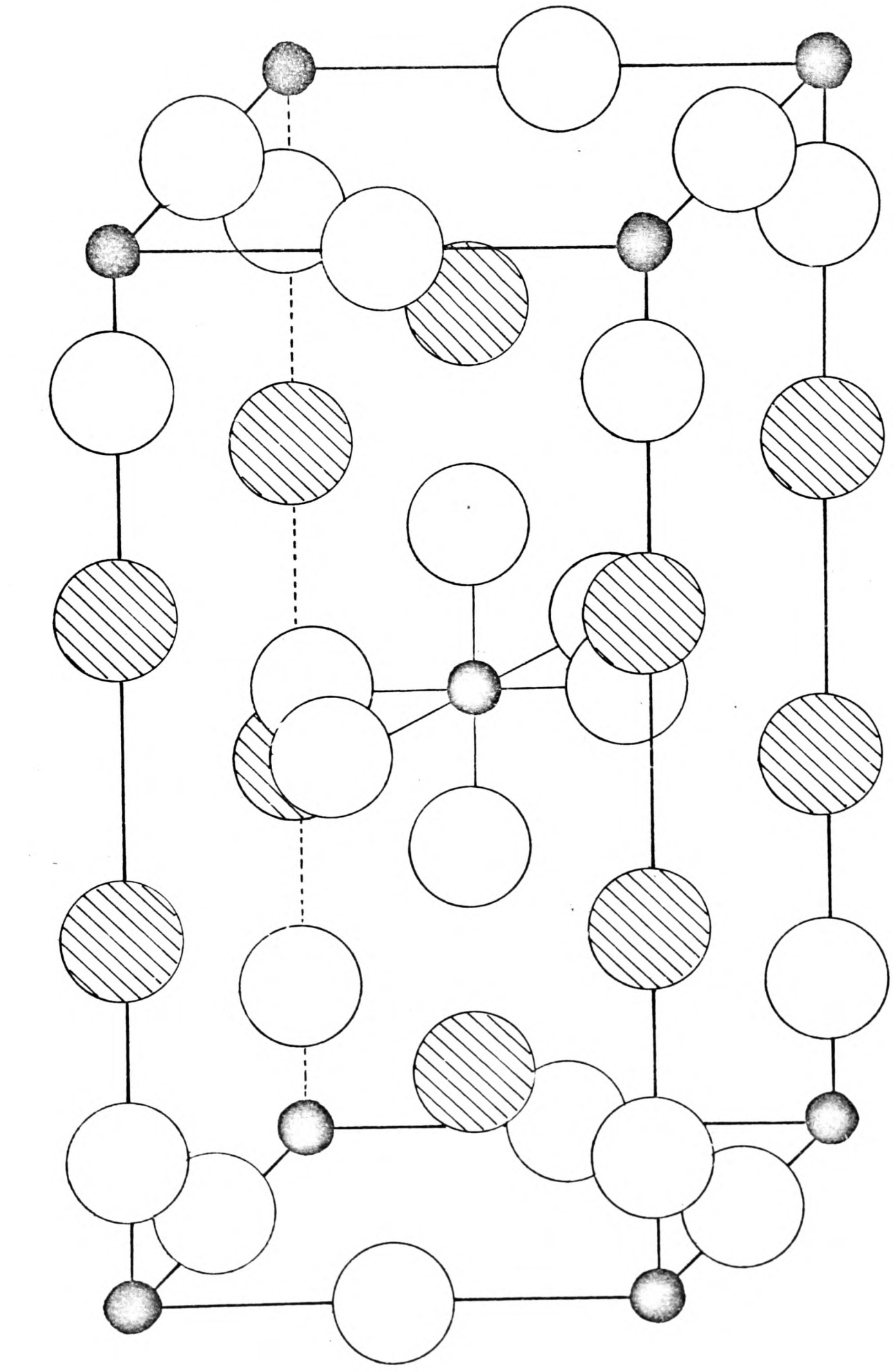
Yeomans, J. M., Stinchcombe, R. B., 1979, J. Phys. C12, 347.

Young, A. P., 1975, J. Phys. C8, L309.

Young, A. P., Stinchcombe, R. B., 1976, J. Phys. C9, 4419.

Young, A. P., 1977, J. Phys. C10, L257.

Figure 1. The crystal structure of Rb_2MnF_4



≡ F ≡ Rb ≡ Mn

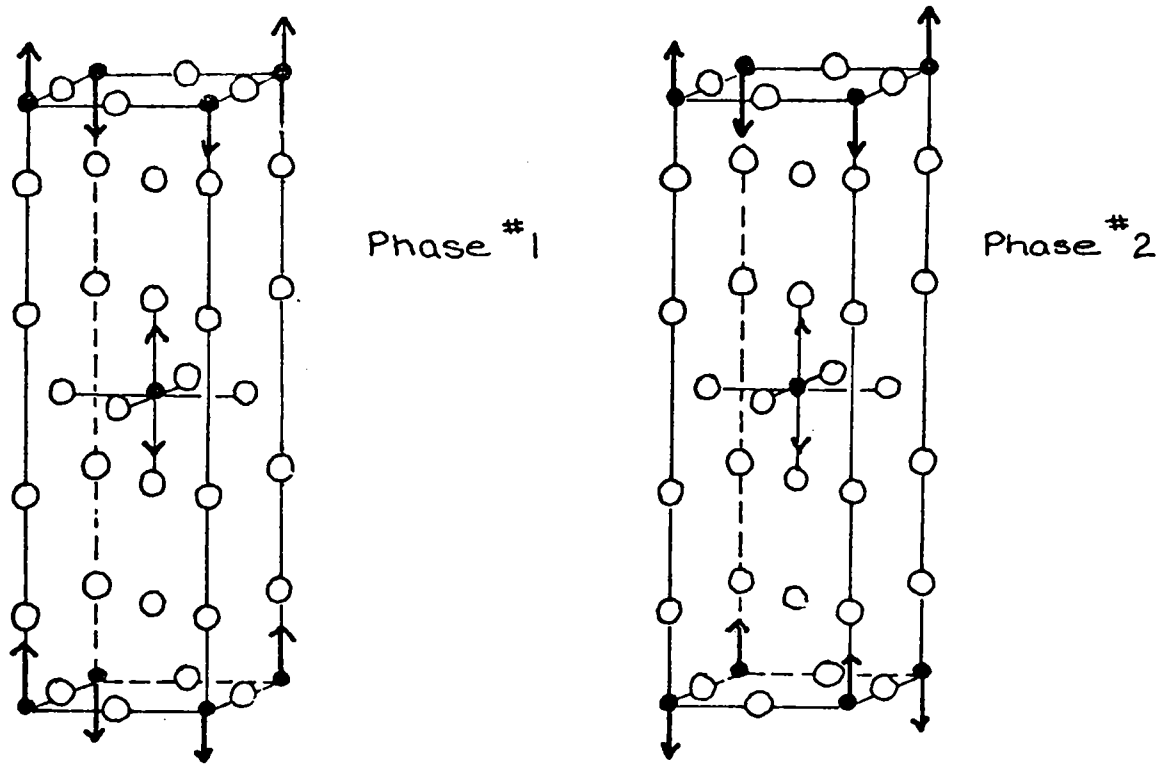


Figure 2. The two magnetic phases which coexist in the ordered phase of Rb_2MnF_4. In phase #1, the next-nearest (n.n.) layers of manganese ions are aligned. In phase #2, the n.n. layers are anti-aligned.

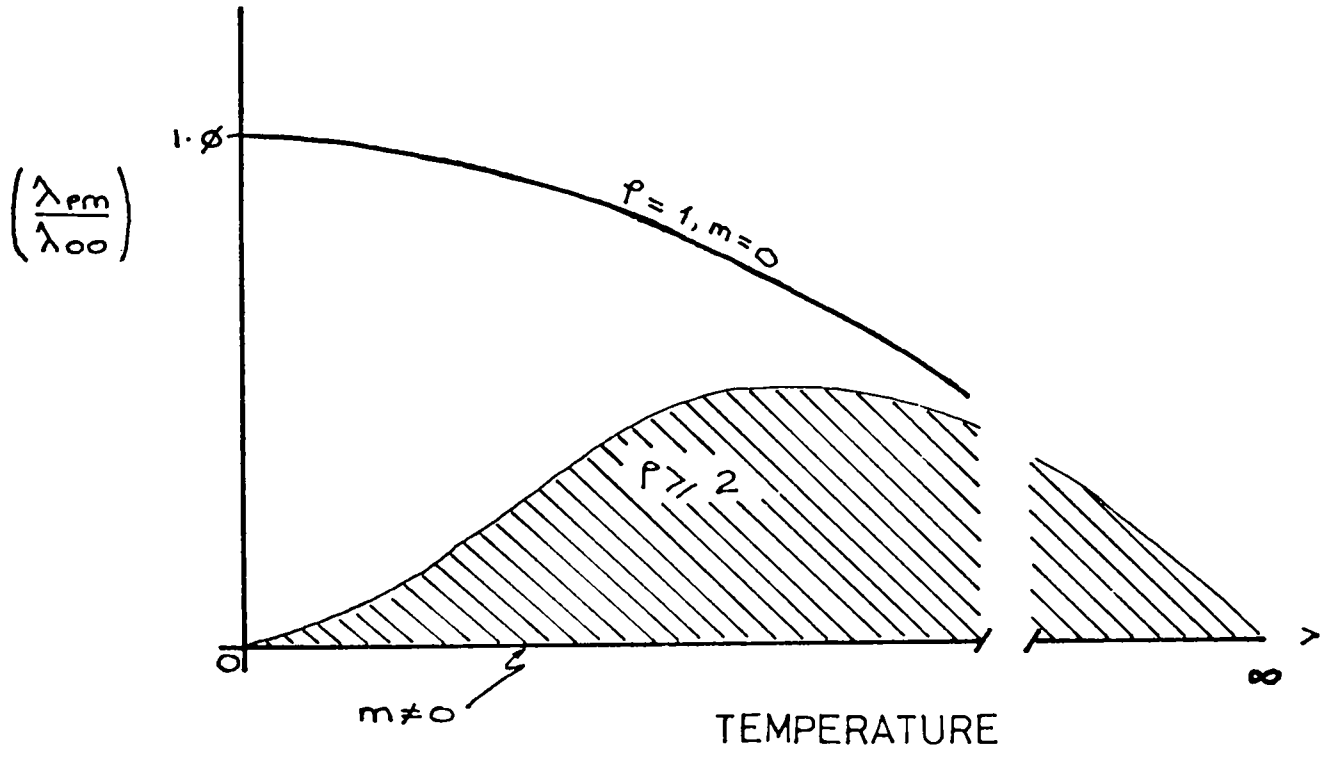


Figure 3. The eigenvalue spectrum behaviour for the Classical Ising Chain. Eigenvalues with $m \neq 0$ are identically zero.

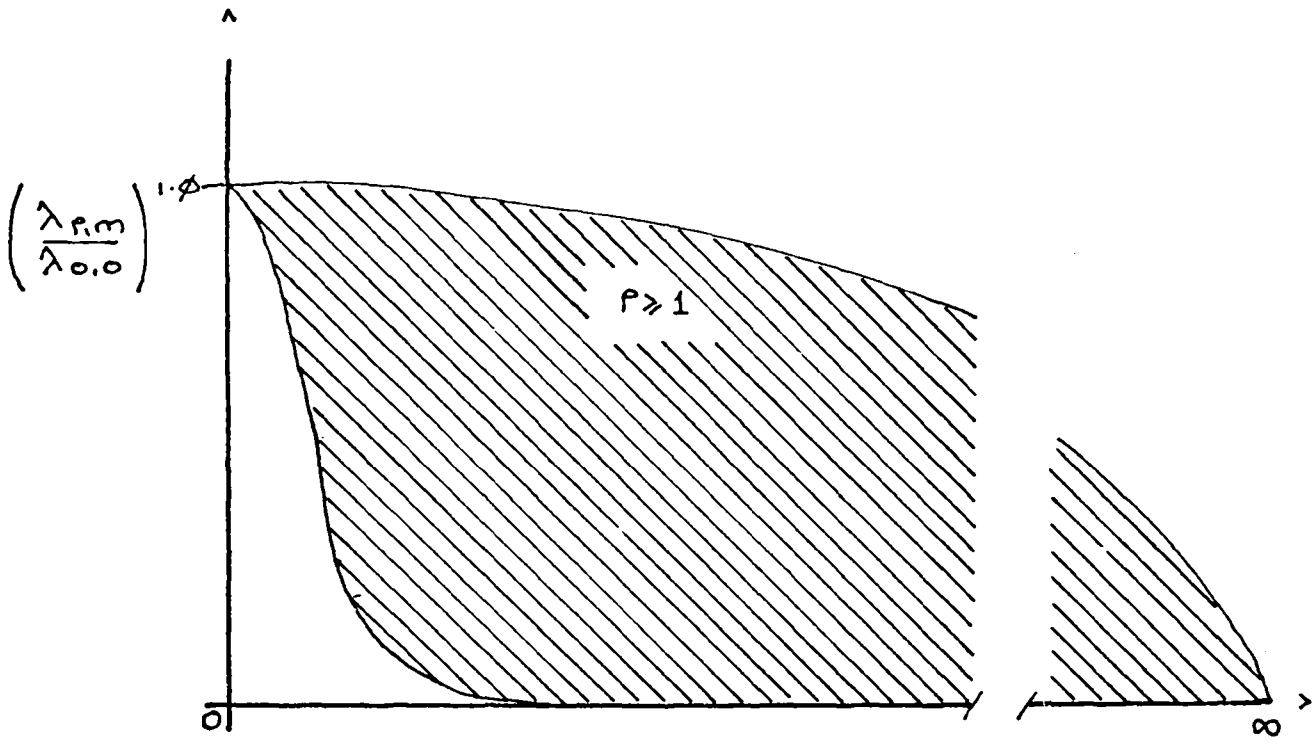


Figure 4. The eigenvalue spectrum behaviour for the Classical Isotropic Heisenberg chain.

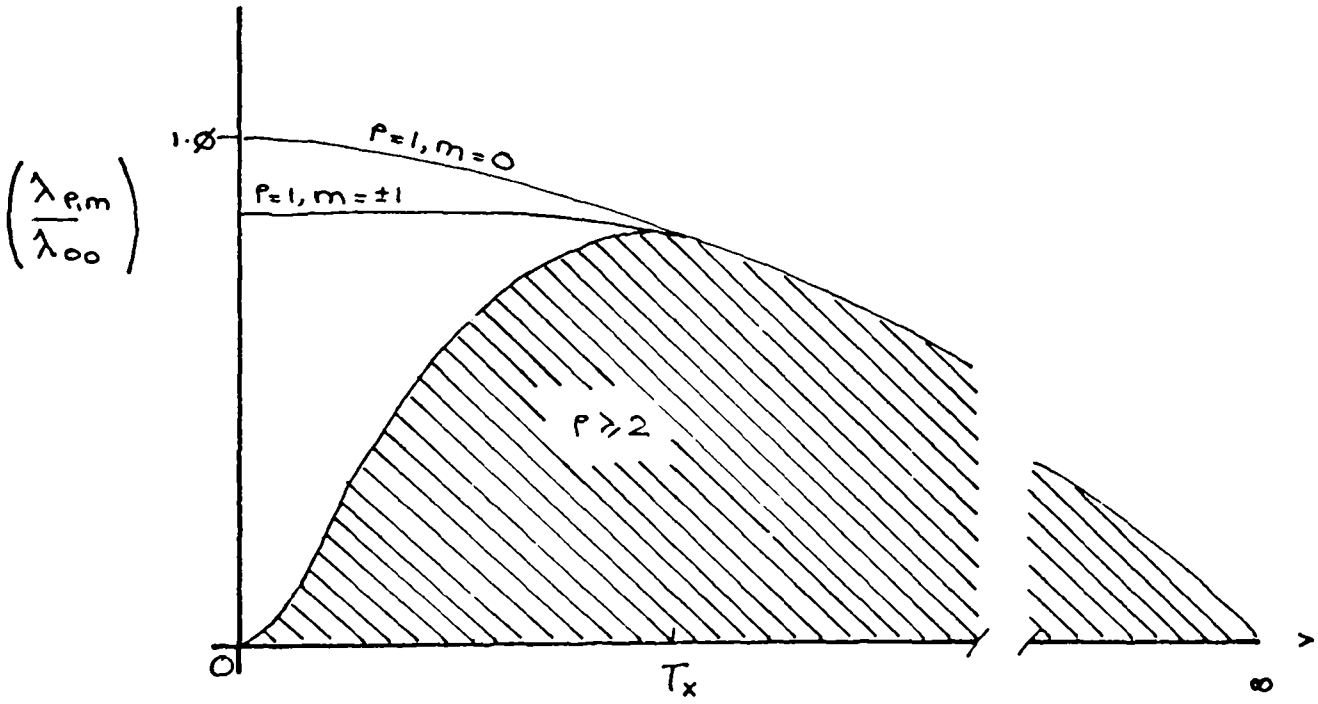


Figure 5. The eigenvalue spectrum behaviour for the weakly anisotropic Heisenberg chain. The crossover temperature, T_x, of the chain is also marked.

Figure 6. Plots of inverse correlation lengths versus temperature obtained from the approximation scheme in Chapter 2.
[See insert between pages 27 and 28 of the text]
The results shown correspond to the anisotropy values:

$\cosh \mu = 10$ (solid line)

$\cosh \mu = 20$ (dashed line)

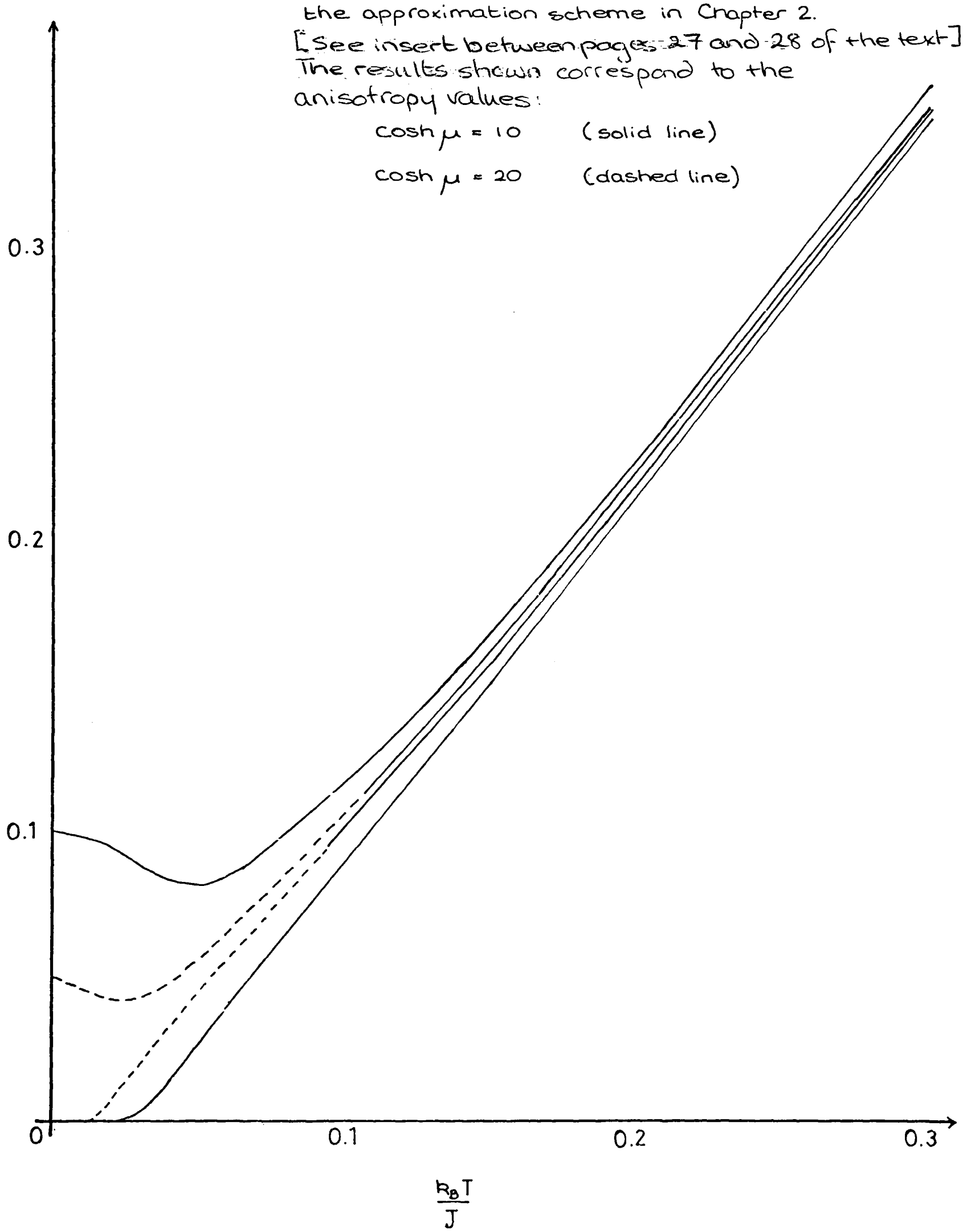


Figure 7. Plot of inverse correlation lengths versus temperature for the weakly anisotropic chain with:

$$\cosh\mu \simeq 8.3$$

from the approximation scheme of Chapter 2.

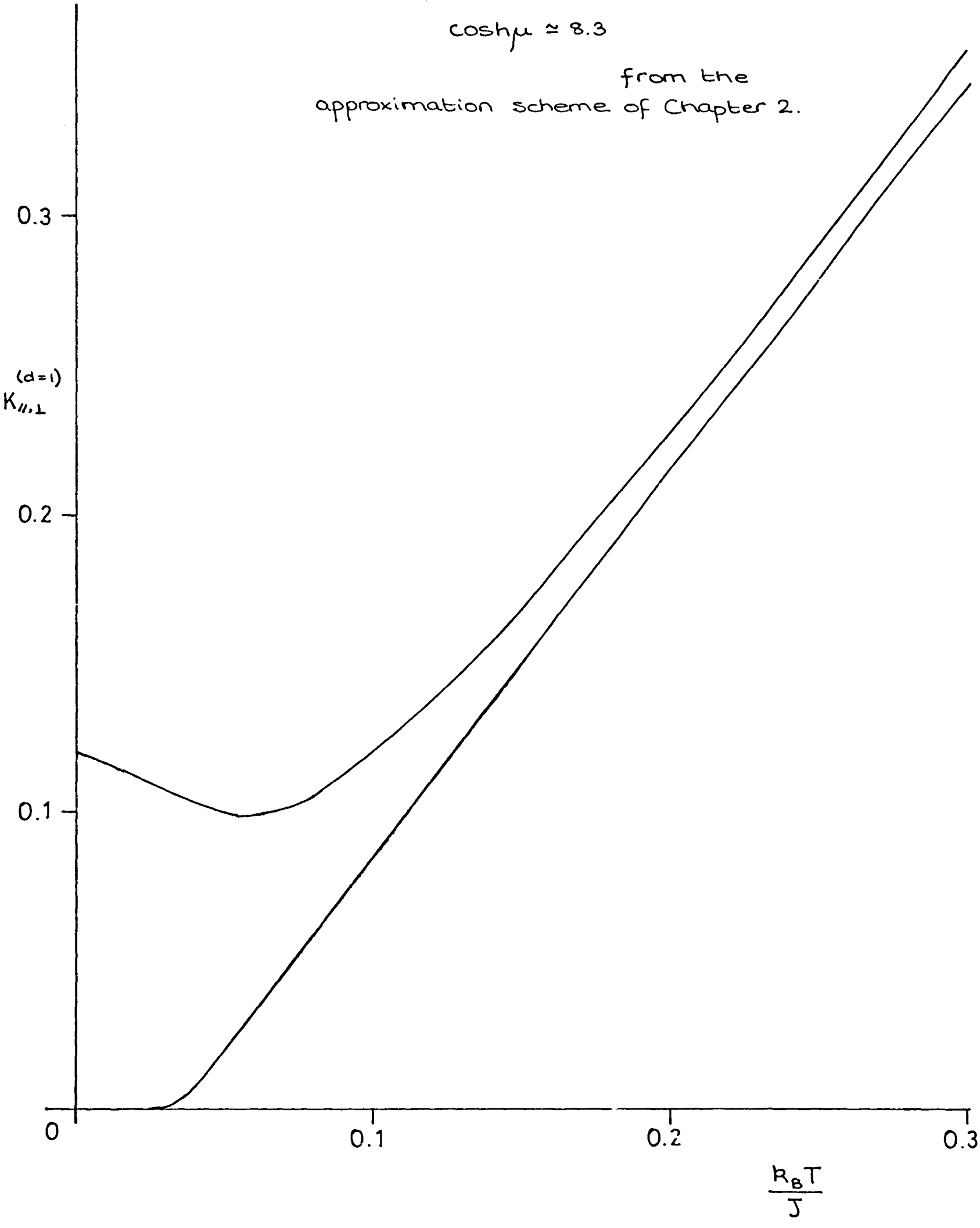


Figure 8. Variation of the longitudinal inverse correlation Length behaviour with dilution in the weakly anisotropic chain. The plots shown are for chains with site/bond concentrations:

$p = 0.9, 0.95, 1.0$

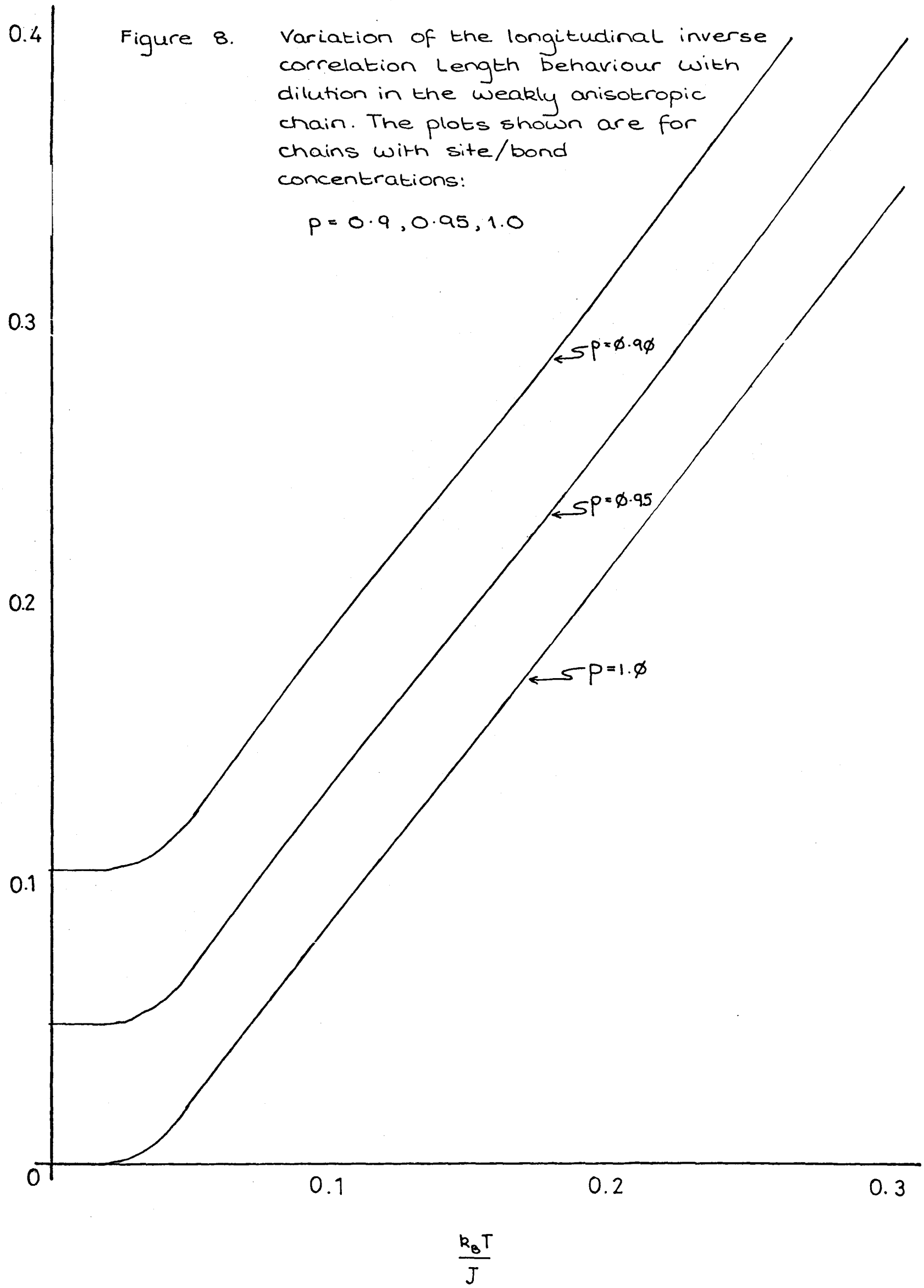


Figure 9. Sketch to show how taking a trace over alternate spins of the one-dimensional system effectively dilates the underlying length scales by a factor, b = 2.

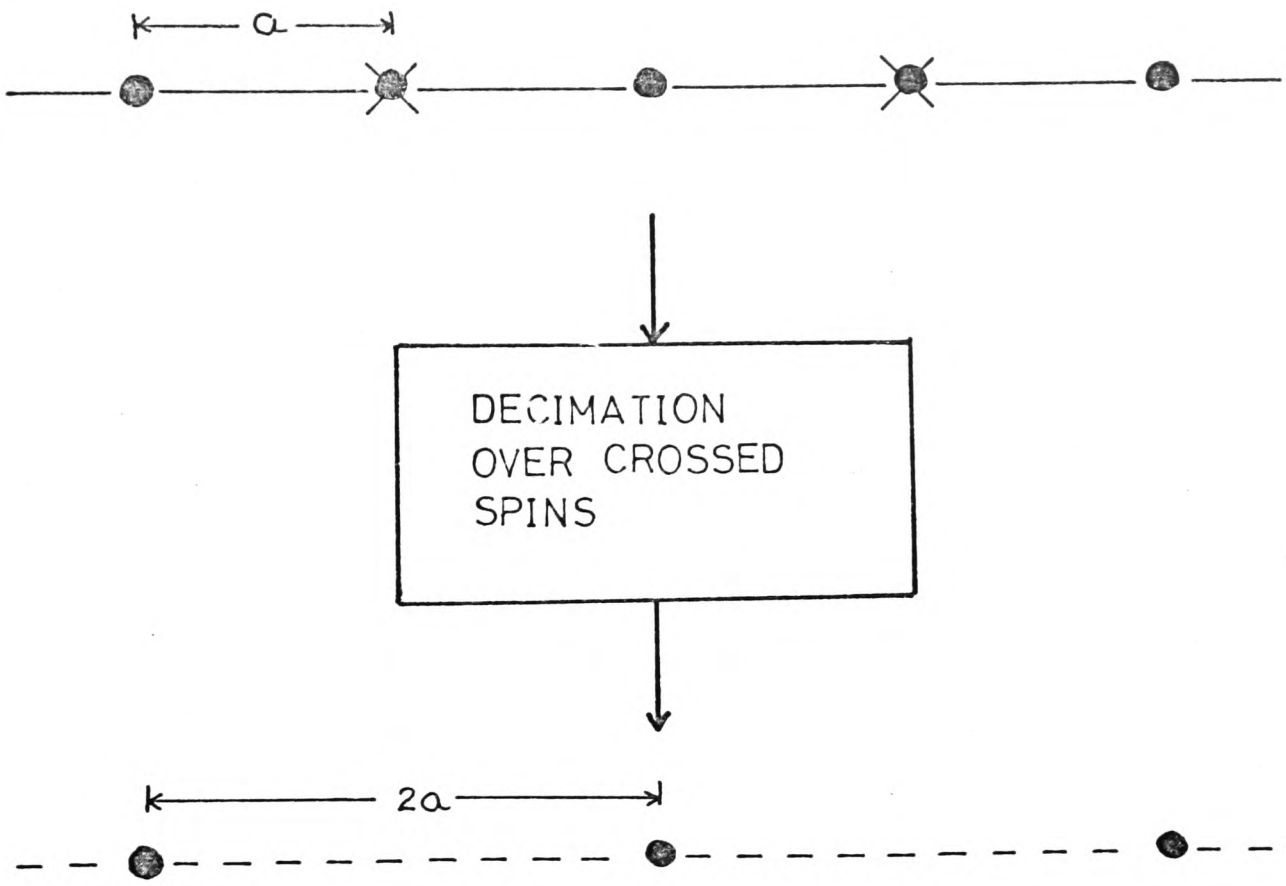
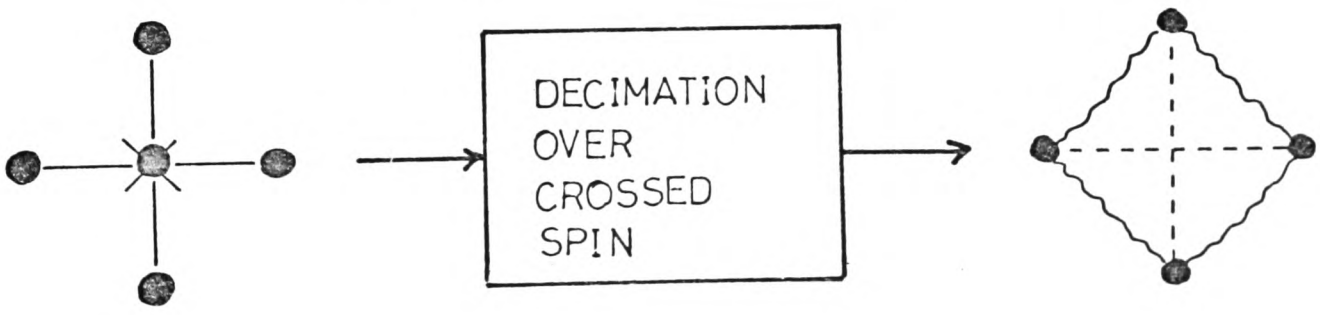


Figure 10 Sketch to show how taking a trace over the central spin of a simple, two-dimensional cluster may introduce higher order couplings.

The dashed lines in the second diagram represent next-nearest neighbour couplings introduced by the decimation process.



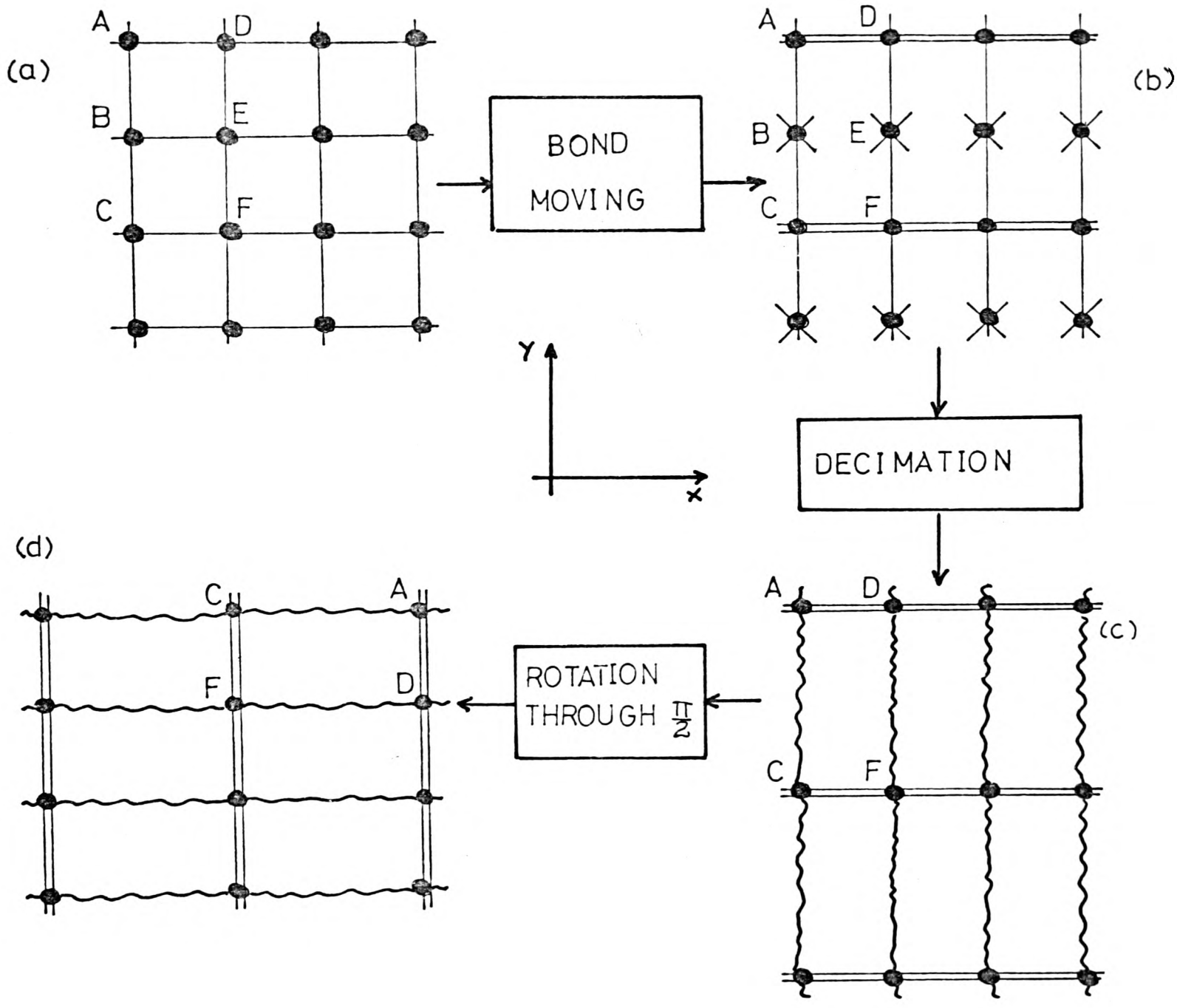


Figure 11. A series of diagrams illustrating the Migdal/Kadanoff bond moving scheme on a square lattice.

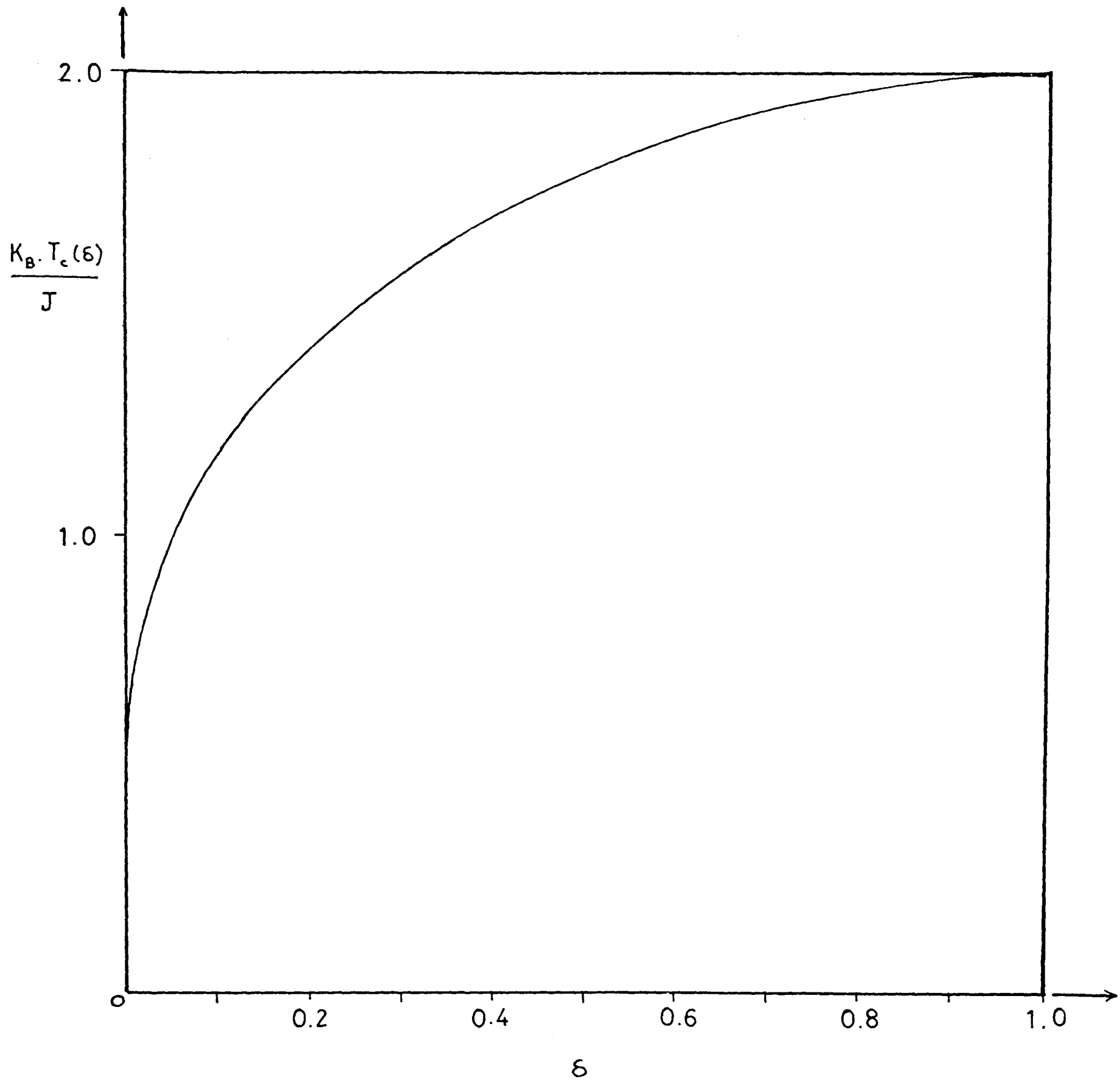


Figure 12. The transition temperature of the pure, two-dimensional Heisenberg model as a function of the anisotropy parameter, δ.

Figure 13. A sketch of the inverse correlation length behaviour in the weakly anisotropic, two-dimensional Heisenberg model. The dashed line indicates the critical temperature, T_c.

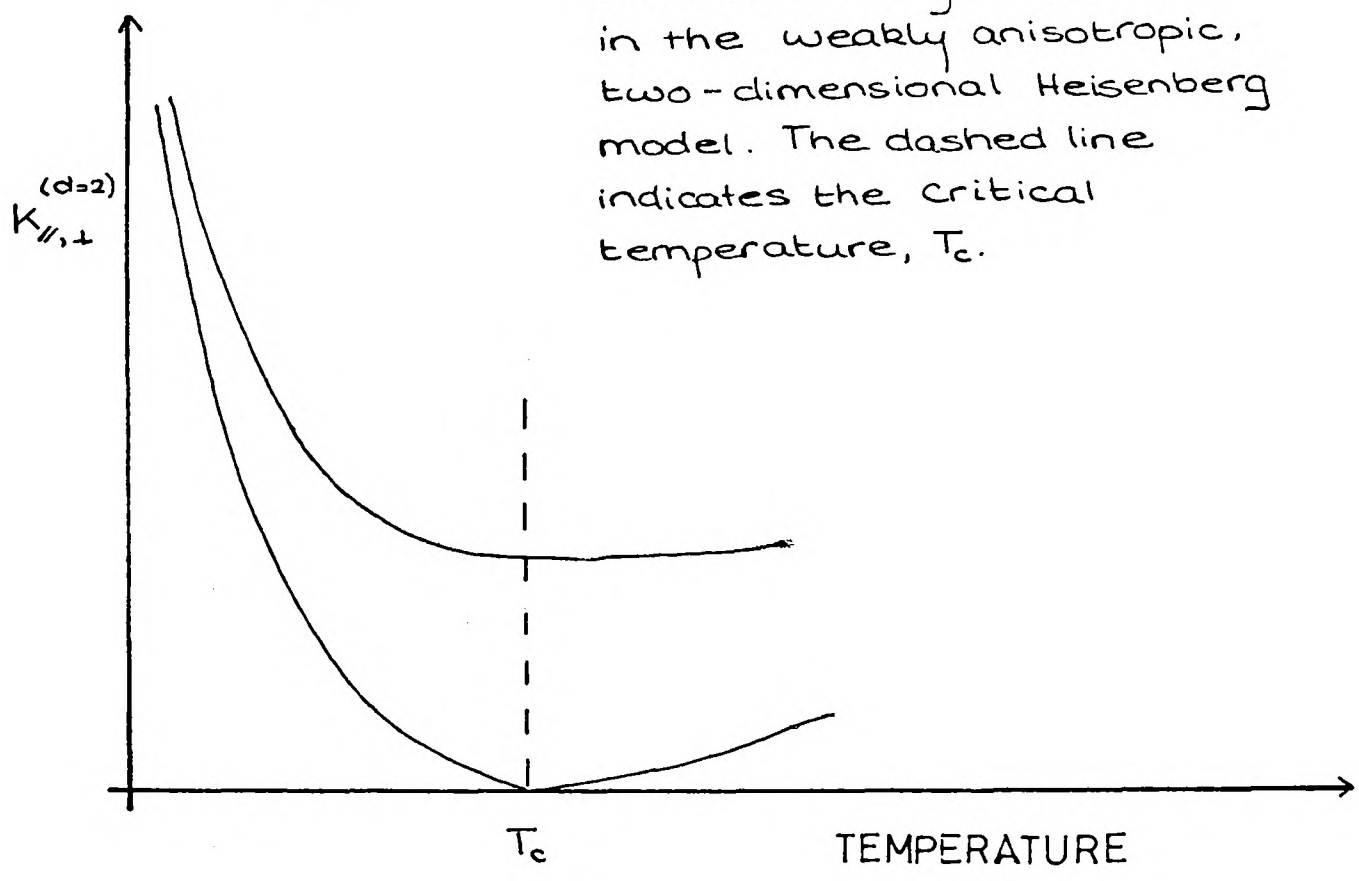
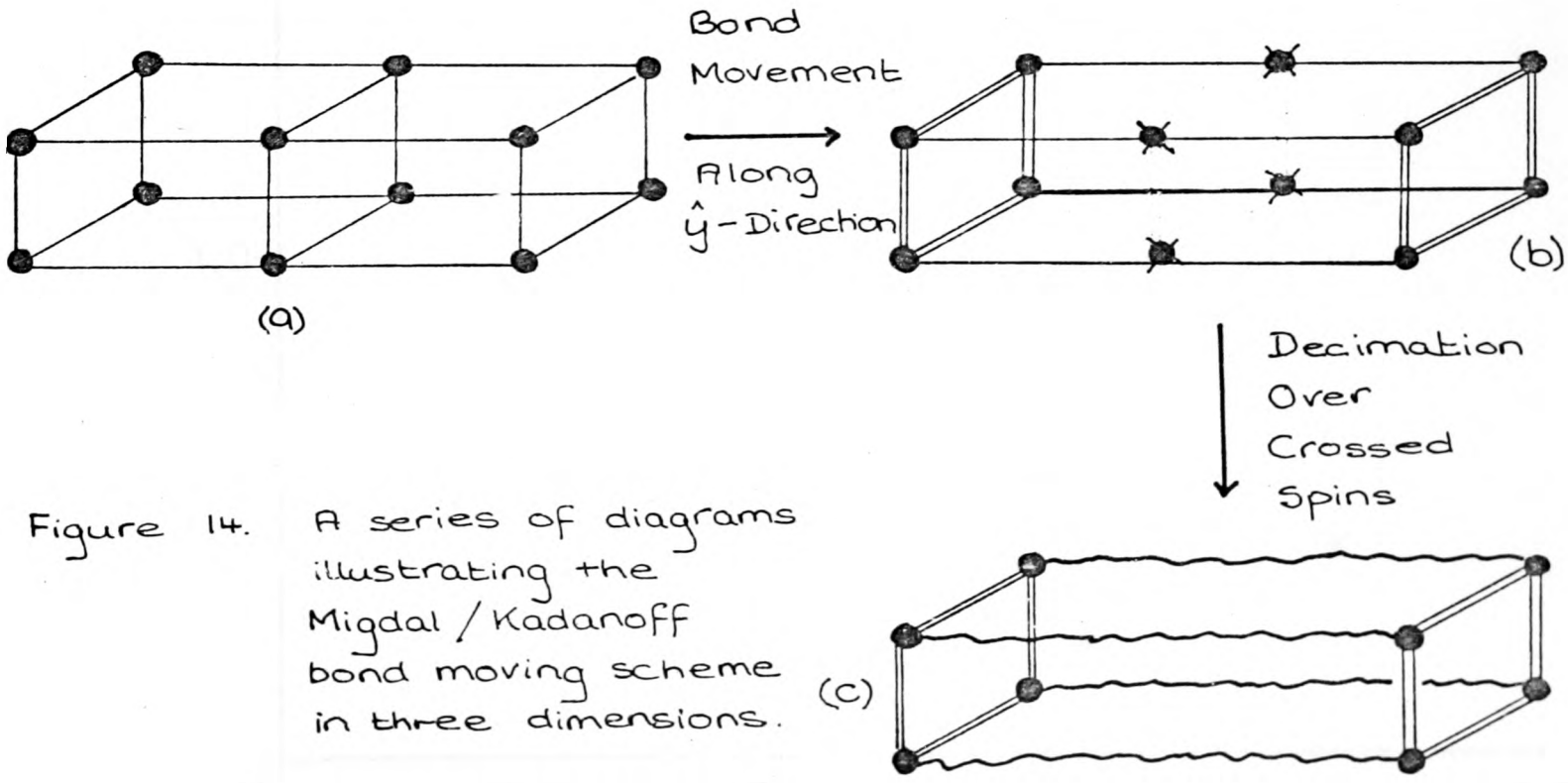


Figure 14. A series of diagrams illustrating the Migdal / Kadanoff bond moving scheme in three dimensions.



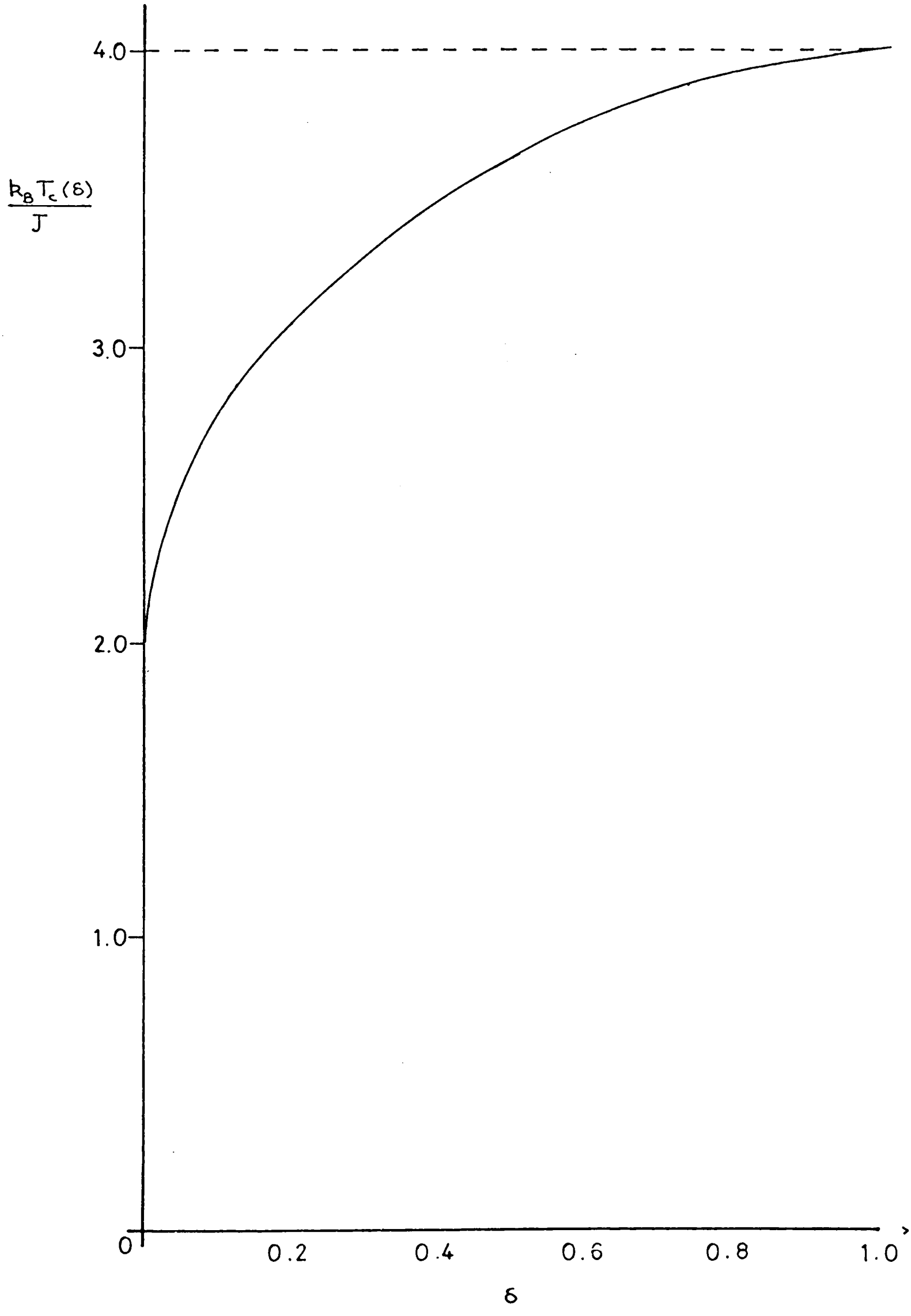


Figure 15. Critical temperature of the pure, three-dimensional Heisenberg model as a function of the anisotropy parameter, δ.

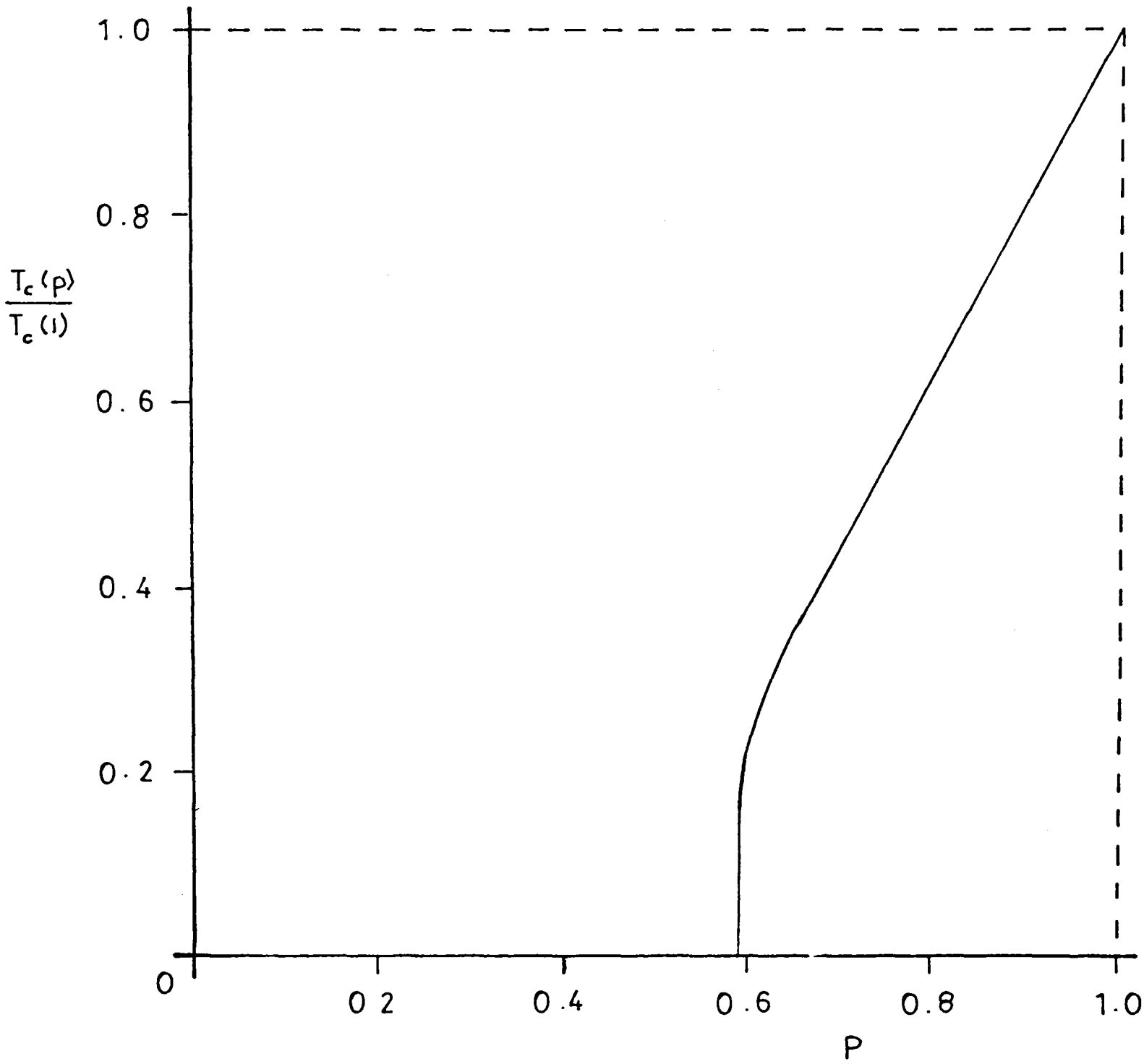


Figure 16. Sketch of the critical temperature of the dilute, weakly anisotropic, two-dimensional Heisenberg model as a function of the magnetic ion concentration.

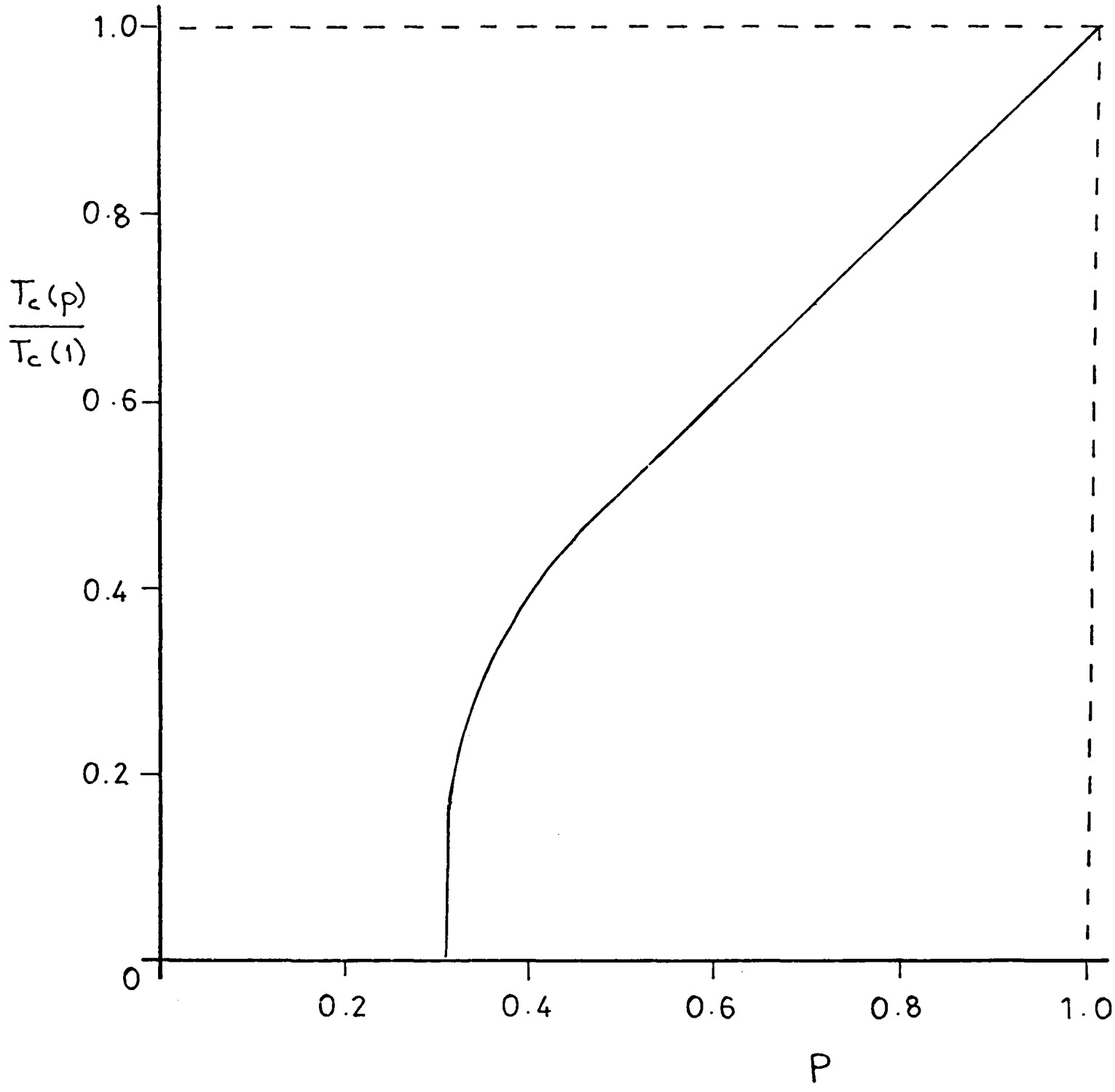


Figure 17. Sketch of the critical temperature of the dilute, weakly anisotropic, three-dimensional Heisenberg model as a function of the magnetic ion concentration.

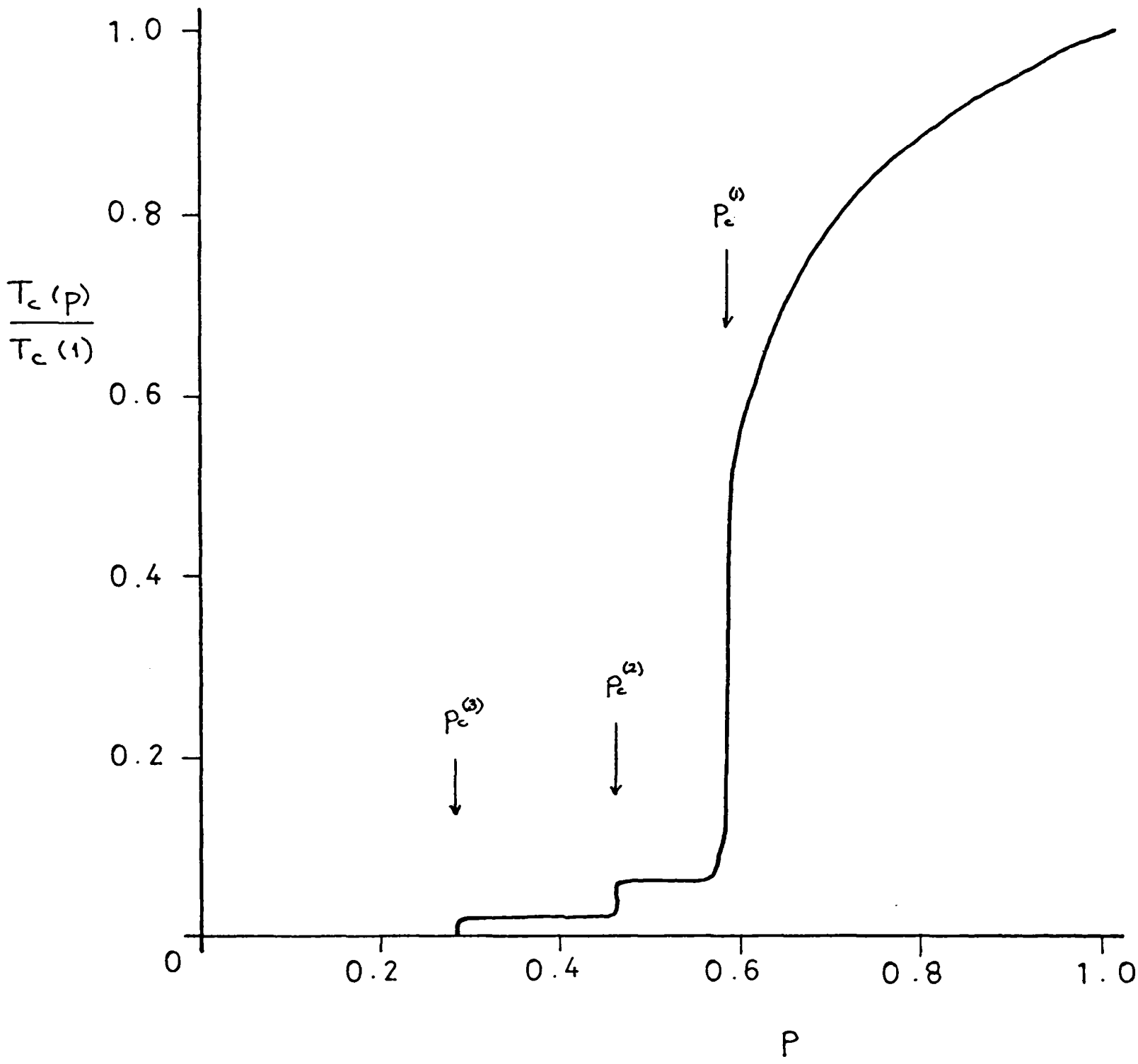


Figure 18. Schematic diagram of the critical temperature as a function of magnetic ion concentration in a real, quasi-two-dimensional model.

$p_c^{(1)}$ represents the critical concentration for a square net with nearest-neighbour interactions only.

$p_c^{(2)}$ represents the critical concentration for a square net in the presence of next-nearest neighbour interactions and $p_c^{(3)}$ for a three-dimensional system.

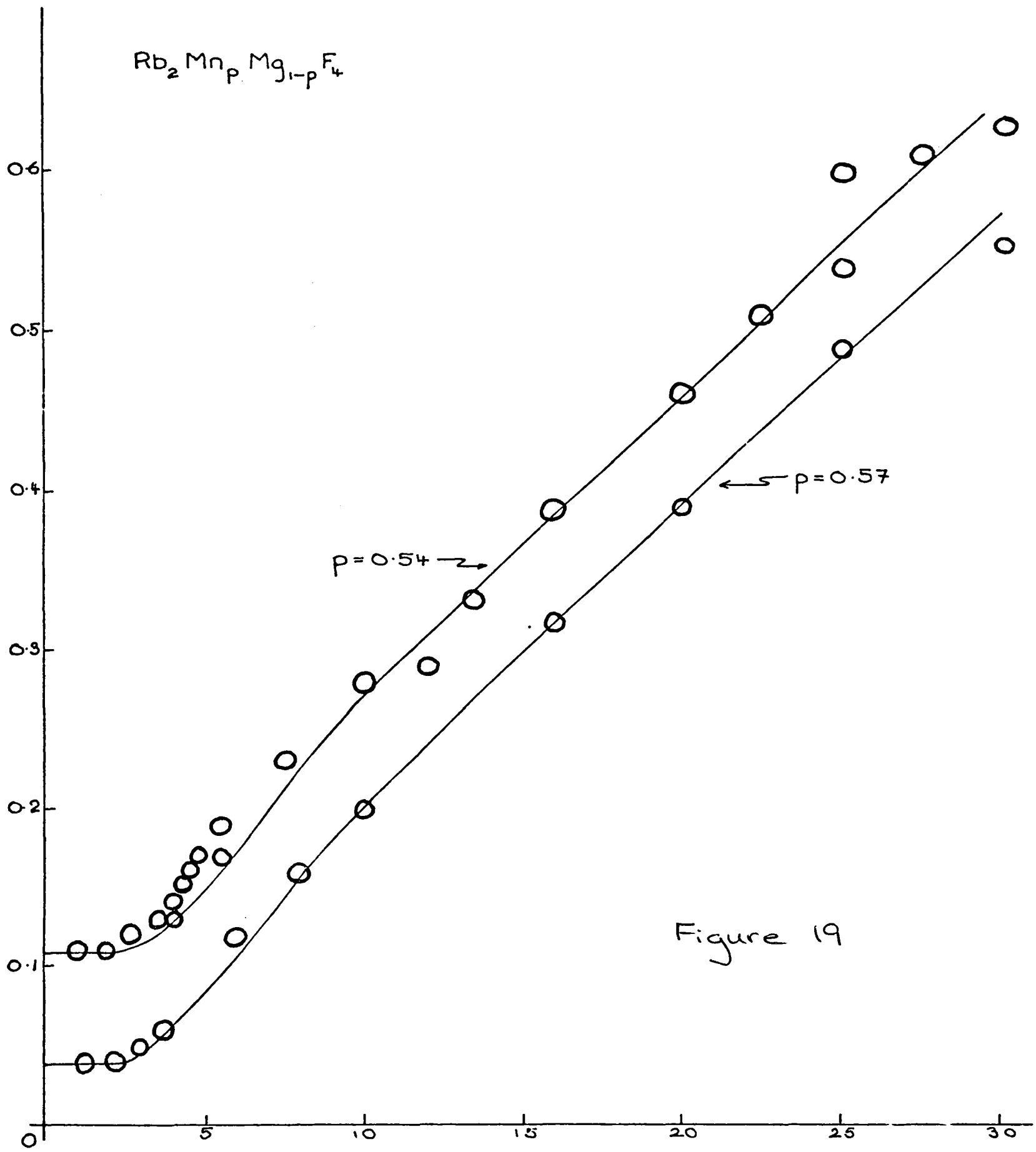


Figure 19

A plot of : $$\frac{1}{\xi_{//}} = \frac{1}{\xi_{//}}(T=0) + a_0 \{K_{//}^{(d=1)}\}^{\nu_c}$$

where: $$\nu_c = \begin{cases} 0.9 : T > T_x \simeq 9K \\ 4/3 : T < T_x \simeq 9K \end{cases} \quad : \quad a_0 = \begin{cases} 1 : T > T_x \\ 2.6 : T < T_x \end{cases}$$

for comparison with the results of Birgeneau et al. (1980) from neutron scattering experiments on the $Rb_2 Mn_p Mg_{1-p} F_4$ system

Experimental points are shown as open circles.

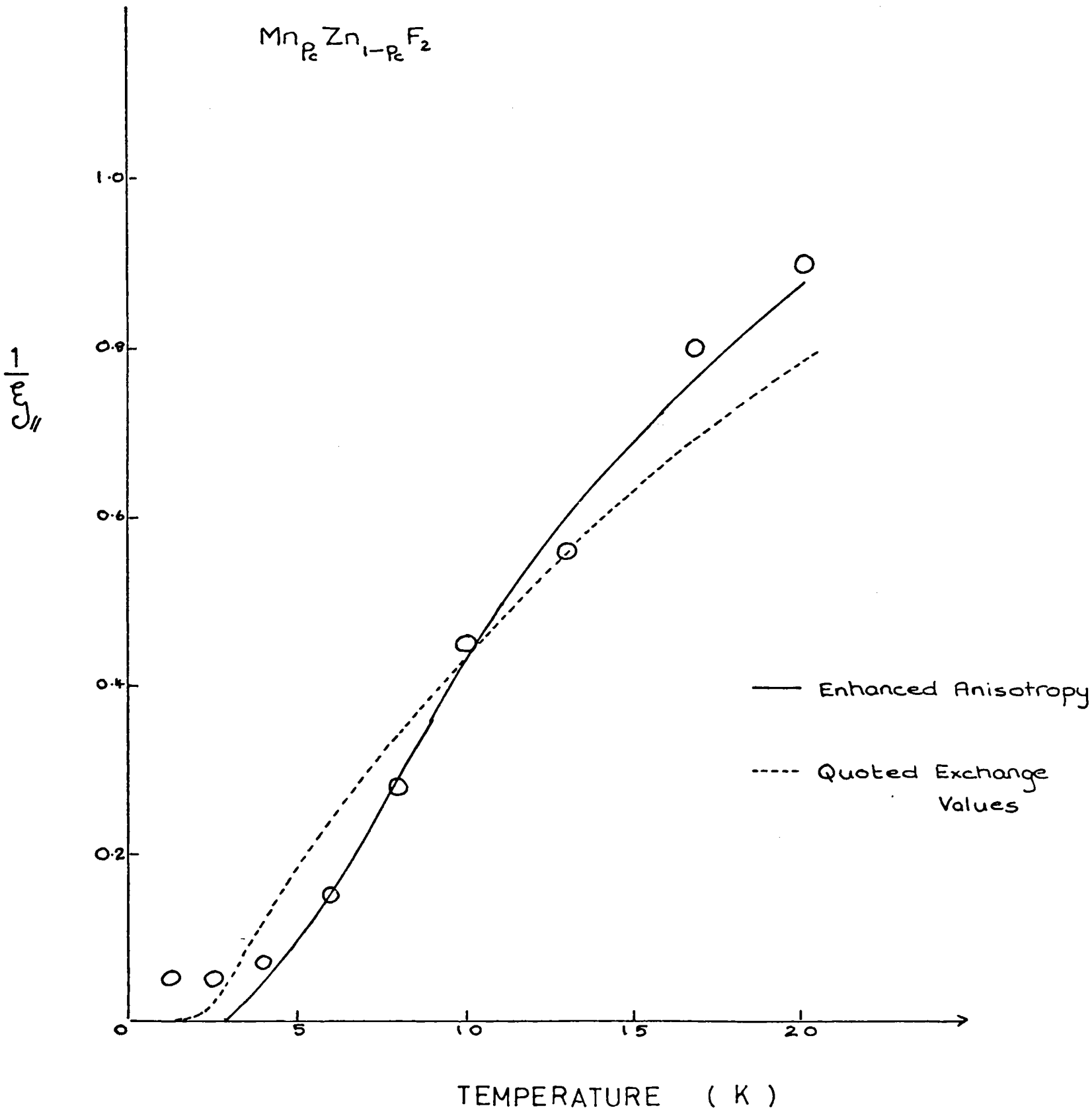


Figure 20. Plots of:

$$\frac{1}{\xi_{//}} = \frac{1}{\xi_{//}}(T=0) + b_0 \left[K_{//}^{(d=1)} \right]^{\nu_t} \quad : \nu_t = 0.7$$

for comparison with the results of neutron-scattering experiments carried out by Cowley et al. on the $Mn_p Zn_{1-p} F_2$ system. The solid curve corresponds to using the exchange constants quoted by Cowley et al. (1977(a)). The dashed line is obtained by multiplying the anisotropy factor, δ, by six. (6).